# The role of lysine acetylation on the regulation of phospholipid homeostasis in yeast

*Louis Dacquay*

A thesis submitted to the
Faculty of Graduate and Postdoctoral Studies
in partial fulfillment of the requirements for the
MSc degree in Biochemistry

Department of Biochemistry, Microbiology and Immunology
Faculty of Medicine
**University of Ottawa**

## Abstract

Actively proliferating cells constantly monitor and re-adjust their metabolic pathways to ensure the replenishment of phospholipids necessary for membrane biogenesis and intracellular trafficking. In *Saccharomyces cerevisiae,* multiple studies have suggested that lysine acetylation has a role in coordinating phospholipid metabolism, yet its contribution towards phospholipid homeostasis remains uncharacterized. In this study we undertook a genetic screen to explore the connection between lysine acetylation and phospholipid homeostasis. We found that mutants of the lysine acetyltransferase complex, NuA4, shared a negative genetic interaction with a mutant of Sec14*,* a lipid-binding protein that regulates Golgi phospholipid composition. Through transcriptome, genetic, cell biology, and chemical analysis, we discovered that the growth defects between NuA4 and Sec14 mutants is likely derived from impaired fatty acid biosynthesis suggesting a role for NuA4 as a positive regulator of fatty acid biosynthesis. Secondly, we discovered that acetylation on the conserved lysine residue K109 inhibits the localization and function of the Oxysterol-Binding Protein Osh4- a lipid-binding protein that antagonizes the function of Sec14 at the Golgi. Furthermore, regulation of Oxysterol-Binding Proteins by acetylation may be a conserved mechanism as we found that Osh1, a homologue of Osh4, was also acetylated on the equivalent lysine residue. Altogether, we have demonstrated that lysine acetylation can target multiple different phospholipid metabolic pathways which implies that it has a very important role for the regulation of phospholipid homeostasis.

## Acknowledgments

I would like to thank my supervisor, Dr. Kristin Baetz, for giving me the opportunity to work in her laboratory. I would also like to thank her for all the mentorship she provided me to help improve my writing and presenting skills.

I would also like to thank the former post-doctoral fellow from our lab, Dr. Michael Kennedy, who provided support and guidance all throughout my Master's degree even after he left the lab. I would also thank him for also helping me improve my writing and presenting skills on top of improving my bench work skills.

A very big thank you to Dr. Sylvain Huard who was always willing to provide help with my experiments and for being very patient with me.

I would also like to thank all the Baetz lab members, both past and present, who've helped me along the way through their friendship and their contributions towards my project: David Czosniak, Michael Cotrut, Jingwen Du, Bo Liao, Trang Pham, Roger Fong, Mila Tepliakova, Amanda Defela, and Meaghan Rollins.

Thank you for other people who helped me with my experiments: Annika Flint and James Butcher (RNA-seq), Danny Salem (fluorescence quantification), Ian Roney and Brendan Camellato (Tet-responsive system), Adam Rudner (various protocols).

I would also like to thank my T.A.C. members, Dr. Jean-François Couture and Dr. Thomas Lagace, for their comments and guidance on my project and thank you Dr. Michael Downey for also providing comments and tips on my project.

# Table of Contents

## List of Figures

## List of Tables

## List of abbreviations

| | |
|---|---|
| CDP-DAG | Cytidine diphosphate diacylglycerol |
| DAG | Diacylglycerol |
| DNA | Deoxyribonucleic acid |
| ER | Endoplasmic reticulum |
| FA | Fatty acid |
| GFP | Green-fluorescent protein |
| GST | Glutathione S-transferase |
| HIS | Histidine |
| ICRE | Inositol/choline response element |
| KAT | Lysine Acetyltransferase |
| KDAC | Lysine Deacetylase |
| LEU | Leucine |
| $OD_{xxx}$ | Optical density (xxx nanometre wavelength) |
| ORP | OSBP-related domain |
| OSBP | Oxysterol-Binding Protein |
| PA | Phosphatidic acid |
| PC | Phosphatidylcholine |
| PE | Phosphatidylethanolamine |
| PI | Phosphatidylinositol |
| PI-4,5-$P_2$ | Phosphatidylinositol-4,5-biphosphate |
| PI-4-P | Phosphatidylinositol-4-phosphate |
| PLD | Phospholipase D |
| PS | Phosphatidylserine |
| PTM | Post-translational modification |
| RNA | Ribonucleic acid |
| rRNA | Ribosomal RNA |
| SC | Synthetic complete |
| SD | Synthetic drop-out |
| SE | Steryl ester |
| TAG | Triacylglycerol |
| TAP | Tandem-affinity purification |
| URA | Uracil |
| WCE | Whole cell extract |
| YPD | Yeast peptone dextrose |

# 1 Introduction

Phospholipids are not only the structural foundation for all cellular membranes but are also pivotal signalling molecules for cellular processes such as proliferation and intracellular trafficking. A vast network of metabolic pathways is responsible to generate these phospholipids. The model organism *Saccharomyces cerevisiae* offers important insights on the mechanisms that regulate lipid metabolism as most genes and pathways remain tightly conserved across all eukaryotes.

Membrane phospholipid composition is in part established by highly conserved families of lipid-binding proteins which, as their name suggests, bind cellular lipids to facilitate lipid transport, modulate enzymatic activity and even regulate the transcription of metabolic genes (reviewed in HENRY *et al.* 2012; OLKKONEN 2013; JACKSON AND BOUVET 2014; TRIPATHI *et al.* 2014). Phospholipid metabolism can also be regulated by signalling pathways such as post-translational modifications. Indeed, it has recently emerged that lysine acetylation contributes to lipid metabolism by regulating both gene expression and the activity of metabolic enzymes (reviewed in DRAZIC *et al.* 2016; MENZIES *et al.* 2016). However, the overall effect of lysine acetylation on the regulation of lipid metabolic pathways remains only partly resolved. The goal of my thesis was to uncover the different mechanisms by which lysine acetylation contributes to phospholipid metabolism. I will begin by describing the pathways and effectors regulating phospholipid metabolism all the while introducing the currently known links between lysine acetylation and phospholipid metabolism.

## 1.1 Lysine Acetylation

### Mechanism of lysine acetylation

Lysine acetylation is a conserved post-translational modification (PTM) found in many different species including yeast and humans (KURDISTANI AND GRUNSTEIN 2003; SHAHBAZIAN

AND GRUNSTEIN 2007). It consists of the reversible addition of an acetyl group on the ε-amino group of a lysine residue on a protein to mask its positive charge. This modification has been found on both histones as well as non-histone proteins implicated in a wide variety of cellular processes (CHOUDHARY *et al.* 2014). Lysine acetylation can have many different effects on proteins which includes inducing conformational changes, modulating protein-ligand interactions, and inducing degradation (XIONG AND GUAN 2012). The enzymes mediating the exchange between the acetylated and the unacetylated form of the residues are the Lysine Acetyltransferases (KATs) and the Lysine Deacetylases (KDACs). In yeast, there are 8 confirmed KATs, 6 more putative or unconfirmed KATs, as well as 10 confirmed KDACs (reviewed in DOWNEY AND BAETZ 2016). Several of these enzymes work within a larger complex that includes other subunits, including the well characterized and essential NuA4 KAT complex.

**NuA4 KAT complex**

NuA4 is a 13 subunit complex composed of the essential lysine acetyltransferase catalytic domain, Esa1, five other essential subunits (Act1, Arp4, Epl1, Swc4, Tra1) and seven non-essential subunits (Eaf1, Eaf3, Eaf5, Eaf6, Eaf7, Yaf9, Yng2) (reviewed in DOYON AND COTE 2004) (**Figure 1.1**). The NuA4 complex is highly conserved with the homologous human KAT complex, Tip60 (CAI *et al.* 2003; reviewed in DOYON *et al.* 2004). The scaffold protein, Eaf1, is critical for NuA4 complex integrity as it attaches the catalytic domain or piccolo-NuA4 domain, Esa1/Yng2/Epl1/Eaf6, to the recruitment module or TINTIN complex, Eaf3/Eaf5/Eaf7 (AUGER *et al.* 2008; MITCHELL *et al.* 2008; CHENG AND COTE 2014; ROSSETTO *et al.* 2014; BHAT *et al.* 2015).

NuA4/Tip60 complex have many defined role and functions within the cells. NuA4 and Tip60 typically localizes within the nucleus in the cells (YAMAMOTO AND HORIKOSHI 1997; GALARNEAU *et al.* 2000), where they regulate chromatin remodelling and gene transcription through the acetylation of histones H4 and H2A-Z (reviewed in LU *et al.* 2009). However, there

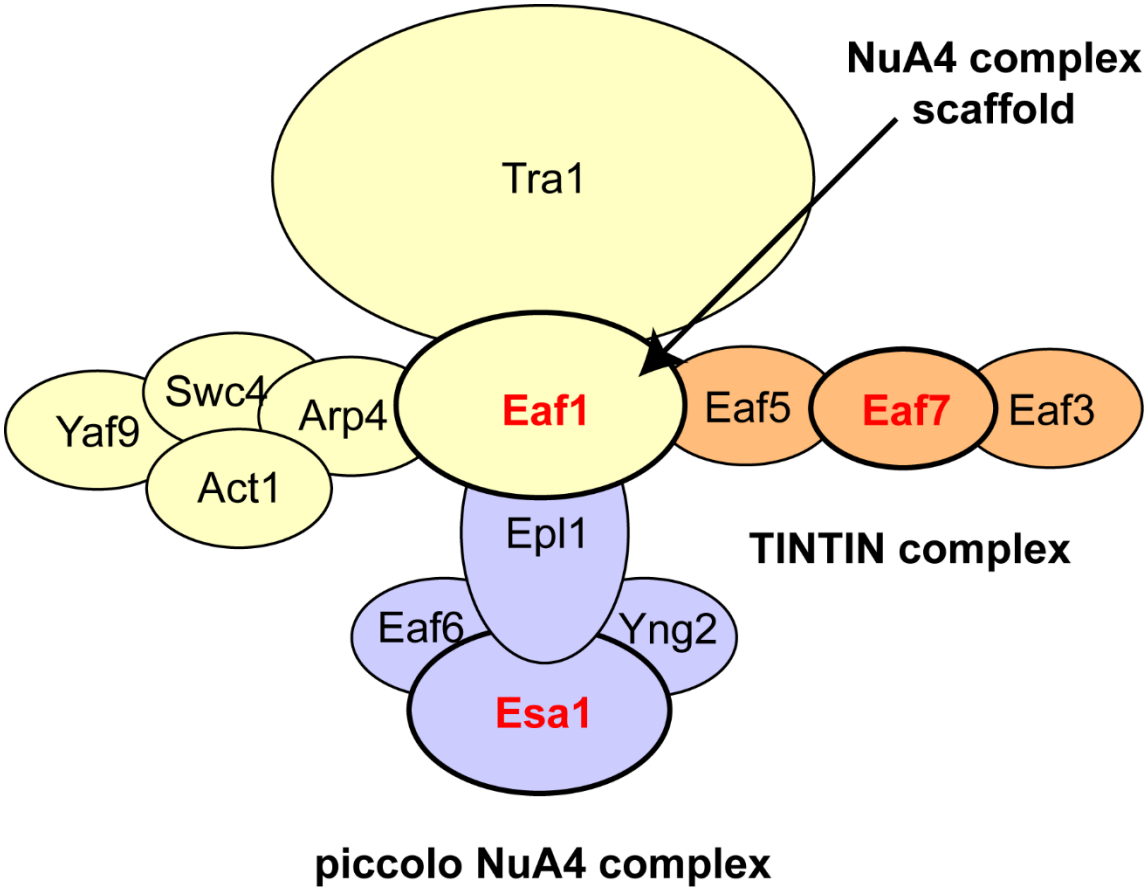
NuA4 complex
scaffold
Tra1
Swc4
Yaf9
Arp4
Act1
Eaf1
Eaf5
Eaf7
Eaf3
Epl1
TINTIN complex
Eaf6
Yng2
Esa1
piccolo NuA4 complex

**Figure 1.1 Current model of the NuA4 lysine acetyltransferase complex.** The 13 subunits of NuA4 are organized with their known physical interactors. In red are the three NuA4 subunits focussed for this project to study the roles and effect of NuA4 mutants on phospholipid homeostasis. Proteins within smaller complexes are organized by colour code: purple= piccolo NuA4 or the catalytic subcomplex; green = TINTIN complex; yellow = other. Figure derived from (CHITTULURU *et al.* 2011)

is also evidence of NuA4/Tip60 localizing outside the nucleus in the cytoplasm under certain conditions (LEE *et al.* 2001; YI *et al.* 2012; YI *et al.* 2014), as well as growing evidence that NuA4 targets non-histone proteins (LIN *et al.* 2009; MITCHELL *et al.* 2011; MITCHELL *et al.* 2013), and the importance of these acetylation sites are only beginning to be understood (reviewed in DOWNEY AND BAETZ 2016).

## 1.2 Phospholipid metabolism

### Major phospholipids biosynthesis pathways

The four phospholipids species that compose the majority of intracellular membranes are phosphatidylcholine (PC), phosphatidylethanolamine (PE), phosphatidylserine (PS), and phosphatidylinositol (PI), all of which derive from the common lipid precursor, phosphatidic acid (PA) (reviewed in HENRY *et al.* 2012) (**Figure 1.2**). *De novo* PA is synthesized at the endoplasmic reticulum (ER) through the incorporation of two fatty acids (FAs) on a glycerol-3-phosphate head-group. PA is subsequently converted to CDP-diacylglycerol (CDP-DAG) at either the ER or the mitochondria (KUCHLER *et al.* 1986), through the activity of the phosphatidate cytidylyltransferase Cds1 (SHEN *et al.* 1996), effectively priming it for phospholipid biosynthesis. Subsequently, the three phospholipids PS, PE, and PC are synthesized from CDP-DAG through the combined activity of several enzymes. First, the PS-synthase Cho1 converts CDP-DAG into PS at the ER by incorporating a serine molecule on the glycerol-3-phosphate head-group (LETTS *et al.* 1983; YAMASHITA AND NIKAWA 1997). Next, PS is converted to PE by the activity of one of two PS-decarboxylases, Psd1 or Psd2, that localizes to the inner mitochondria membrane and the Golgi/vacuole, respectively (CLANCEY *et al.* 1993; TROTTER *et al.* 1993; TROTTER *et al.* 1995; VOELKER 1997). Finally, PE is converted to PC at the ER by the activity of the PE-methyltransferase Cho2/Pem1 and the phospholipid-methyltransferase Opi3/Pem2 (KODAKI AND YAMASHITA 1987). Alternatively, PC and PE can also be synthesized through a salvage pathway, also referred to as the Kennedy pathway. In this

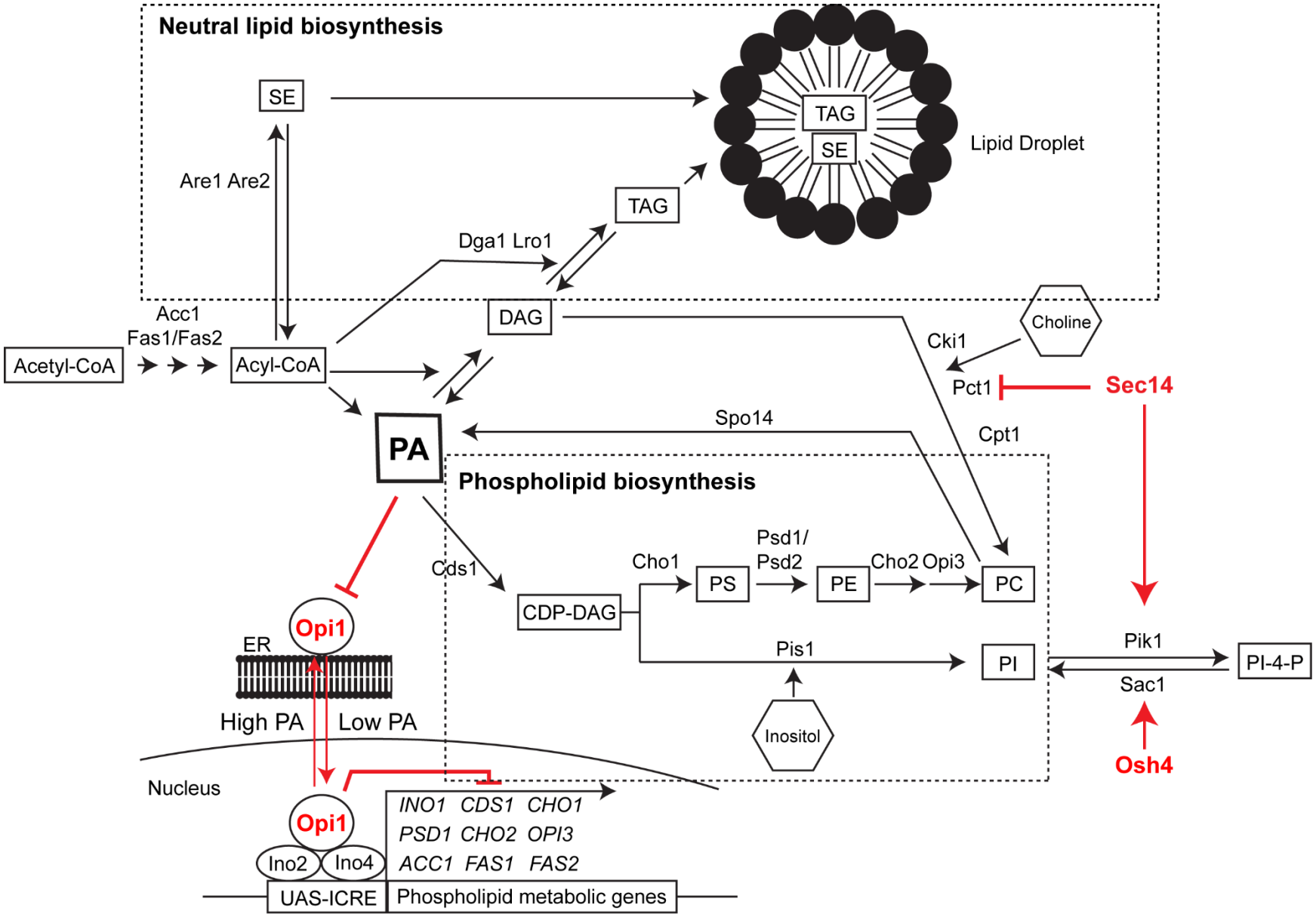
Neutral lipid biosynthesis
SE
TAG
SE
Lipid Droplet
Are1 Are2
TAG
Dga1 Lro1
Acc1
Fas1/Fas2
Acetyl-CoA
Acyl-CoA
DAG
Choline
Cki1
Pct1
Sec14
Spo14
Cpt1
PA
Phospholipid biosynthesis
Cds1
Cho1
PS
Psd1/
Psd2
PE
Cho2 Opi3
PC
CDP-DAG
Opi1
ER
High PA
Low PA
Pis1
PI
Pik1
PI-4-P
Sac1
Inositol
Osh4
Nucleus
Opi1
Ino2
Ino4
INO1 CDS1 CHO1
PSD1 CHO2 OPI3
ACC1 FAS1 FAS2
UAS-ICRE
Phospholipid metabolic genes

**Figure 1.2 Overview of phospholipid and neutral lipid metabolism.** Key lipid metabolic proteins are indicated in black to demonstrate their enzymatic activities. Lipid species are indicated in black rectangles. Abbreviations: Phosphatidic acid (PA), Diacylglycerol (DAG), Triacylglycerol (TAG), Steryl esters (SE), Cytidine diphosphate diacylglycerol (CDP-DAG), Phosphatidylinositol (PI), Phosphatidylserine (PS), Phosphatidylethanolamine (PE), Phosphatidylcholine (PC), Phosphatidylinositol-4-phosphate (PI-4-P). In red are three lipid-binding proteins that help coordinate phospholipid homeostasis by either regulating transcription (Opi1) or by regulating enzymatic activities (Sec14 and Osh4).

pathway, ethanolamine and choline provided for by the residing media is transported into the cells and directly incorporated as head-groups on the glycerophosphate backbone of DAG through the CDP-ethanolamine pathway and the CDP-choline pathway by enzymes that localizes on vesicular structures, the mitochondria, or the ER (HUH *et al.* 2003; NATTER *et al.* 2005; GIBELLINI AND SMITH 2010). Unlike the other phospholipids, PI is synthesized at the ER in a completely distinct pathway dependent on inositol which is directly incorporated on CDP-DAG by the PI synthase, Pis1 (NIKAWA AND YAMASHITA 1984; NIKAWA AND YAMASHITA 1997). Together, these four lipids provide most of the necessary components for membrane assembly which is instrumental for cellular proliferation and division

**Neutral lipid biosynthesis pathways**

When cells are in stationary phase, or are not actively proliferating, excess phospholipids and fatty acids can be stored within lipid droplets in the form of neutral lipids through the generation of triacylglycerols (TAGs) and steryl esters (SE) (**Figure 1.2**). TAGs are generated predominately by the activity of the acyltransferases Dga1 and Lro1 (OELKERS *et al.* 2000; OELKERS *et al.* 2002). The two acyltransferases, Are1 and Are2 are necessary for the production of SEs but can also contribute to TAG biosynthesis (YANG *et al.* 1996; SANDAGER *et al.* 2002). Although TAG and SE biosynthesis is not required for cell survival as a strain lacking all four neutral lipid biosynthesis genes, *dga1Δlro1Δare1Δare2Δ,* remains viable and can proliferate (SANDAGER *et al.* 2002), their synthesis does allow the cells to efficiently store FAs for energy purposes and to buffer the toxic effect of over-accumulated FAs (reviewed in MULLNER AND DAUM 2004). Conversely, under conditions where FAs are required, such as in actively proliferating cells, the hydrolysis of TAGs and SEs provides readily available substrate for creating new membranes (reviewed in KOHLWEIN 2010).

**PI-4-Phosphate metabolic pathways**

A smaller yet no less important class of lipids are the phosphoinositides, which are the phosphorylated-derivatives of PI. The inositol head-group of PI can be phosphorylated on the three available hydroxyl groups (D3, D4, D5) in every different combination, each of which confer a specific function or signal to the lipid. A well characterized phosphoinositide subspecies is PI-4-phosphate (PI-4-P) that plays both the role of a precursor for secondary messenger molecules as well as a signalling molecule itself for the recruitment of specific proteins to membranes (reviewed in DELAGE *et al.* 2013). PI-4-P metabolism is controlled by the activity of PI-kinases and PI-phosphatases. In yeast, there are three known PI-4-kinases of which two contribute to most of the PI-4-P produced: Pik1 and Stt4 (FLANAGAN *et al.* 1993; YOSHIDA *et al.* 1994a; AUDHYA *et al.* 2000; HAN *et al.* 2002). Although they have the same catalytic activity, Pik1 and Stt4 have different functions. Pik1 localizes both on Golgi membranes as well as within the nucleus whereas Stt4 localizes predominately at the plasma membrane (AUDHYA AND EMR 2002; STRAHL *et al.* 2005). Pik1-dependent PI-4-P production is essential for the secretion and trafficking of Golgi vesicles, whereas Stt4-dependent PI-4-P production is instead essential for actin cytoskeleton organisation suggesting that distinct pools of PI-4-P are required for different functions (AUDHYA *et al.* 2000). In the case of vesicular trafficking, PI-4-P can be used as a recruitment platform for various trafficking effectors, such as GTPases and membrane coating proteins (reviewed in TAN AND BRILL 2014). PI-4-P also provides the substrate required to produce the PI-4,5-$P_2$ subspecies of phosphoinositides catalyzed by the PM-localized Mss4 PI-4,5-kinase (DESRIVIERES *et al.* 1998; HOMMA *et al.* 1998). Much like PI-4-P, PI-4,5-$P_2$ also has unique essential functions that include providing substrate for phospholipase C, recruiting protein effectors for various membrane functions, and regulating the enzymatic activities of some proteins (reviewed in DELAGE *et al.* 2013). The dephosphorylation of PI-4-P and PI-4,5-$P_2$ is catalyzed by PI-phosphatases. Sac1 is the major PI-4-phosphatase that's localized at the endoplasmic reticulum (ER) but has been shown to shuttle to the Golgi in nutrient-limited conditions (HUGHES *et al.* 2000; FAULHAMMER *et al.* 2005). Unlike the kinases, Sac1 is not

essential in yeast but its null mutation causes accumulation of PI-4-P within the cells, vacuole morphological defects, and accumulation of lipid droplets (FOTI *et al.* 2001).

**Regulation of phospholipid homeostasis**

Although I only briefly introduced the enzymes responsible for the metabolism of the major phospholipids, the objective was to illustrate the complexity and intricacies of phospholipid biosynthesis (**Figure 1.2**). One can truly appreciate how remarkable it is that cells can create and maintain specific lipid compositions for each distinct membrane. Tight regulation of this phospholipid homeostasis over different growth phases and in different stress conditions is crucial for the viability of cells. Several different effectors for regulating homeostasis have been identified of which I will present three of particular interest: Opi1, Sec14, and Osh4.

## 1.3 Transcriptional regulation of phospholipid metabolic genes by Opi1-mediated repression

One mechanism used for regulating phospholipid homeostasis under different growth conditions is driven by Opi1- a transcriptional repressor of phospholipid biosynthesis genes. The coordination of phospholipid homeostasis by Opi1 under inositol-depleted conditions has been extensively studied and provides a key example of transcriptional regulation of the phospholipid gene network.

**Lipid changes under inositol-depleted conditions**

In inositol-depleted conditions, intracellular phospholipid composition undergoes drastic remodeling. As inositol is a necessary substrate for PI synthesis, under inositol-depleted conditions the rate of PI synthesis are rapidly decreased which leads to an accumulation of its precursor, PA (BECKER AND LESTER 1977). The accumulation of PA then leads to the increase production of TAGs and SEs in lipid droplets, effectively storing excessive and potentially toxic lipids (GASPAR *et al.* 2011). Upon the re-introduction of inositol, the opposite effect occurs in that PA and TAGs are rapidly consumed in favor of PI synthesis (GASPAR *et al.* 2011). Cells unable

to synthesize or hydrolyze TAGs and SEs have severe growth defects under inositol-depleted conditions (GASPAR *et al.* 2011). Moreover, these mutants exhibit decreased growth rate upon re-introduction of inositol and an extended lag phase upon re-introduction to nutrient rich media suggesting that TAG and SE turnover pathways are important for stress response and cellular proliferation (PETSCHNIGG *et al.* 2009; GASPAR *et al.* 2011). Similar fluctuations of TAGs and PA have also found between cells in different growth phases. The levels of TAGs are increased when cells enter into stationary phase, and are rapidly decreased when cells re-enter logarithmic growth phase (reviewed in KOHLWEIN 2010). Additionally, TAG turnover appear to play an important role during cell cycle events (KURAT *et al.* 2009). In summary, the regulatory mechanism of lipid homeostasis under inositol-depleted conditions offers important insight on the regulation of lipid metabolism under stress and provides incentives for discovering additional mechanisms behind the regulation of lipid metabolism.

**Inositol biosynthesis**

Inositol is a metabolite required for the synthesis of all inositol-containing lipids including PI, phosphatidylinositides, inositol phosphates, and inositol-containing sphingolipids, but it can also be used as a key metabolic signalling molecule (reviewed in HENRY *et al.* 2014). Inositol can either be provied for by the residing media or, if needed, be synthesized *de novo* through the enzymatic conversion of glucose-6-phosphate to inositol in  through the cytoplasmic inositol-3-phosphate synthase, Ino1 (DONAHUE AND HENRY 1981). The Ino1 gene, *INO1,* is one of several genes whose expression is regulated by the availability of inositol/choline (HIRSCH AND HENRY 1986). Under inositol-depleted conditions, cells require *INO1* expression in order to survive (CULBERTSON AND HENRY 1975; DEAN-JOHNSON AND HENRY 1989). A genome wide screen has led to the identification of multiple mutants which confer growth defects under inositol-depleted conditions mainly due to their inability to derepress and transcriptionally activate *INO1* (VILLA-GARCIA *et al.* 2011).

**Transcriptional regulation of ICRE-containing genes**

The promoter region of *INO1* includes multiple copies of upstream repressing sequence called inositol/choline-responsive elements (ICRE) that contains a conserved repeat element ($UAS_{ICRE}$) found in different gene promoters of many phospholipid metabolic genes (**Table 1.1**) as well as other stress response pathways (LOPES *et al.* 1993; BACHHAWAT *et al.* 1995). The transcription factors required to activate transcription of ICRE-regulated genes are Ino2 and Ino4 (LOEWY AND HENRY 1984; HOSAKA *et al.* 1994). Ino2 and Ino4 form a heterodimer which contain basic helix-loop-helix domains that binds to the *INO1* promoter and other ICRE-containing genes (SCHULLER *et al.* 1992; AMBROZIAK AND HENRY 1994; SCHULLER *et al.* 1995; SCHWANK *et al.* 1995). Ino2 then recruits histone remodelers Ino80 and Snf2 as well as histone acetylases Esa1 and Gcn5 to the promoter region to acetylate histone tails and displace the surrounding nucleosomes (SUKA *et al.* 2001; ESPOSITO *et al.* 2010; KONARZEWSKA *et al.* 2012). Repression of the transcription of *INO1* and ICRE-regulated genes is mediated by Opi1 (GREENBERG *et al.* 1982; HIRSCH AND HENRY 1986; WHITE *et al.* 1991). Opi1 can directly bind to Ino2 as well as the co-repressors Sin3 and Ssn6 to recruit histone deacetylases and repress ICRE-regulated genes (WAGNER *et al.* 2001; JASCHKE *et al.* 2011; GRIGAT *et al.* 2012).

**Opi1-dependent regulation of ICRE-containing genes**

Intracellular inositol levels signal the cells to either switch ON or OFF the ICRE-regulated genes (reviewed in HENRY *et al.* 2014) (**Figure 1.3**). In nutrient rich conditions or inositol-supplemented conditions, PA and CDP-DAG levels are rapidly consumed in favor of PI synthesis leading to the translocation of the transcriptional repressor Opi1 from the ER to the nucleus where it represses the transcription of ICRE-containing genes (LOEWEN *et al.* 2003; LOEWEN *et al.* 2004) (**Figure 1.3A**). In inositol-depleted conditions, PI synthesis is substantially decreased leading to increased levels of PA (BECKER AND LESTER 1977). Opi1, which contains a

**Table 1.1 ICRE-regulated phospholipid biosynthesis genes and function**

| Gene name* | Description** |
|---|---|
| ***INO1*** | Inositol-3-phosphate synthase |
| ***CDS1*** | Phosphatidate cytidylyltransferase |
| ***CHO1*** | Phosphatidylserine synthase |
| ***PSD1*** | Phosphatidylserine decarboxylase |
| ***CHO2*** | Phosphatidylethanolamine methyltransferase |
| ***OPI3*** | Methylene-fatty-acyl-phospholipid synthase |
| ***EKI1*** | Ethanolamine kinase |
| ***EPT1*** | Ethanolamine phosphotranferase |
| ***CKI1*** | Choline kinase |
| ***CPT1*** | Choline phosphotransferase |
| ***SAH1*** | S-adenosyl-L-homocysteine hydrolase |
| ***SAM2*** | S-adenosylmethionine synthetase |
| ***PGS1*** | Phosphatidylglycerolphosphate synthase |
| ***PCT1*** | Cholinephosphate cytidylyltransferase |
| ***ITR1*** | Myo-inositol transporter |
| ***ITR2*** | Myo-inositol transporter |
| ***CTR1*** | Choline/ethanolamine transporter |
| ***FAS1*** | Beta subunit of fatty acid synthetase |
| ***FAS2*** | Alpha subunit of fatty acid synthetase |
| ***ACC1*** | Acetyl-CoA carboxylase |

* Gene list created using reviews (CARMAN AND HAN 2011; HENRY *et al.* 2014) as reference.
** Descriptions obtained from the Saccharomyces Genome Database (SGD) http://www.yeastgenome.org/

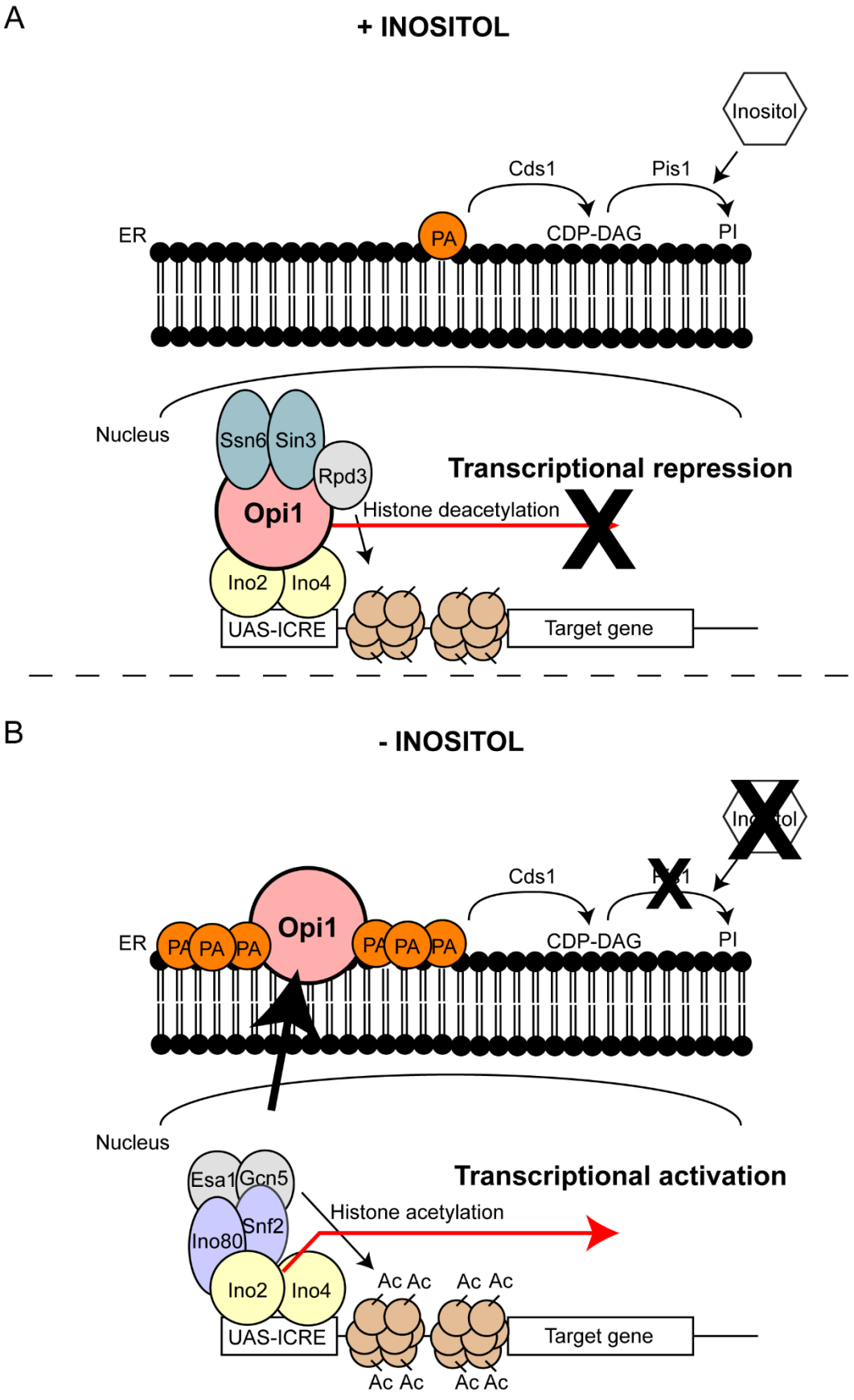
A
+ INOSITOL
Inositol
Cds1
Pis1
ER
PA
CDP-DAG
PI
Nucleus
Ssn6
Sin3
Rpd3
Transcriptional repression
Opi1
Histone deacetylation
Ino2
Ino4
UAS-ICRE
Target gene
B
- INOSITOL
Cds1
ER
PA
PA
PA
Opi1
PA
PA
PA
CDP-DAG
PI
Nucleus
Esa1
Gcn5
Transcriptional activation
Histone acetylation
Ino80
Snf2
Ino2
Ino4
Ac Ac
Ac Ac
UAS-ICRE
Target gene
Ac Ac
Ac Ac

**Figure 1.3 Current understanding of the mechanism regulating transcription of ICRE-containing genes.** Under inositol-supplemented conditions, Cds1 and Pis1 rapidly consume PA and CDP-DAG to make PI. The transcriptional repressor, Opi1, resides in the nucleus and binds to the transcription factor, Ino2. The heterodimer Ino2/Ino4 are bound to the $UAS_{ICRE}$ binding motif in front of ICRE-regulated target genes. Opi1 recruits the chromatin remodelers Sin3 and Ssn6 as well as the lysine deacetylase Rpd3 leading to the deacetylation of histones surrounding the promoter region of ICRE-regulated target genes. Altogether, this leads to *transcriptional repression* of ICRE-regulated target genes. **B)** Under inositol-depleted conditions, PI synthesis is inhibited, leading to the accumulation of PA at the ER. Opi1, which contains a PA-binding domain, shuttles from the nucleus to the ER, thus releasing the Ino2/Ino4 transcription factors. Ino2 subsequently recruits the chromatin remodelers, Ino80 and Snf2, as well as the lysine acetylases, Esa1 and Gcn5, to promote the acetylation and displacement of nucleosomes from the promoter region of the target genes. Altogether, this leads to *transcriptional activation* of ICRE-regulated target genes. Detailed explanation of Opi1-regulated transcriptional repression of ICRE-containing genes is reviewed in (HENRY *et al.* 2014).

PA-binding domain, will preferentially bind to PA localized at the ER, which then leads to the derepression and transcription of ICRE-regulated genes (LOEWEN *et al.* 2004) (**Figure 1.3B**). Mutants that overproduce and excrete excess inositol (Opi- phenotype) are characteristic of an *opi1Δ* mutant (GREENBERG *et al.* 1982).

### Lysine acetylation and Opi1-mediated transcription of phospholipid genes

High-throughput genomic screens have identified many other mutants that similarly derepress *INO1* transcription and causes an Opi- phenotype including multiple mutants of the NuA4 complex (*EAF1, EAF3, EAF5, EAF7, YAF9,* and *ESA1*) (HANCOCK *et al.* 2006; SALAS-SANTIAGO AND LOPES 2014). Despite evidence that NuA4 localizes to and acetylates the histones on the *INO1* promoter, NuA4 is not required for the transcriptional activation of *INO1* (SUKA *et al.* 2001; KONARZEWSKA *et al.* 2012) suggesting that the Opi- phenotype of NuA4 mutants is due to an uncharacterized role for NuA4 in the regulation of ICRE-containing genes as well as phospholipid homeostasis. NuA4 subunits are unique among Opi- mutants as they also negatively interact with a mutant of the phospholipid-remodelling protein Sec14, providing an opportunity to dissect the particular role of NuA4 in phospholipid metabolism. Alternatively, mutants of the SAGA KAT complex and the Set3 KDAC complex have both been found to exhibit an inositol auxotrophy phenotype (Ino-) providing evidence once again that additional KAT/KDACs might be involved in phospholipid homeostasis (VILLA-GARCIA *et al.* 2011). Despite increasing evidence of its participation in Opi1-regulated transcription of phospholipid metabolic genes, the role of lysine acetylation and NuA4 on this process has been sparingly studied.

## 1.4 Sec14: role and function within the Golgi vesicular trafficking pathway

### The conserved lipid-binding protein Sec14

Sec14, like Opi1, is another example of a lipid-binding protein that can regulate phospholipid metabolic pathways (**Figure 1.4A**). Sec14 was initially identified as one of 23 essential genes required for the yeast secretory pathway (NOVICK *et al.* 1980). The temperature

sensitive mutant, *sec14-G266N* (*sec14-1$^{ts}$*), is unable to survive at 37°C due to defects in Golgi-derived vesicular trafficking characterized by its inability to secrete invertase (BANKAITIS *et al.* 1989). Sec14 was subsequently identified as a lipid-transfer protein with capacity to transfer PI and PC between membranes *in-vitro* (AITKEN *et al.* 1990; BANKAITIS *et al.* 1990). The Golgi trafficking defects in *sec14-1$^{ts}$* are caused by the depletion of PI-4-P pools in the cells (HAMA *et al.* 1999) (**Figure 1.4B**). Furthermore, overexpression of the PI-4 kinase Pik1 can suppress both PI-4-P depletion and Golgi trafficking defects of *sec14-1$^{ts}$* suggesting that Sec14 has a role in positively regulating PI-4-P metabolism (HAMA *et al.* 1999). It was later demonstrated that Sec14 can physically stimulate the kinase activity of Pik1 *in-vitro* and that the PI-binding affinity, but not the PC-binding affinity, was required for this function (SCHAAF *et al.* 2008). Yet, specific inhibition of either PI or PC binding affinity by point mutation inhibits genetic complementation of a *sec14* background suggesting binding of both PI and PC are essential for its function (SCHAAF *et al.* 2008). The PC-bound form for Sec14 is necessary for accomplishing a secondary function which is the inhibition of the rate-limiting enzyme of the PC metabolic pathway, Pct1 (SKINNER *et al.* 1995). This model is further supported by evidence demonstrating that inhibition of Sec14 was shown to cause an increase of PC levels at the Golgi (MCGEE *et al.* 1994). Altogether, the data suggests that Sec14 coordinates the metabolism of PI-4-P with PC in order to sustain a lipid environment at the Golgi necessary for vesicular trafficking (summarized in GHOSH AND BANKAITIS 2011).

**The *sec14* bypass phenotype**

By manipulating either PI-4-P or PC metabolic, the lethal phenotype of a Sec14-deficient strain can be suppressed, which is often referred to as the “bypass” pathway. The first method of bypassing the Sec14 essential function is by deleting Cki1 or any other members of the CDP-choline pathway responsible for PC biosynthesis, which is called the *CKI1*-dependent *sec14* bypass (CLEVES *et al.* 1991) (**Figure 1.4C**). The CDP-choline pathway is one of the pathways

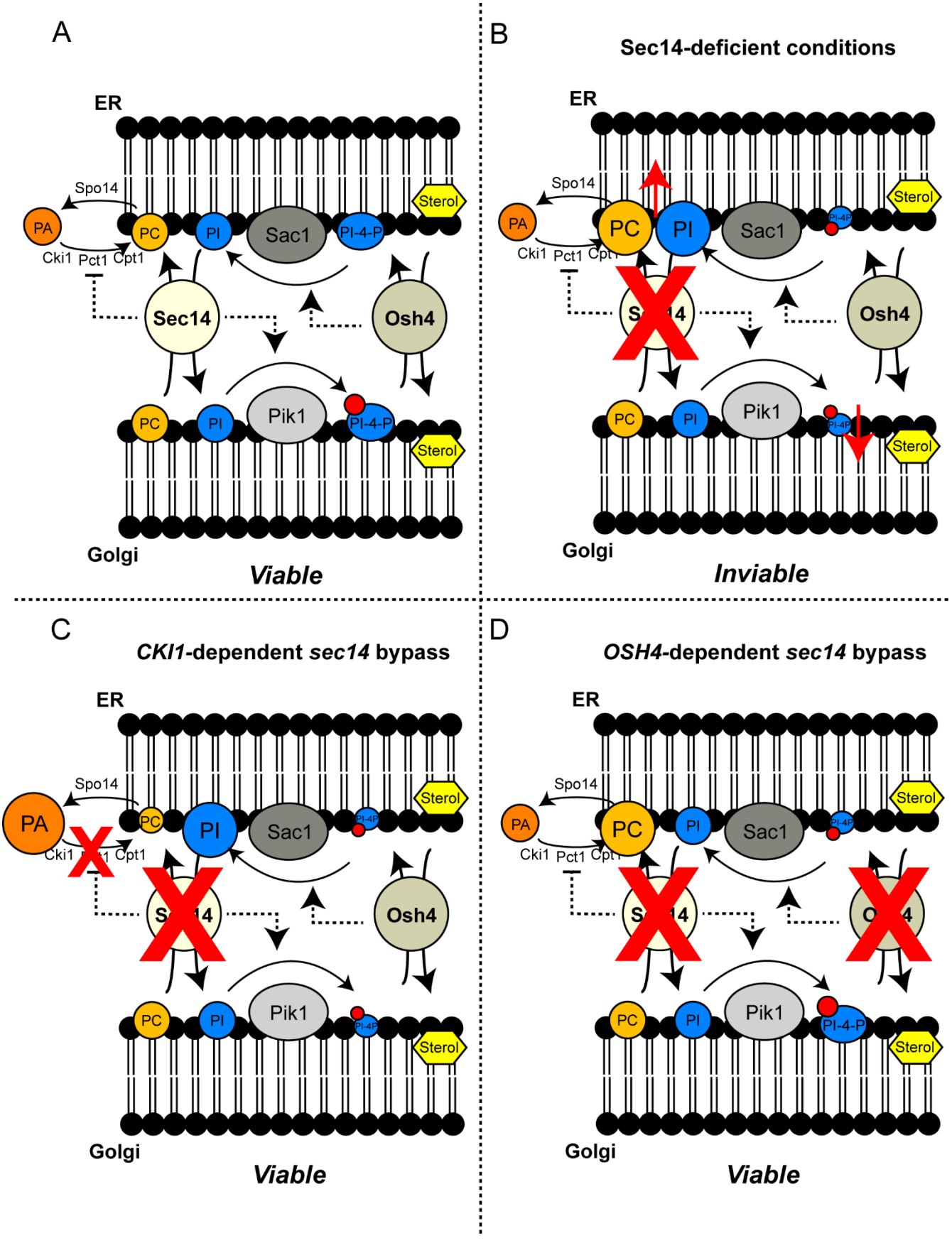
A
ER
Spo14
PA
PC
PI
Sac1
PI-4-P
Sterol
Cki1 Pct1 Cpt1
Sec14
Osh4
Pik1
Golgi
Viable
B
Sec14-deficient conditions
Inviable
C
CKI1-dependent sec14 bypass
Viable
D
OSH4-dependent sec14 bypass
Viable

**Figure 1.4 Current model for Sec14 and Osh4-mediated regulation of Golgi membrane phospholipid composition.A)** The PI/PC transfer protein Sec14 transports PI to the Golgi in exchange for PC and stimulates the PI-kinase Pik1 to produce PI-4-P. Subsequently, PC is transported back to the ER in exchange for another PI molecule and the cycle restarts. Sec14 also prevents further production of PC by inhibiting the activity of Pct1- the rate limiting enzyme of the CDP-choline pathway. Conversely, the PI-4-P/sterol transfer protein Osh4 antagonizes the function of Sec14 by transporting PI-4-P from the Golgi to the ER in exchange for a sterol molecule. PI-4-P is subsequently dephosphorylated by the PI-4-phosphatase Sac1 and the cycle restarts. **B)** In Sec14-deficient conditions, PI-4-P levels are depleted and PC levels are increased which prevents Golgi-derived vesicular trafficking and causes lethality. **C)** By deleting *CKI1* or any other genes with the CDP-choline pathway, cells can adapt to the loss of Sec14 by preventing PC biosynthesis. Inhibiting PC biosynthesis is sufficient to restore viability to Sec14-deficent cells. **D)** By deleting *OSH4*, cells can adapt to Sec14-deficient conditions by replenishing PI-4-P levels, thus restoring viability to Sec14-deficient cells. Detailed explanation of Sec14/Osh4-regulated Golgi phospholipid metabolism is reviewed in (GHOSH AND BANKAITIS 2011; TRIPATHI *et al.* 2014).

responsible for the synthesis of PC at the expense of PA (DOWD *et al.* 2001). The second method of bypassing the Sec14 essential function is by deleting the Oxysterol-Binding Protein homologue, Osh4/Kes1, which is called the *OSH4*-dependent *sec14* bypass (FANG *et al.* 1996) (**Figure 1.4D**). Osh4 directly antagonizes Sec14-stimulated Pik1 activity by promoting the depletion of Golgi-localized PI-4-P via activation of the PI-4-P phosphatase Sac1 (FANG *et al.* 1996; LI *et al.* 2002; FAIRN *et al.* 2007; STEFAN *et al.* 2011).

Although *OSH4*-dependent and *CKI1*-dependent *sec14* bypass pathways have distinct features, both bypass pathways converge towards the activity of the phospholipid D (PLD) enzyme Spo14. Spo14 is a P-4,5-$P_2$ activated PLD enzyme that contributes to *sec14* bypass by catalyzing the hydrolysis of PC to PA, a function required for both *OSH4*-dependent and *CKI1*-dependent *sec14* bypass (ROSE *et al.* 1995; PATTON-VOGT *et al.* 1997; SREENIVAS *et al.* 1998; XIE *et al.* 1998; FAIRN *et al.* 2007). In recent models, it was suggested that Spo14 regulates Golgi-trafficking in the absence of Sec14 by regulating trafficking effectors (MENDONSA AND ENGEBRECHT 2009). In *sec14* conditions, Spo14 activity is increased leading to increased turnover and hydrolysis of PC (SREENIVAS *et al.* 1998). This increase in activity is dependent on Sec14-homologues, called Sfh proteins, which stimulates PI-4-P synthesis through the alternative PI-4 kinase Stt4 and provides the necessary precursor for Mss4-catalyzed PI-4.5-$P_2$ synthesis (YOSHIDA *et al.* 1994b; LI *et al.* 2000; RUDGE *et al.* 2004). Moreover, overexpression of Sec14 homologues, including Sfh2, suppresses the lethality of a *sec14* background in a Spo14-dependent manner (LI *et al.* 2000).

**Lysine acetylation and Sec14-mediated phospholipid metabolism**

Sec14-deficient mutants also exhibit growth defects under inositol-depleted conditions (PATTON-VOGT *et al.* 1997), which in contrast to the Opi- phenotype, is associated with an inability to derepress *INO1* expression leading to decreased inositol biosynthesis under conditions lacking an exogenous source of inositol (CULBERTSON AND HENRY 1975; VILLA-

GARCIA *et al.* 2011). Synthetic genetic screens identified *eaf7*Δ, a subunit of NuA4, as one of several mutants which displays a growth defect in combination with the temperature sensitive mutant, *sec14-1*$^{ts}$ (CURWIN *et al.* 2009). A separate high-throughput synthetic dosage lethal screen found that overexpression of *OSH4*, a gene whose function directly antagonizes Sec14 by depleting phosphatidylinositol 4-phosphate (PI-4-P), (FANG *et al.* 1996; LEBLANC AND MCMASTER 2010; ALFARO *et al.* 2011) resulted in decreased viability in the NuA4 mutants *eaf5Δ*, *eaf7Δ* and lethality in *yng2Δ*, providing evidence that NuA4 mutants are sensitive to conditions where PI-4-P levels are limited. In a third synthetic dosage lethal screen, the KDAC mutant, *rpd3Δ*, was found to be sensitive to *OSH4* overexpression providing evidence that other KAT/KDAC enzymes might be involved in Sec14/ PI-4-P metabolism. Yet, much like the case for Opi1-mediated phospholipid homeostasis, the role for lysine acetylation within the Sec14 and PI-4-P metabolic pathway remains unresolved.

## 1.5 Oxysterol-Binding Proteins

### Lipid-binding affinity of Oxysterol-Binding Proteins

Oxysterol-Binding Proteins (OSBPs) are a conserved class of lipid-binding proteins found in yeast and humans. In mammalian cells, there are 12 genes encoding for 16 different OSBPs, deemed OSBP-related proteins (ORPs) while in *S. cerevisiae,* there are seven genes encoding for seven OSBP-homologues called Osh proteins (BEH *et al.* 2001; LEHTO *et al.* 2001). The proteins were originally identified as OSBPs (KANDUTSCH *et al.* 1984; TAYLOR *et al.* 1984); however, OSBPs have since been demonstrated to bind a variety of lipid-ligands including sterols, PS, PI-4,5-$P_2$, and, more importantly, PI-4-P (LI *et al.* 2002; IM *et al.* 2005; DE SAINT-JEAN *et al.* 2011; MAEDA *et al.* 2013). The crystal structure of the conserved domain of OSBPs reveals a β-barrel enclosed with a lid, allowing the protein to extract and sequester lipids from membranes *in-vitro* (IM *et al.* 2005). Selectively mutating the residues involved in lipid-binding severely affects functionality both *in-vivo* and *in-vitro* implying that OSBPs lipid-binding affinities

are at the core of their functions (IM *et al.* 2005; RAYCHAUDHURI *et al.* 2006; DE SAINT-JEAN *et al.* 2011). However, it is currently unknown if or how OSBPs lipid-binding affinities are regulated. Its affinity for PI-4-P is particularly interesting because, unlike with the other lipid-ligands, the residue involved in PI-4-P binding are conserved throughout the entire family of proteins and several OSBPs have been found to be able to bind to PI-4-P including Osh3, Osh4, and Osh6 in yeast and OSBP, ORP4, ORP5, ORP8, and ORP9 in mammals (reviewed in TONG *et al.* 2016). This suggests that PI-4-P binding is the principal lipid-ligand for all OSBPs.

**Osh proteins regulate PI-4-P metabolism**

In yeast, deletion of the seven Osh proteins is lethal; but, the expression of any one Osh proteins, at correct dosage, is sufficient for the cells to survive (BEH *et al.* 2001). Cells lacking expression of all seven Osh proteins show a significant increase in PI-4-P levels comparable to the effect of deleting the PI-4-P phosphatase Sac1 (STEFAN *et al.* 2011). Furthermore, overexpression of *OSH4* causes a significant decrease in PI-4-P levels and impairs growth dependently on Sac1 expression (LEBLANC AND MCMASTER 2010; ALFARO *et al.* 2011). Finally, Osh proteins have been found to directly stimulated the activity of Sac1 *in-vitro* (STEFAN *et al.* 2011). Therefore, the main function of OSBP has been hypothesized to be the regulation of PI-4-P metabolism through the stimulation of Sac1. To date, the mechanism behind the stimulation of Sac1 is at least partially resolved. The PI-4-P-binding affinity of Osh4 ability is required for Sac1 stimulation (STEFAN *et al.* 2011). Additionally, stimulation of Sac1 activity *in-vivo* is dependent on proper localization of a subfraction of Osh4 to Golgi/endosomes through its PIP-binding domain (LI *et al.* 2002; MOUSLEY *et al.* 2012). Current model for Osh4 suggests that the protein carries PI-4-P from the Golgi to the ER in a cyclical fashion (DE SAINT-JEAN *et al.* 2011) (**Figure 1.4**). Furthermore, this exchange coupled with the stimulation of Sac1 activity would ensure a definite direction for the exchange between PI-4-P and sterols (STEFAN *et al.* 2011). A similar model has been proposed for the function of the mammalian OSBP

protein suggesting a conserved role for all ORPs in the regulation of PI-4-P metabolism through intermembrane trafficking (OLKKONEN 2015). However, it should be noted that Oxysterol-Binding Proteins do not share all the same function. For example, the previously mentioned *OSH4*-dependent *sec14* bypass is a unique feature of Osh4 that does not extend to any other Osh proteins (FANG *et al.* 1996; BEH *et al.* 2001).

**Lysine acetylation and Osh proteins**

Several high-throughput acetylome studies have uncovered acetylation sites on Osh4 (HENRIKSEN *et al.* 2012; DOWNEY *et al.* 2015; MADSEN *et al.* 2015). One of the sites identified in these studies, lysine K109, is directly implicated in the PI-4-P binding affinity of the protein (DE SAINT-JEAN *et al.* 2011) suggesting that lysine acetylation could potentially regulate the lipid-binding affinity and the function of Osh4. Although other Osh proteins have not been identified in any of these screens, the highly conserved nature of these proteins and their PTMs suggests that lysine acetylation could potentially regulate more OSBPs. Altogether, this suggests another possibility for how lysine acetylation could contribute to phospholipid metabolism.

## 1.6 Hypothesis

Based on the presented evidence, we hypothesize that lysine acetylation is regulating Sec14/Osh4 mediated phospholipid metabolism and maintenance. To investigate this claim, we pursed two different aims in pursuit of the numerous targets and pathways likely affected by lysine acetylation:

**Aim #1:** Study the effect of lysine acetyltransferases and lysine deacetylases on PI-4-P and phospholipid metabolic pathways

**Aim #2:** Study the effect of lysine acetylation on the function of Osh4 and other Oxysterol-Binding Proteins

# 2 Materials and Methods

## Yeast strains, plasmids, and media

The yeast strains and the plasmids used in this study are listed in **Table S1** and **Table S2**, respectively. Strains were generated either by standard mating methods or a PCR-mediated gene insertion/deletion technique for mutants with defective mating (LONGTINE *et al.* 1998). In each case, multiple colonies for each generated strains were confirmed by PCR. Strains from the Deletion Mutant Array (DMA) collection (GE, CAT# YSC1053) and the GFP collection (Thermo, CAT#95702) were confirmed by PCR. Plasmids generated for this study were created using Seamless Ligation Cloning Extract (SLICE) method (ZHANG *et al.* 2014). Tetracycline/doxycycline inducible promoter (ptet) was a gift from M. Kaern lab (RONEY *et al.* 2016). Strains and plasmids from other sources are as indicated. All yeast cells were grown in standard nutrient rich media, YPD, for most experiments, or synthetic media (synthetic drop-out (SD) or synthetic complete (SC)) for selecting markers or for inositol-depletion experiment. For media plates, a final concentration of 20 g/L of agar (BioShop®, CAT#AGR001.1) was added to the liquid media before autoclaving. SC-inositol media was made using 6.7 g/L of YNB with ammonium sulfate, without inositol (Millipore, CAT#4027-412) and 2 g/L of standard amino acid complete mix. The most common source of inositol, myo-inositol (Sigma, CAT#I5125), was used for inositol repleted conditions doxycycline at a final concentration of 75 µM. Doxycycline (Sigma, CAT#D3447), cerulenin (Sigma, CAT#C2389) or $dH_2O$ was added to media after autoclaving to the concentration desired.

## Spot assays

Cultures were grown in YPD or SD media, as indicated, at 30°C prior to being diluted to an $OD_{600}$ of 0.1 and 4 times 10-fold serial dilutions ($OD_{600}$= 0.1, 0.01, 0.001, and 0.0001) were spotted on selected plates and incubated for two to three days at the indicated temperatures. Images of spot assays were taken with the Bio-Rad Chemidoc™ XRS system under EPI-white light illumination and auto-exposure setting.

**Protein lysate**

Yeast strains were pre-inoculated overnight in liquid media (YPD or SD media) at 25°C. After which, samples were re-inoculated at $OD_{600}$=0.1 in liquid media (YPD or SD media) and grown at 30°C until mid-log growth phase ($OD_{600}$=0.5-0.6), then harvested by centrifugation, washed in water, aliquoted in 1.5 mL microcentrifuge tubes and flash frozen in liquid nitrogen. Cell pellets were re-suspended in lysis buffer (0.1 M sodium phosphate buffer pH=7.0, 100 mM NaCl (Sigma, CAT#S7653-5KG), 2 mM EDTA (EMD, CAT#4050-1KG), 10 mM sodium butyrate (Sigma, CAT#B5887-5G), 2 mM DTT (Sigma, CAT#D9779-10G) , 0.6 mM PMSF (Sigma, CAT#78830-5G), 1 mM sodium orthovanadate (Sigma, CAT#S6508-50G), 1% w/v NP-40 (Roche, CAT#11754599001), protease inhibitor cocktail tablet (Roche, CAT# 4693159001)) and lysed mechanically by vortex with glass beads. Cell debris and glass beads were removed by centrifugation. Whole cell extract (WCE) was diluted in Laemmli loading dye and stored at -80°C.

**Immunoprecipitation**

Ten to fifteen milligrams of whole cell extract (WCE) were added to pre-washed GFP-Trap®_M magnetic beads (Chromotek, gta-20 CAT# ACT-CM-GFA0050) and incubated at -4°C for 1h on an end-to-end rotator. The magnetic beads were collected with a magnet, washed 5 times in lysis buffer and re-suspended in 1X Laemmli loading dye (40mM Tris pH=6.8 (Wisent, CAT#600-125-IK), 2% w/v SDS (Wisent, CAT#800-100-cl), 0.02% w/v Bromophenol Blue (Sigma, CAT#B5525-5G), 10% v/v glycerol (Fisher, CAT#G33-4)). Immunoprecipitated (IP) samples were eluted from beads (65°C, 15 min) and 2-mercaptoethanol (Sigma, CAT#M3148-25ML) was added to a final concentration of 100 mM, to reduce disulfide bonds, before storage at -80°C.

**Detection of lysine acetylation by mass spectrometry**

Mass spectrometry service was provided by Dr. Daniel Figeys lab (UOttawa) and Dr. Anne-Claude Gingras lab (UToronto). IP samples were separated by SDS-PAGE, and resulting gel was stained using a coomassie-based protocol (MERRIL 1990). Protein band was cut out and dried in 1.5 mL microcentrifuge tubes before being sent to respective labs. Resulting samples were analyzed by LC-MS/MS and acetylation sites were identified using a Mascot search engine, as previously described (Mitchell et al., 2013).

**Immunoblotting**

The prepared samples (IP and/or WCE) were boiled at 95°C for 10min prior to separation by SDS-PAGE on a linear SDS-polyacrylamide gel (7%-9%). Western blotting was performed using a semi-dry transfer apparatus from Bio-Rad (Trans-Blot SD Semi Dry Electrophoretic Transfer Cell; CAT#170-3940). Protein transfer was performed for 1 hour using constant milliamps (mA) based on the following calculation: 0.8mA x area of gel x # of gels. Acetylation was detected by using 1/500 dilution of mouse α-acetyl lysine IgG (α-AcK) (Cell Signaling, CAT#9681). Other primary antibodies used were: rabbit α-G6PDH IgG (1/10000 dilution) (Sigma, CAT#A9521) as a loading standard, mouse α-GFP IgG (1/5000 dilution)(Roche, CAT#11814460001), rabbit α-GST IgG (1/10000 dilution)(Invitrogen, CAT#A5800) and rabbit α-Osh4 IgG (1/10000 dilution)(gift from C. Beh lab). Secondary antibodies used were peroxidase-conjugated goat α-rabbit IgG (1/10000) (Chemicon; CAT#AP307P), and peroxidase-conjugated goat α-mouse IgG (1/5000) (Bio-Rad; CAT#170-6516), where appropriate. Blocking and primary incubations were performed with 5% milk (w/v) in TBS-T (0.1% Tween20 (v/v); VWR, CAT#CA95017-122L), except the Cell Signaling anti-

acetyl lysine antibody which was performed in 5% BSA (w/v) in TBS-T (0.1% Tween20 (v/v); VWR, CAT#CA95017-122L). Secondary incubations were all done with 5% milk (w/v) in TBS-T (0.1% Tween20 (v/v); VWR, CAT#CA95017-122L). Primary incubations were carried out overnight at 4°C and secondary incubations at room temperature for 1 hour. Chemiluminescence was detected using Immobilon Western Chemiluminescent HRP substrate (Millipore; CAT#WBKLS0500) and developed on a ChemiDoc XRS system (Bio-Rad; CAT#170-8070).

**Osh4 quantitative immunoblotting**

The prepared samples (WCE) were boiled at 95°C for 10min prior to separation by SDS-PAGE using the TGX Stain-Free™ FastCast™ Acrylamide Kit (7.5%) (BioRad, CAT#1610181). Strain-Free gels were activated in gel under ultraviolet light for 1 min using the Bio-Rad imaging tool. After which, immunoblotting was performed using a semi-dry transfer apparatus from Bio-Rad (Trans-Blot Turbo™ Transfer System, CAT#1704155). Protein transfer was performed for 7 min at constant voltage (25 V) on nitrocellulose membranes. After transfer, membranes were exposed under ultraviolet light to measure total protein content per lane using the Bio-Rad imaging software which was subsequently used to normalize immunoblots. Then, membranes were blocked for 30 min with 5% w/v milk in TBS-T (0.1% Tween; VWR, CAT#CA95017-122L) Primary antibodies used was rabbit α-Osh4 IgG (1/10000 dilution) (gift from C. Beh lab). Secondary antibody used was peroxidase-conjugated goat α-rabbit IgG (1/10000 dilution) (Chemicon, CAT#AP307P). Primary incubations were carried out overnight at 4°C and secondary incubations at room temperature for 1 hour. Chemiluminescence was detected using Immobilon Western Chemiluminescent HRP substrate (Millipore, CAT#WBKLS0500) and developed on a ChemiDoc XRS system (Bio-Rad, CAT#170-8070). Quantification of images were performed on the Bio-Rad Image Lab™ software using total protein content per lane to normalize Osh4 signal following protocol defined by Bio-Rad (TAYLOR AND POSCH 2014).

**RNA-seq**

The strains *sec14-1$^{ts}$* (CMY505) and *sec14-1$^{ts}$eaf1Δ* (YKB3935) were grown in triplicate in 50 mL of YPD at 30°C to mid-log phase ($OD_{600}$=0.5), then shifted to pre-warmed YPD media at 33.5°C for two hours before harvesting, washing with $dH_2O$, and flash-freezing on dry ice. Cells were subsequently lysed by resuspending pellets in 100 µL of lyticase reaction solution (1.2 M sorbitol, Sigma CAT# S1876; 1 mg/mL lyticase Sigma, CAT #SRE0018) and incubated at 30°C for 30 min. RNA was purified using the RNA mini-kit (Ambion, CAT#12183018A) following the yeast extraction protocol as suggested by the manufacturers. Purified RNA extracts were then twice treated with DNaseI (Promega, CAT#M6101) for 1h at 37°C each time followed by a phenol/choloroform extraction. After two DNaseI treatments, purified RNA was resuspended in 30 µL of RNase-free water. Three micrograms of purified RNA spiked with 1.5 µg of ERCC RNA control (Ambion, CAT#4456740) was depleted of ribosomal RNA (rRNA) using the Ribo-Zero Gold rRNA depletion kit for yeast (Illumina, CAT#MRZY1306) and resuspended in 10 µL of RNase-free water. Successful depletion of the 18S and 26S ribosomal RNA was confirmed using the Agilent Bioanalyzer RNA 6000 Pico quantification kit (Agilent Technologies, CAT#5067-1513).

Whole transcriptome RNA-seq libraries were prepared using the Ion Total RNA-Seq Kit V2 (Life Technologies, CAT#4479789) and the Ion-Xpress RNA-seq Barcode 1-16 kit (Life Technologies, CAT#4475485) according to the manufacturer's recommendations using 50 ng of input rRNA depleted total RNA. The size distribution and yield of the final barcoded RNA-seq libraries was assessed using the Agilent Bioanalyzer High Sensitivity DNA quantification kit (Agilent Technologies, CAT#5067-4626). All six RNA-seq libraries were multiplexed and sequenced on the Life Technologies Ion Torrent Proton platform using a single Ion Proton Chip.

Resulting reads were aligned against the *Saccharomyces cerevisiae* S288c genome (version GCF_000146045.2_R64) using the TMAP aligner provided with the Torrent Suite

(v5.0.4). Raw sequencing reads have been deposited at the NCBI SRA archive under accession number PRJNA350552. Variation in sample processing during rRNA depletions and library construction was assessed using the ERCC analysis plugin (v5.0.0.0). The number of reads aligning to each annotated transcript was determined using bedtools (v2.17.0) (QUINLAN AND HALL 2010). Differential expression of transcripts between *sec14-1*$^{ts}$ and *sec14-1*$^{ts}$*eaf1Δ* was determined using DESeq2 (v1.10.1) (LOVE *et al.* 2014). Transcripts with a fold change ≥2 and an adjusted *p* value ≤0.05 were considered to be differentially expressed. GO-term analysis of enriched biological processes was conducted by using the DAVID bioinformatic online database (https://david.ncifcrf.gov) (HUANG DA *et al.* 2009). Significantly downregulated or upregulated genes were clustered into functionally related groups using the Gene Functional Classification Tool. The highest ranking Biological Process term (BP-term) was subsequently assigned for each group.

**qRT-PCR**

RNA extracts were prepared as above but without rRNA depletion. Two micrograms of purified RNA was reverse transcribed using the High Capacity cDNA Reverse Transcriptase Kit (Applied Biosciences, CAT#4368814) and resulting cDNA was diluted 1/10 for qRT-PCR. Transcript levels were measured using the SsoFast™ EvaGreen® Supermix for qPCR (Bio-Rad, CAT#172-5201) with the Bio-Rad MiniOpticon Real-Time PCR system and CFX manager software. Primers used for qRT-PCR are as listed: 1) *INO1* Forw.: 5'-TCTCTGTTGCCCATGGTTAG-3' Rev: 5'-CTTCAAGCGTTGTTGCAG-AT-3'; 2) *FAS1* Forw: 5'-TGAAGGTGTTCCATCTCCAA-3' Rev: 5'-CGACTAGATTCTT-CGCACCA-3'; *FAS2* Forw: 5'-GCCAGAACAAGATGG-GAAAT-3' Rev*:* 5'-TGTATG-GACGACCCTTCAAA-3'; *CDS1* Forw: 5'-GCCATGGTGGT-ATCACAGAC-3' Rev: 5'-TCTGCTTGTCGTTCAGGTTC-3'; *YEH1* Forw: 5'-TTCTCAG-GGCACTACACAGG-3' Rev: 5'-AAGGGACCAGGATACACTGC-3'; *BCP1* Forw: 5'-

TGATTAATATGCCACCG-GAA-3' Rev: 5'-ATGTTTGTCATCGCCAAGTG-3'; *TDH3* Forw: 5'-CTGTCAAGTTGAACAAGGAAACCAC-3' Rev: 5'-CAACGTGTTCAACCAAGT-CGACAA-3'; *ACT1* Forw:5'-GCCTTCTACGTTTCCATCCA-3' Rev: 5'-CGTAAATTGGA-ACGACGTGA-3'. A standard curve was constructed using a five times five-fold serial dilution series of pooled cDNA sample from the original individual RT reactions starting at a 1/5 dilution. *TDH3* and *ACT1* were used as the internal reference genes for normalization of relative expression levels (PFAFFL 2001) using the BioRad CFX Manager™ software. Three biological and two technical replicates were used for each sample. Statistical analyses were completed using a two-tailed unpaired t-test ($p \leq 0.05$) with the GraphPad Prism software.

**Lipid droplet**

Cultures were grown in SC media at 30°C to mid-log growth phase ($OD_{600}$=0.5), washed in $dH_2O$, and transferred to SC-inositol media supplemented with and without 75 µM of myo-inositol and grown for 2 hours at 30°C. Cells were subsequently incubated with 10µM BODIPY® 493/503 (LifeTechnologies, CAT#D3922) for 10min at room temperature in their residing media and washed with $dH_2O$. Cells were pelleted, re-suspended in SC media, and loaded onto prewashed microscope slide with coverslips. Images were taken using the CellVoyager™ CV1000 disk confocal microscope (Yokogawa Electric Corporation, Musashino Tokyo, Japan). Brightfield (20% intensity,100 ms exposure time, 100% gain) and BODIPY fluorescence, using FITC filters (25% intensity, 50 ms exposure time, 20% gain) were taken across multiple fields of view to capture at least 100 cells on the 100X oil-immersion objective. Images for each field of view were taken at 0.2 µm steps for a total of 30 images. Image analysis was done using a custom MATLAB script. Bright field images were first thresholded using an adaptive thresholding algorithm. The resulting thresholded images were segmented using our MATLAB script that incorporated previously published code (RICICOVA *et al.* 2013), as well as our own code which makes use of functions found in the MATLAB Image Processing Toolbox. The cell

outlines obtained through segmentation were used to quantify the area (in pixels) and total fluorescence from the fluorescence images. Fluorescence was quantified using the middle z-stack for each cell. Fluorescence density was calculated by dividing total fluorescence by area. A total of three biological replicates with over 100 cells were analysed for each sample. Statistical analyses were performed by one-way ANOVA with the Tukey's multiple comparisons test using the GraphPad Prism software.

**Osh4 and Osh1 point mutant generation**

Sets of two primers were designed to generate either acetylated lysine mimic (lysine (K) to glutamine (Q)) or unacetylated mimic (lysine (K) to arginine (R)) on specified residue. Each primer set was designed using the QuickChange® Primer Design program available on the Agilent website (http://www.genomics.agilent.com/primerDesignProgram.jsp) by substituting a single amino acid. For K to Q mutants, specified lysine codon, AAA or AAG, was changed to glutamine codon CAA or CAG, respectively. For K to R mutants, specified lysine codon, AAA or AAG, was changed to arginine codon AGA or AGG, respectively. All the primer designed are as followed: A) Osh4 K109Q**:** Forw: 5'-ATGAATCCTTAGGTTCTGAGAAACA-ACCTTTGAACCCATTTCTAG-3' Rev: 5'-CTAGAAATGGGTTCAAAGGTTGTTTCTCAGAA-CCTAAGGATTCAT-3'; K109R: Forw: 5'-AATGAATCCTTAGGTTCTGAGAAAAGACCTTTGAA-CCCATTTCTAG-3' Rev: 5'-CTAGAAATGGGTTCAAAGGTCTTTTCTCAGAACCTAAGGAT-TCATT-3'; K168Q: Forw: 5'-AAGCTGCAAGGCTACAACCAAATTCAAGCCAGTTTCAC-3' Rev: 5'-GTGAAACTGGCTTGAATTTGGTTGTAGCCTTGCAGCTT-3'; K168R: Forw: 5'-GCTGCA-AGGCTACAACCAAATTAGAGCCAGTTTCAC-3' Rev: 5'-GTGAAACTGGCTCTAATTTGG-TTGTAGCCTTGCAGC-3'; K247Q: Forw: 5'-TACTTTTCTGGTAAAAAGAATTCATTCCAGG-CAAGAATTTACAAAGACTC-3' Rev: 5'-GAGTCTTTGTAAATTCTTGCCTGGAATGAATTCT-TTTTACCAGAAAAGTA-3'; K247R: Forw: 5'-GGCTACTTTTCTGGTAAAAAGAATTCATTCA-GGGCAAGAATTTACAAA-3' Rev: 5'-TTTGTAAATTCTTGCCCTGAATGAATTCTTTTTACCA-

GAAAAGTAGCC-3' B) Osh1 K874Q: Forw: 5'-GTAAGGGGTTGAATGGTTGAGACACTCTG-TTAGTGGT-3' Rev: 5'- ACCACTAACAGAGTGTCTCAACCATTCAACCCCTTAC-3'; K874R: Forw: 5'- TAAGGGGTTGAATGGTCTAGACACTCTGTTAGTGGTAG-3' Rev: 5'-CTACCACT-AACAGAGTGTCTAGACCATTCAACCCCTTA-3'. Mutagenesis of plasmids encoding Osh4 or Osh1 was performed using QuickChange® Lightning Site-Directed Mutagenesis kit (Agilent; CAT#210519) following the manufacturer's instruction. Briefly, complete 50 µL PCR reaction mix with 100 ng of plasmid and 125 ng of each primer were mixed together in PCR reaction tubes. Reaction tubes were subjected to the following PCR cycling parameter: Step 1) 95°C for 2min; Step 2) 95°C for 20 sec; Step 3) 60°C for 10 sec; Step 4) 68° for 30 sec/kb of plasmid length; Step 5) Repeat Step 2-4 18 times; Step 6) 68°C for 5 min. After PCR cycling, each reaction was treated with 2 µL of DpnI enzyme provided in the kit for 5 min at 37°C. Finally, 2 µL of each reaction were transformed in competent DH5α cells and plated on LB +ampicillin media and incubated at 37°C for 16 hours. Positive colonies were grown overnight in LB +ampicillin at 37°C and mutated plasmids were recovered using plasmid Miniprep kit (Bio-Basic, CAT#BS614-250Preps). Mutated plasmids were confirmed by sequencing using the TCAG DNA Sequencing facility in Toronto (http://www.tcag.ca/facilities/dnaSequencingSynthesis.html).

**Osh4-GFP and Osh1-GFP localization**

Cultures were grown in selective media at 30°C to mid-log phase ($OD_{600}$= 0.5), re-suspended in SC media and spread on microscope slides with cover glass. Microscopy was performed using a Leica DMI 6000 fluorescent microscope (Leica Microsystems GmbH, Wetzler Germany), equipped with a Sutter DG4 light source (Sutter Instruments, California, USA), Ludl emission filter wheel with Chroma band pass emission filters (Ludl Electronic Products Ltd., NY, USA) and Hamamatsu Orca AG camera (Hamamatsu Photonics, Herrsching am Ammersee, Germany). Brightfield (0.07 sec exposure time, 100% gain) and GFP fluorescence, using the FITC filters (1 sec exposure time, 100% gain) were taken across multiple fields of view to

capture at least 80 cells on the 63X oil-immersion objective. Images for each field of view were taken at 0.2 µm steps for a total of 30 images using the Velocity 4.3.2 Build 23 (Perkin Elmer). Quantification of Osh4 localization was done manually by inspecting the presence of at least one distinct foci within the cell across 80 cells from three biological replicates. Statistical analysis was performed by one-way ANOVA with Tukey's multiple comparisons test using the GraphPad Prism software.

**Recombinant Osh4 protein purification for *in-vitro* assay**

Plasmid encoding wildtype (PKB261), K109Q (PKB262), and K109R (PKB263) GST-tagged Osh4 recombinant protein as well as the GST empty vector (PKB292) were transformed in BL21 competent cells. Cultures for each strain were grown overnight in 1L of LB media + 25 µg/mL chloramphenicol (Sigma, CAT# C0378-5G), 100 µg/mL ampicillin (Wisent, 400-110-XG), and 1 mM IPTG (Sigma, CAT# I6758-1G). Cells were pelleted by centrifugation (5 min, 3000 rpm) and 2-5ml of lysis buffer (125 mM Tris-HCl pH 7.5 (Wisent, CAT#600-125-IK), 150 mM NaCl (Sigma, CAT#S7653-5KG), protease inhibitor cocktail tablet (Roche, CAT# 4693159001), 1 mg/mL lysozyme (Sigma; CAT# 62970-1G-F)) were added per mg of wet weight. Samples were subsequently incubated for 30 min on ice. After which, samples were sonicated for 30 sec at power level 5 followed by DNaseI I treatment (5µg/ml) (Promega, CAT#M6101). Then, lysates were centrifuged for 30 min at 12500 rpm. Resin bead for purification (Sigma, CAT# M8032-100G) were prepared by washing resin in empty column with lysis buffer, and centrifuging at 500g for 5 min to sediment resin. Resin beads were diluted as 50 % slurry by adding 200 µl of lysis buffer if 200 µl of resin was initially prepared. Protein lysates were added to resin on column and incubated at room temperature for 30 min to ensure binding. Resin beads were washed by adding 5x volume of bed volume of lysis buffer. Afterwards, proteins were eluted by adding elution buffer (50 mM Tris-HCl, pH 8.0 (Wisent, CAT#600-125-IK); 10mM reduced glutathione (Sigma, CAT# G4251 L)) and incubated at room temperature for 10 min

followed by elution through the column into 1.5 mL microcentrifuge tubes. Finally, purified protein concentration was measured by spectrophotometry and final concentration was adjusted to 1 mg/mL of protein in 50% glycerol stock. Protein expression was confirmed by staining SDS-PAGE gels using a coomassie-based protocol (MERRIL 1990).

**Lipid-binding assay**

PI (Avanti Polar Lipids, CAT# 840042P) and PI-4-P (Avanti Polar Lipids, CAT#840045P) in chloroform/methanol stock (2:1) were serially diluted in chloroform at indicated amounts. Dilutions were spotted on pre-washed (chloroform washed) nitrocellulose membrane and dried at room temperature. Purified GST, GST-Osh4, GST-osh4-K109Q, and GST-osh4-K109R GST (4 µg/mL) in PBS were incubated with blocked membranes overnight. Thereafter, membranes were washed 3 times with PBS and immunoblotted using primary α-Osh4 IgG (1/10000 dilution) (gift from C. Beh lab) and secondary peroxidase-conjugated goat α-rabbit IgG (1/10000 dilution) (Chemicon, CAT#AP307P). Chemiluminescence was detected using Immobilon Western Chemiluminescent HRP substrate (Millipore; CAT#WBKLS0500) and developed on a ChemiDoc XRS system (Bio-Rad; CAT#170-8070).

***In-vitro* Sac1 assay**

Protocol was largely derived from previously established method (STEFAN *et al.* 2011). Catalytic domain of Sac1 ($Sac1^{1-522}$) (PKB266) was purified from BL21 cells, similarly to Osh4 protein but with some differences. Lysis buffer used was slightly different (50 mM Tris-HCl pH 8.0 (Wisent, CAT#600-125-IK), 300 mM NaCl (Sigma, CAT#S7653-5KG), 10mM imidazole (Sigma, CAT#I2399-100G), 1 mg/mL lysozyme (Sigma; CAT# 62970-1G-F). For the washing steps, 5mM of 2-mercaptoethanol (Sigma, CAT#M3148-25ML), was added to the lysis buffer. Elution buffer used was lysis buffer + 250mM of imidazole (Sigma, CAT#I2399-100G). After elution, purified $Sac1^{1-522}$ was dialyzed in dialysis buffer (50mM Tris-HCl, pH6.8 (Wisent, CAT#600-125-IK), 150mM NaCl (Sigma, CAT#S7653-5KG), 2mM DTT (Sigma, CAT#D9779-

10G)). Simarly, Osh4 protein samples were dialyzed in dialysis buffer. Concentration was measured by spectrophometry and adjusted to 1 mg/ml in 50% glycerol. For assay, diC8 PI4P stock (Echelon, CAT#P4008) was diluted in chloroform to 250 µM and 50 µL were aliquoted into each tube for the assay and dried under N2 gas. Dried lipid film was rehydrated in 50 µL of reaction buffer/dialysis buffer. Buffer or 300 ng of purified $Sac1^{1-522}$ with or without 3 µg of purified Osh4, $osh4^{K109Q}$, or $osh4^{K109R}$ protein were added to individual reaction tubes with rehydrated lipids. Reaction mix was incubated for 10 min at 25°C and stopped with 40 mM N-ethylmaleimide (Sigma, CAT#E3876). After which, 50 µL of each reaction mix were added to each well of a 96 well plate. Standard curve for PI-4-P were 2X serial dilutions from 8000 pmol to 500 pmol in duplicates. 100 µL of Biomol green reagent (Enzo, CAT#BML-AK111-0250) was added to each well and incubated for 20 min before reading absorbance at $OD_{620}$. Results shown are averages from three separate experiments. Statistical analyses were performed by one-way ANOVA with Sidak's multiple comparisons test: ** = $p< 0.05$; n.s.= not significant.

# 3 Chapter 1: NuA4 regulates the *sec14* bypass and phospholipid homeostasis

## 3.1 Brief introduction

Several pieces of evidence suggested a connection between lysine acetylation and the regulation of phospholipid homeostasis, particularly with regards to phosphatidylinositol-4-phosphate (PI-4-P) metabolism and inositol metabolism. Two high-throughput genetic screens found that mutants of the NuA4 KAT complex members caused growth defects when either Sec14 was inactivated or when Osh4 was hyperactivated- two conditions where PI-4-P levels are depleted (CURWIN *et al.* 2009; MITCHELL *et al.* 2011). Furthermore, several NuA4 mutants display increased expression of the inositol-3-synthase Ino1, and increased production of inositol- a key metabolite used as a signal for transcriptional regulation of phospholipid metabolic genes containing inositol-choline responsive elements (ICREs) within their promoters (HANCOCK *et al.* 2006; HENRY *et al.* 2014; SALAS-SANTIAGO AND LOPES 2014). Our initial goal was to determine which of the several lysine acetyltransferases (KATs) and lysine deacetylases (KDACs) display defects in phospholipid regulation, specifically in regards to PI-4-P-depleted conditions. For this purpose, we undertook a genetic screen with non-essential deletion mutants of KAT and KDAC catalytic subunit or complex members to determine their effect under PI-4-P depleted conditions.

Here we report that of all the KAT and KDAC mutants screened, mutants of three separate NuA4 complex subunits (Eaf1, Eaf7, Esa1) displayed the strongest and most consistent negative growth defects under both Sec14-deficient conditions and *OSH4*-overexpression conditions. Furthermore, we found that NuA4 mutants increased the growth defects of *sec14-1*$^{ts}$ under inositol-depleted conditions, instead of suppressing it. Transcriptional analysis of *sec14-1*$^{ts}$*eaf1Δ* cells determined that while the transcription of *INO1* is derepressed by over 2-fold, the transcription of other ICRE-containing genes was not. This suggests that the

growth defects of NuA4 mutants with *sec14-1$^{ts}$* under inositol-depleted conditions likely involve a mechanism that extends beyond *de novo* inositol biosynthesis. In fact, we find that ***eaf1Δ*** cells have decreased lipid droplet formation which implies defects in the biosynthesis of triacylglycerols (TAGs) and steryl esters (SEs). Through genetic and chemical approaches, we determine that the genetic interaction between *sec14-1$^{ts}$* and ***eaf1Δ*** potentially reflects a role for NuA4 in fatty acid biosynthesis. Altogether our work identifies a role for NuA4 in the regulation of phospholipid metabolism through the fatty acid biosynthesis pathway and lipid droplet formation.

## 3.2 Results:

### 3.2.1 Identifying the KATs and KDACs regulating phospholipid homeostasis through complementary genetic screens.

To begin our investigation into the role of lysine acetylation on phospholipid homeostasis, we attempted to identify the KAT and KDAC mutants that were sensitive to PI-4-P-depleted conditions. For this purpose, we screened a collection of non-essential deletion mutants for KATs and KDACs (**Table 3.1**), and compared their growth under two conditions which deplete PI-4-P levels.

**Table 3.1 Lysine Acetyltransferases (KATs) and Lysine Deacetylases (KDACs) mutants used for genetic screens**

| KAT mutant | KDAC mutant |
|---|---|
| *eaf1Δ** | *rpd3Δ* |
| *rtt109Δ* | *sir2Δ* |
| *elp3Δ* | *hda1Δ* |
| *gcn5Δ* | *hos1Δ* |
| *hat1Δ* | *hos2Δ* |
| *sas2Δ* | *hos3Δ* |
| *sas3Δ* | *hst1Δ* |
| *hpa2Δ* | *hst2Δ* |
| *hpa3Δ* | *hst3Δ* |
| | *hst4Δ* |

*Eaf1 is a non-essential subunit of the NuA4 KAT complex

Notable exceptions to our list of KATs and KDACs mutants are Eco1, which is an essential gene, and the putative KATs, Lys20, Lys21, Spt10, and Taf1, which are unconfirmed catalytic domains (reviewed in DOWNEY AND BAETZ 2016). Another noticeable absent KAT is Esa1, which is the essential catalytic domain of NuA4 (reviewed in DOYON AND COTE 2004). Instead of using an Esa1 mutant, we used a deletion mutant for one of NuA4s non-essential subunit, Eaf1.

The KATs and KDACs deletion mutants where first subjected to Sec14 inactivation. The temperature sensitive Sec14 mutant, *sec14-1$^{ts}$*, is inactive at higher temperatures causing PI-4-P depletion and Golgi trafficking defects (BANKAITIS *et al.* 1989; CLEVES *et al.* 1989; HAMA *et al.* 1999). Double mutants of *sec14-1$^{ts}$* and non-essential KAT and KDAC mutants were screened to identify mutants that either increase or decrease the growth defects of *sec14-1$^{ts}$*. While most genetic backgrounds did not affect the growth defects of *sec14-1$^{ts}$,* the KAT deletion mutants, ***eaf1Δ***, ***rtt109Δ***, and ***elp3Δ***, all increased the growth defects of *sec14-1$^{ts}$* compared to the wildtype background at semi-permissive temperatures (33.5°C) with ***eaf1Δ*** having the most dramatic effect (**Figure 3.1A**). In contrast, none of the KDAC deletion mutants appear to affect the growth of *sec14-1$^{ts}$* (**Figure 3.1B**).

In a complementary screen, we compared the growth defect of overexpressing *OSH4*-the genetic antagonist of Sec14 (FANG *et al.* 1996). Overexpression of Osh4 causes a similar negative effect on growth as Sec14 inactivation caused by depletion of PI-4-P levels through the hyperactivation of the PI-4-P phosphatase Sac1 (LEBLANC AND MCMASTER 2010; ALFARO *et al.* 2011; MOUSLEY *et al.* 2012). For this screen, *OSH4* expression was controlled by a tetracycline-inducible promoter generated through the genetic manipulation of a galactose-inducible promoter (RONEY *et al.* 2016). We confirmed the overexpression-induced toxicity by spot assay for both the wildtype *OSH4* and the sterol-binding deficient *osh4-Y97F* (**Figure 3.2A**). As a negative control, media containing raffinose without tetracycline was used to prevent any leaky expression of *OSH4* that might be caused by residual effect of the galactose-inducible promoter.

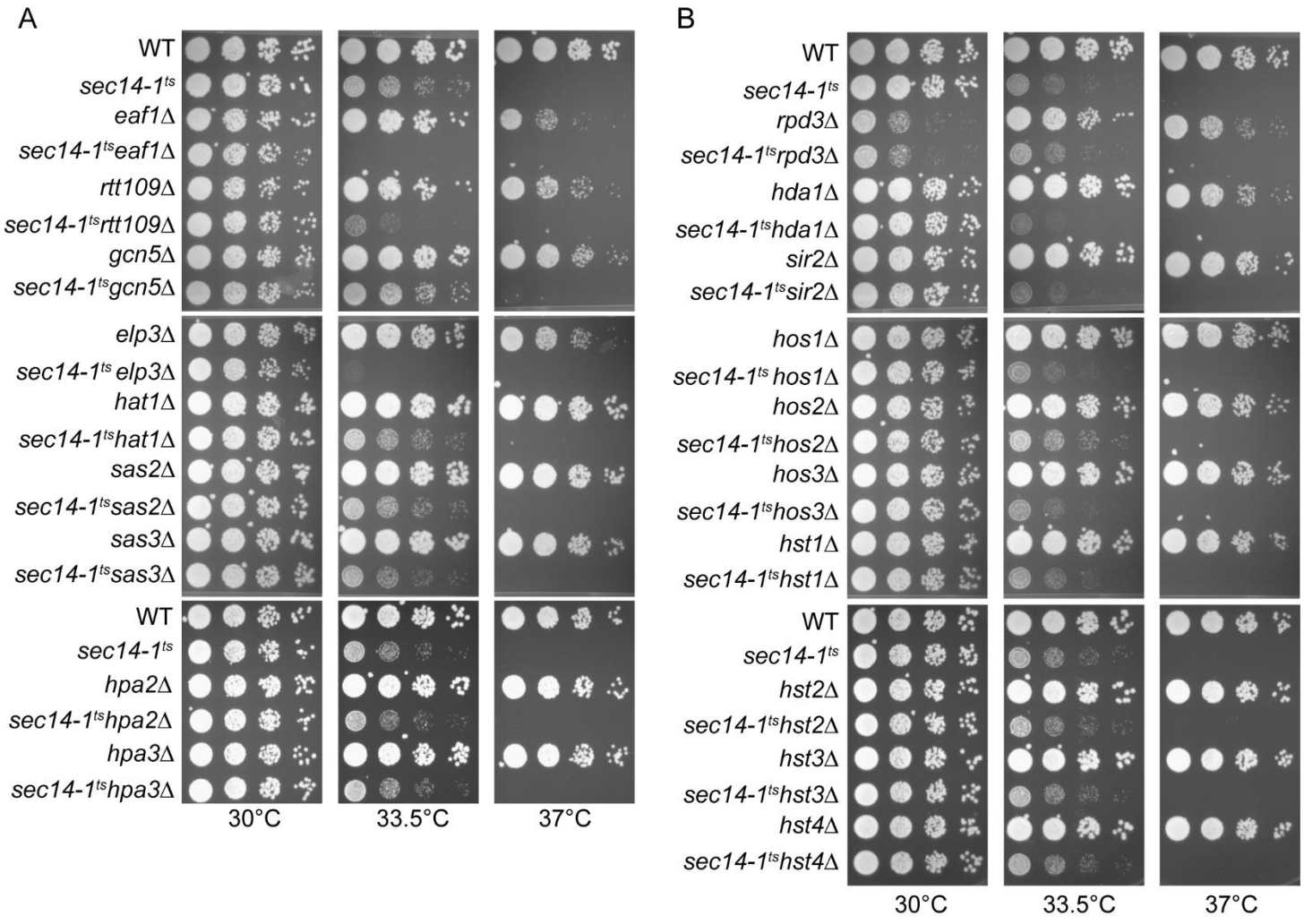
A
WT
sec14-1ts
eaf1Δ
sec14-1tseaf1Δ
rtt109Δ
sec14-1tsrtt109Δ
gcn5Δ
sec14-1tsgcn5Δ
elp3Δ
sec14-1ts elp3Δ
hat1Δ
sec14-1tshat1Δ
sas2Δ
sec14-1tssas2Δ
sas3Δ
sec14-1tssas3Δ
WT
sec14-1ts
hpa2Δ
sec14-1tshpa2Δ
hpa3Δ
sec14-1tshpa3Δ
30°C
33.5°C
37°C
B
WT
sec14-1ts
rpd3Δ
sec14-1tsrpd3Δ
hda1Δ
sec14-1tshda1Δ
sir2Δ
sec14-1tssir2Δ
hos1Δ
sec14-1ts hos1Δ
hos2Δ
sec14-1tshos2Δ
hos3Δ
sec14-1tshos3Δ
hst1Δ
sec14-1tshst1Δ
WT
sec14-1ts
hst2Δ
sec14-1tshst2Δ
hst3Δ
sec14-1tshst3Δ
hst4Δ
sec14-1tshst4Δ
30°C
33.5°C
37°C

**Figure 3.1 Systematic screening of KAT and KDAC mutants reveal that deletion mutants of *EAF1*, *RTT109*, *ELP3* display negative genetic interactions with *sec14-1$^{ts}$*.** To determine if KAT or KDAC activity would affect the growth of *sec14-1$^{ts}$*, wildtype (WT; YKB1079) and an array of non-essential KAT **(A)** or KDAC (**B**) deletion mutant strains (**Table 3.1**) were crossed with *sec14-1$^{ts}$* (YKB3145). Cultures were grown in YPD at 30°C prior to being diluted to an $OD_{600}$ of 0.1 and 4 times 10-fold serial dilutions were spotted on YPD for two days at 30°C, 33.5°C, or 37°C. Representative images from three separate experiments are shown.

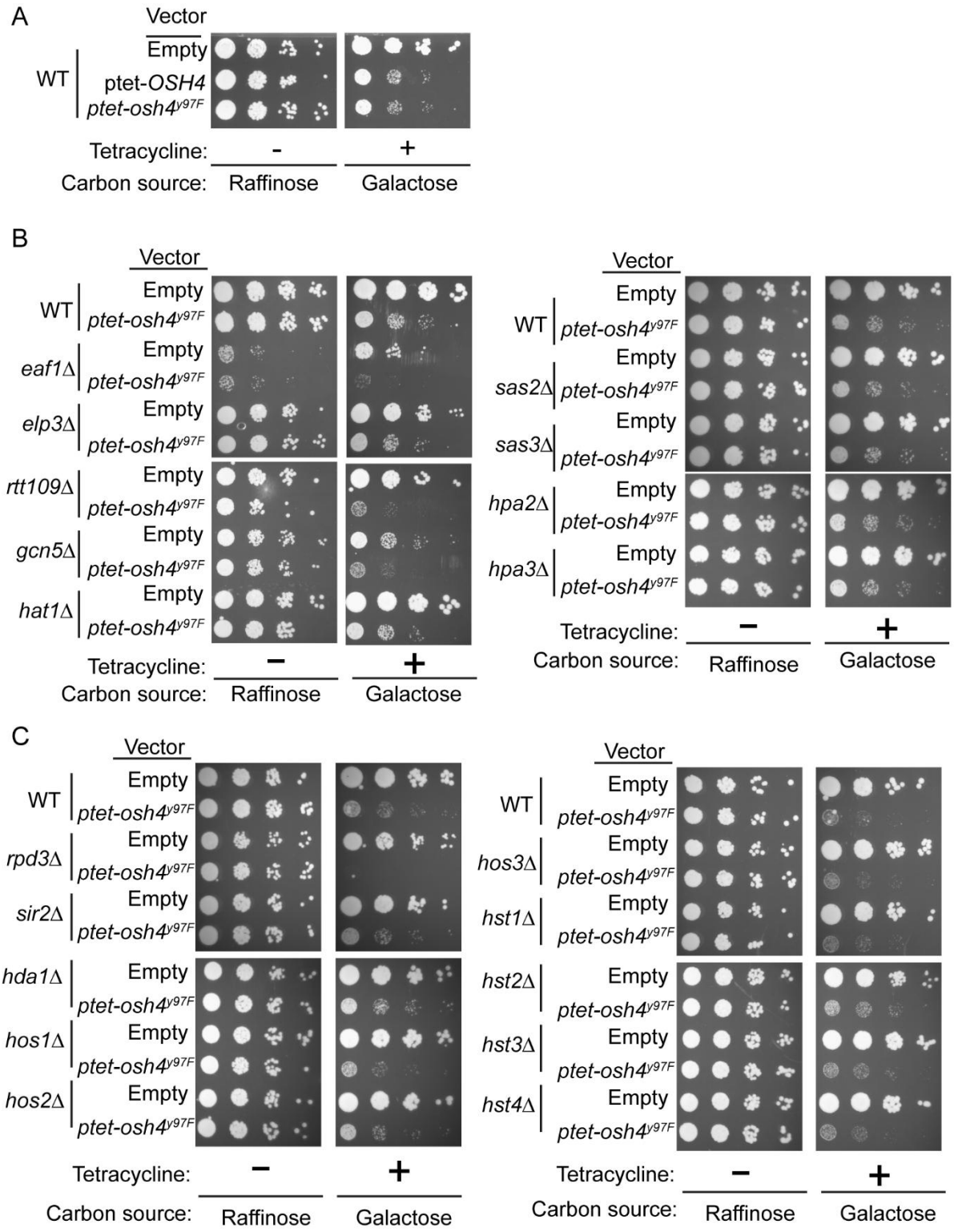
A
Vector
Empty
WT
ptet-OSH4
ptet-osh4y97F
Tetracycline: - +
Carbon source: Raffinose Galactose
B
Vector
WT
Empty
ptet-osh4y97F
eaf1Δ
elp3Δ
rtt109Δ
gcn5Δ
hat1Δ
sas2Δ
sas3Δ
hpa2Δ
hpa3Δ
Tetracycline: − +
Carbon source: Raffinose Galactose
C
rpd3Δ
sir2Δ
hda1Δ
hos1Δ
hos2Δ
hos3Δ
hst1Δ
hst2Δ
hst3Δ
hst4Δ

**Figure 3.2 Systematic screening of KAT and KDAC mutants reveal that deletion of *EAF1*, *RTT109*, *GCN5*, and *RPD3* increase *osh4-Y97F* overexpression-induced toxicity. A)** *OSH4* overexpression-induced toxicity levels are similar between wildtype *OSH4* construct and sterol-binding deficient mutant, *osh4*$^{Y97F}$. Wildtype yeast strain (YKB1079) was transformed with either an empty vector (pRS413), a tetracycline inducible reporter with *OSH4* (ptet-*OSH4*; PKB299) or sterol-binding deficient mutant (ptet-*osh4*$^{Y97F}$; PKB302). Cultures were grown in SD–His at 30°C prior to being diluted to an $OD_{600}$ of 0.1 and 4 times 10-fold serial dilutions were spotted on non-inducible media (Raffinose, - tetracycline) or inducible media (Galactose, + 10 ng/ml tetracycline) for three days at 30°C. Representative images from three separate experiments are shown. **B)** and **C)** To determine if KAT or KDAC activity could modulate *osh4-Y97F* overexpression-induced toxicity, wildtype (WT; YKB1079) and an array of non-essential KAT (B) or KDAC (C) deletion mutant strains (**Table 3.1**) were transformed with an empty vector (pRS413), or *osh4-Y97F* under a tetracycline-inducible reporter (*ptet-osh4*$^{Y97F}$; PKB302). Cultures were grown in SD–His at 30°C prior to being diluted to an $OD_{600}$ of 0.1 and 4 times 10-fold serial dilutions were spotted on non-inducible media (Raffinose, - tetracycline) or inducible media (Galactose, + 10 ng/ml tetracycline) for three days at $30^0$C. Representative images from three separate experiments are shown.

Both *OSH4* and *osh4-Y97F* caused growth defects under inducible conditions (galactose + tetracycline). However, the use of the sterol-binding deficient mutant, *osh4-Y97F*, over the wildtype *OSH4* construct was favoured due to its specific interaction with PI-4-P, instead of sterols (IM *et al.* 2005; MOUSLEY *et al.* 2012). *osh4-Y97F* was overexpressed in all the KAT/KDAC deletion mutants and growth was compared by spot assays under inducible conditions (Galactose, + tetracycline). Of all the KAT mutants, only ***eaf1Δ***, ***rtt109Δ***, and ***gcn5Δ*** displayed a relatively increased growth defect compared to wildtype when *osh4-Y97F* was overexpressed, with ***eaf1Δ*** having the most pronounced effect (**Figure 3.2B**). Additionally, the KDAC mutant ***rpd3Δ*** also displayed a relatively increased growth defects when *osh4-Y97F* overexpression (**Figure 3.2C**).

Only ***eaf1Δ*** and ***rtt109Δ*** consistently displayed a negative interaction to both PI-4-P depleted conditions (**Figure 3.1-3.2**). This led us to focus our attention on these particular genes. To determine if ***eaf1Δ*** and ***rtt109Δ*** negative interactions with PI-4-P depleted conditions were epistatic, we compared the growth of the double mutant, ***eaf1Δrtt109Δ***, to the single mutant strains with and without *sec14-1$^{ts}$* (**Figure 3.3**). At normally permissive temperatures (30°C), the ***eaf1Δrtt109Δ*** double mutant displayed an additive effect on the growth defect of *sec14-1$^{ts}$* compared to the single mutants. This non-epistatic interaction suggests that Eaf1 and Rtt109 are not working within the same pathway, but, more likely, in parallel pathways to buffer *sec14-1$^{ts}$*. Furthermore, the effects of ***eaf1Δ*** on PI-4-P-depleted conditions appear relatively more deleterious than the effect of ***rtt109Δ***. Therefore, we decided to focus our attention on the role of Eaf1 and its related complex, NuA4, on the regulation of phospholipid homeostasis.

### 3.2.2 NuA4 subunits all share a genetic interaction with Sec14

Eaf1 is the structural component of the conserved NuA4 KAT complex consisting of 13 different subunits (SMITH *et al.* 1998; MITCHELL *et al.* 2008). Given that ***eaf1Δ*** was hypersensitive to PI-4-P deficient conditions, we anticipated that a similar sensitivity would be

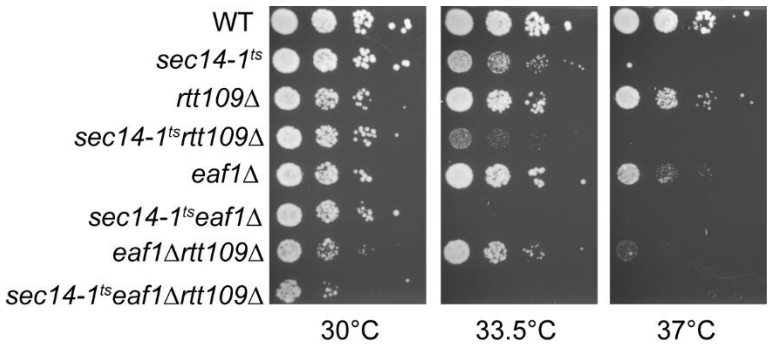
WT
sec14-1ts
rtt109Δ
sec14-1tsrtt109Δ
eaf1Δ
sec14-1tseaf1Δ
eaf1Δrtt109Δ
sec14-1tseaf1Δrtt109Δ
30°C
33.5°C
37°C

**Figure 3.3 *eaf1*Δ *rtt109*Δ double mutant displays additive effect on *sec14-1$^{ts}$* growth defects.** Wildtype (WT; YKB1079), *sec14-1$^{ts}$* (YKB3144), *rtt109*Δ (YKB4073), *sec14-1$^{ts}$rtt109*Δ (YKB4074), *eaf1*Δ (YKB3333), *sec14-1$^{ts}$eaf1Δ* (YKB3935), *eaf1Δ rtt109Δ* (YKB4083), and *sec14-1$^{ts}$ eaf1Δ rtt109Δ* (YKB4084) cultures were grown in YPD at 30°C prior to being diluted to an $OD_{600}$ of 0.1 and 4 times 10-fold serial dilutions were spotted on YPD media for two days at 30°C, 33.5°C, or 37°C. Representative images of three separate experiments are shown.

shared across other NuA4 mutant strains. To confirm this, we assessed the effect of two other NuA4 mutants, ***eaf7Δ*** and *esa1-L254P*$^{ts}$, on Sec14 inactivation and *OSH4* overexpression (**Figure 3.4**). *esa1-L254P*$^{ts}$ is a temperature-sensitive mutant allele of the essential catalytic gene *ESA1* (CLARKE *et al.* 1999). As expected, both ***eaf7Δ*** and *esa1-L254P*$^{ts}$ increased the growth defects of *sec14-1*$^{ts}$ compared to wildtype at semi-permissive temperature (**Figure 3.4A**). Similarly, both ***eaf7Δ*** and *esa1-L254P*$^{ts}$ strains increased the growth defects towards *OSH4* overexpression compared to wildtype at a similar extent as ***eaf1Δ*** (**Figure 3.4B**). This suggests that the entire NuA4 complex is required to buffer the effect of Sec14 inactivation and Osh4 overexpression. Additionally, we determined that the role of NuA4 within this pathway were not simply due to regulation of either endogenous or induced Osh4 protein levels (**Figure 3.5**). In conclusion, we have determined that the NuA4 complex is required to buffer the toxic effect of Sec14 inactivation and *OSH4* overexpression suggesting a role for NuA4 in the regulation of phospholipid homeostasis.

### 3.2.3 NuA4 is required for both *OSH4*- and *CKI1*-dependent *sec14* bypass.

We next sought to determine the cause of the genetic interaction between NuA4 mutants and *sec14-1*$^{ts}$. Mutations within PI-4-P or PC metabolic pathways can suppress *sec14* mutants and are known as "*sec14* bypass" pathways. Deletion of *OSH4/KES1*, encoding for a conserved PI-4-P binding protein which activates the Sac1 PI-4-P phosphatase, can restore viability to the temperature-sensitive *sec14-1*$^{ts}$ strain, by preventing PI-4-P depletion (FANG *et al.* 1996; FAIRN *et al.* 2007; STEFAN *et al.* 2011). Alternatively, deletion of *CKI1,* or any genes within the CDP-choline pathway, can also restore viability to the *sec14-1*$^{ts}$ strain by inhibiting PC biosynthesis and preventing PA depletion (CLEVES *et al.* 1989; CLEVES *et al.* 1991; PATTON-VOGT *et al.* 1997). Therefore, we wanted to determine whether deletion of *OSH4* or *CKI1* could bypass the synthetic lethality observed in a *sec14-1*$^{ts}$***eaf1Δ*** double mutant. Although deletion of *OSH4,* could, as expected, completely suppress the growth defects of *sec14-1*$^{ts}$ at 37°C, the growth of

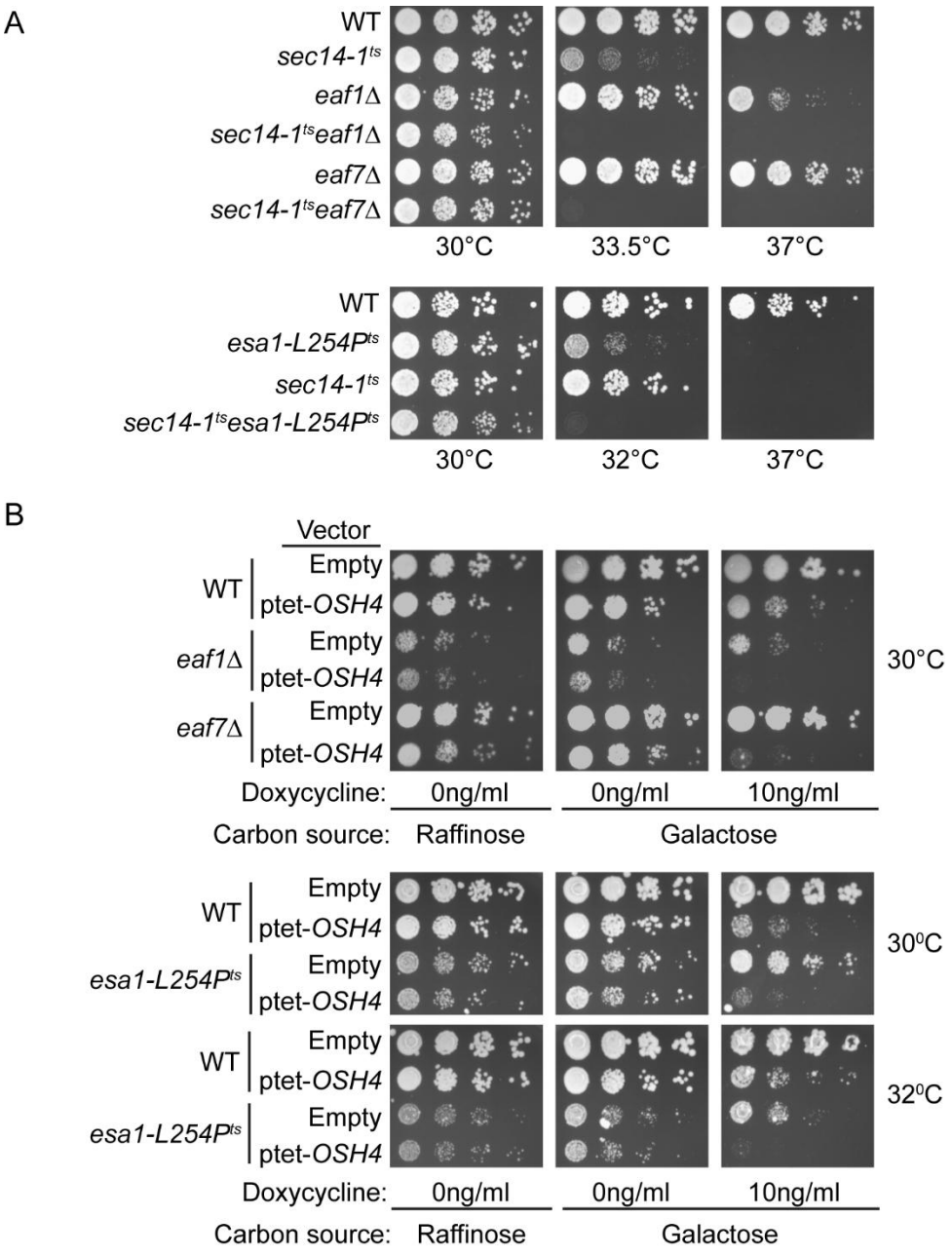
A
WT
sec14-1ts
eaf1Δ
sec14-1tseaf1Δ
eaf7Δ
sec14-1tseaf7Δ
30°C
33.5°C
37°C
WT
esa1-L254Pts
sec14-1ts
sec14-1tsesa1-L254Pts
30°C
32°C
37°C
B
Vector
WT
Empty
ptet-OSH4
eaf1Δ
Empty
ptet-OSH4
eaf7Δ
Empty
ptet-OSH4
30°C
Doxycycline:
0ng/ml
0ng/ml
10ng/ml
Carbon source:
Raffinose
Galactose
WT
Empty
ptet-OSH4
esa1-L254Pts
Empty
ptet-OSH4
30°C
WT
Empty
ptet-OSH4
esa1-L254Pts
Empty
ptet-OSH4
32°C
Doxycycline:
0ng/ml
0ng/ml
10ng/ml
Carbon source:
Raffinose
Galactose

**Figure 3.4 NuA4 mutants are hypersensitive to PI-4-P-depleted conditions. A)** NuA4 mutants display negative genetic interactions with *sec14-1$^{ts}$*. Wildtype (WT; YKB1079), *sec14-1$^{ts}$* (YKB3144), ***eaf1***Δ (YKB3333), *sec14-1$^{ts}$* ***eaf1Δ*** (YKB3935), ***eaf7***Δ (YKB3292), *sec14-1$^{ts}$* ***eaf7***Δ (YKB4068), *esa1-L254P$^{ts}$* (YKB4236), and *sec14-1$^{ts}$ esa1-L254P$^{ts}$* (YKB4242) cultures were grown in YPD at 30°C prior to being diluted to an $OD_{600}$ of 0.1 and 4 times 10-fold serial dilutions were spotted on YPD for two days at 30°C, 32°C, 33.5°C, or 37°C. Representative images from three separate experiments are shown. **B)** *OSH4* overexpression-induced toxicity is increased in NuA4 mutants. Wildtype (WT; YKB1079), ***eaf1***Δ (YKB3333), ***eaf7***Δ (YKB3292), and *esa1-L254P$^{ts}$* (YKB4236) were transformed with an empty vector (pRS415), or with a vector containing *OSH4* under a tetracycline-inducible GAL promoter (ptet-*OSH4*; PKB321). Cultures were grown in SD-His at 30°C prior to being diluted to an $OD_{600}$ of 0.1 and 4 times 10-fold serial dilutions were spotted on non-inducible media (Raffinose, - tetracycline) or inducible media (Galactose, + 10 ng/ml tetracycline) for three days at 30°C or 32°C.

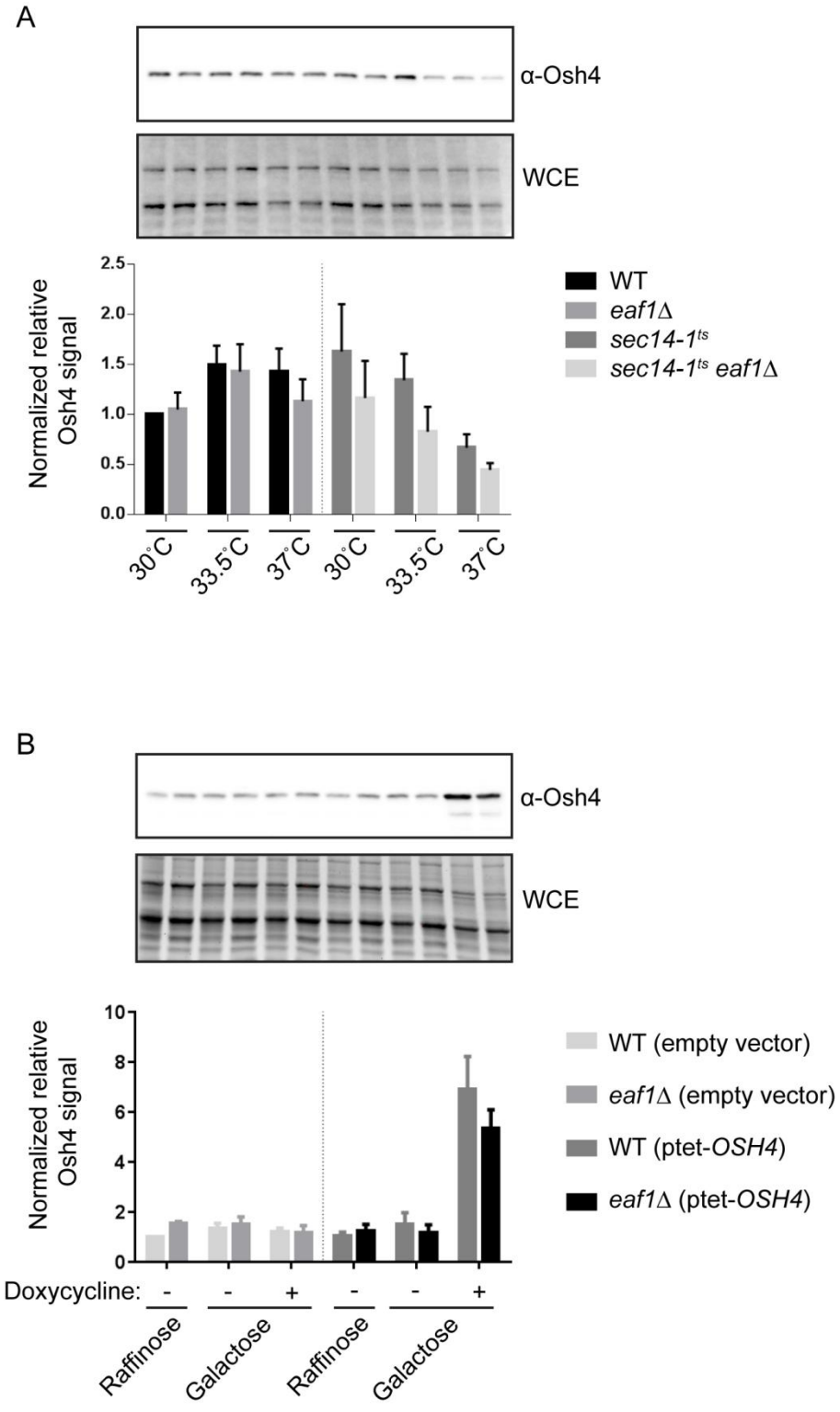
A
α-Osh4
WCE
Normalized relative Osh4 signal
2.5
2.0
1.5
1.0
0.5
0.0
30˚C
33.5˚C
37˚C
30˚C
33.5˚C
37˚C
WT
eaf1Δ
sec14-1ts
sec14-1ts eaf1Δ
B
α-Osh4
WCE
Normalized relative Osh4 signal
10
8
6
4
2
0
Doxycycline: - - + - - +
Raffinose
Galactose
Raffinose
Galactose
WT (empty vector)
eaf1Δ (empty vector)
WT (ptet-OSH4)
eaf1Δ (ptet-OSH4)

**Figure 3.5 *EAF1* deletion mutant does not affect Osh4 protein levels A)** Protein levels of Osh4 were compared wildtype (WT; YKB1079), *sec14-1$^{ts}$* (YKB3144), ***eaf1*Δ** (YKB3333), and *sec14-1$^{ts}$**eaf1Δ*** (YKB3935). Cultures were grown in YPD at 30°C prior to being shifted in preheated YPD media for four hours at 30°C, 33.5°C, or 37°C. **B)** Protein levels of Osh4 were compared in wildtype (WT; YKB1079) and ***eaf1*Δ** (YKB3333) transformed with an empty vector (pRS415), or with a vector containing *OSH4* under a tetracycline-inducible GAL promoter (ptet-*OSH4*; PKB321). Cultures were grown in SD-His at 30°C prior to being shifted to non-inducible media (Raffinose, - tetracycline) or inducible media (Galactose, + 10ng/ml tetracycline) for four hours at 30°C. Whole cell lysates were prepared and 12 µg resolved on 7.5% SDS-PAGE gel, and subjected to Western blot analysis with α-Osh4 antibodies. Osh4 signal was normalized to total protein amount loaded in each well, shown below the immunoblot. using the methods described in (TAYLOR AND POSCH 2014). Top panel is representative immunoblot image of three separate biological replicates. Bar graph displays the mean normalized signal (N=3, +S.E.M.) of Osh4 for each sample relative to A) WT 30°C sample, and B) WT with empty vector (Raffinose) sample.

of the triple mutant strain *sec14-1$^{ts}$eaf1Δosh4Δ* was only partially rescued at 33.5°C, and remained inviable at 37°C (**Figure 3.6A**). Similarly, *cki1Δ* was unable to completely suppress the growth defects of *sec14-1$^{ts}$eaf1Δ* at 33.5°C and was unable to grow at 37°C (**Figure 3.6A**). As this may reflect the temperature sensitivity and growth defects of *eaf1*Δ cells (AUGER *et al.* 2008; AUESUKAREE *et al.* 2009), we also determined the suppression capability of *osh4Δ* and *cki1Δ* on *sec14-1$^{ts}$eaf7*Δ and *sec14-1$^{ts}$esa1-L254P$^{ts}$*. While deletion of *OSH4* could rescue *sec14-1$^{ts}$eaf7*Δ at 33.5°C, only partial rescue could be achieved at 37°C (**Figure 3.6B**). In contrast deletion of *CKI1* resulted in minimal suppression of *sec14$^{ts}$eaf7*Δ at 37°C (**Figure 3.6B**). While deletion of *OSH4* and *CKI1* could partially suppress the *sec14-1$^{ts}$esa1-L254P$^{ts}$* at 33.5$^{o}$C, no suppression was detected at 37°C, suggesting that the essential function of Esa1 is likely not phospholipid metabolism (**Figure 3.6C**). However, it must be noted that suppression of *sec14-1$^{ts}$eaf1*Δ is background dependent, as deletion of *OSH4*, but not *CKI1*, can completely suppress *sec14-1$^{ts}$eaf1*Δ in a different strain background, SEY6210/SEY6211 (Huang *et al.* 2016; preparing for submission to *Cell*).

Since both *OSH4*-dependent and *CKI1*-dependent Sec14-bypass pathways requires phosphatidic acid (PA) and the activity of the Phospholipase D Spo14 (PATTON-VOGT *et al.* 1997; SREENIVAS *et al.* 1998; XIE *et al.* 1998), we sought to assess if NuA4 and Spo14 worked within the same pathway. We compared the growth of the double mutant *eaf1Δspo14Δ* and triple mutant *sec14-1$^{ts}$eaf1Δspo14Δ* with their respective single and double mutants (**Figure 3.7A**). As previously determined, the *sec14-1$^{ts}$spo14Δ* displayed a growth defect upon increased temperature (CURWIN *et al.* 2009). We also determined that the double mutant *eaf1Δspo14Δ* displays a synthetic growth defect at 30°C compared to the single mutants, and that this growth defect is increased in combination with *sec14-1$^{ts}$* (**Figure 3.7A**). In contrast, the negative genetic interaction between *eaf1Δ* and *spo14Δ* were not seen between *eaf7Δ* and *esa1-L254P$^{ts}$* with *spo14Δ* (**Figure 3.7B-C**). Eaf7 has been found both within NuA4 and as part

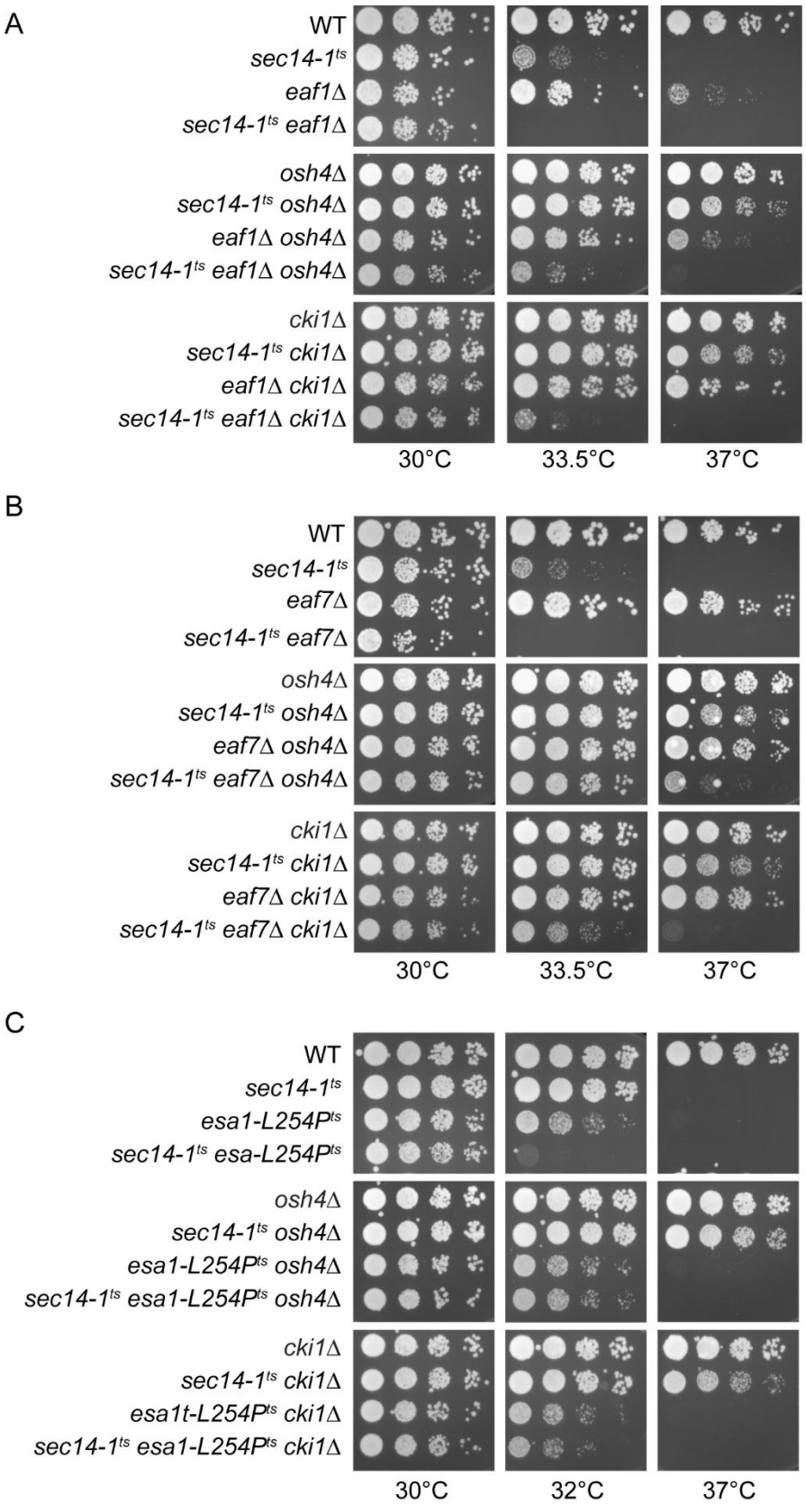
A
WT
sec14-1ts
eaf1Δ
sec14-1ts eaf1Δ
osh4Δ
sec14-1ts osh4Δ
eaf1Δ osh4Δ
sec14-1ts eaf1Δ osh4Δ
cki1Δ
sec14-1ts cki1Δ
eaf1Δ cki1Δ
sec14-1ts eaf1Δ cki1Δ
30°C
33.5°C
37°C
B
WT
sec14-1ts
eaf7Δ
sec14-1ts eaf7Δ
osh4Δ
sec14-1ts osh4Δ
eaf7Δ osh4Δ
sec14-1ts eaf7Δ osh4Δ
cki1Δ
sec14-1ts cki1Δ
eaf7Δ cki1Δ
sec14-1ts eaf7Δ cki1Δ
30°C
33.5°C
37°C
C
WT
sec14-1ts
esa1-L254Pts
sec14-1ts esa-L254Pts
osh4Δ
sec14-1ts osh4Δ
esa1-L254Pts osh4Δ
sec14-1ts esa1-L254Pts osh4Δ
cki1Δ
sec14-1ts cki1Δ
esa1t-L254Pts cki1Δ
sec14-1ts esa1-L254Pts cki1Δ
30°C
32°C
37°C

**Figure 3.6 NuA4 mutants impairs *OSH4*¬- and *CKI1*-dependent *sec14* bypass.A)** *EAF1* deletion mutant, **B)** *EAF7* deletion mutant, and **C)** *ESA1* temperature-sensitive mutant impair *OSH4*- and *CKI1*-dependent *sec14* bypass. Wildtype (YKB1079), *sec14-1$^{ts}$* (YKB3144), ***eaf1Δ*** (YKB3333), *sec14-1$^{ts}$**eaf1Δ*** (YKB3935), ***osh4***Δ (YKB3343), *sec14-1$^{ts}$**osh4***Δ (YKB3344), ***eaf1Δ osh4Δ*** (YKB4056), *sec14-1$^{ts}$**eaf1Δ osh4Δ*** (YKB4061), ***cki1***Δ (YKB4273), *sec14-1$^{ts}$**cki1***Δ (YKB4275), ***eaf1Δ cki1Δ*** (YKB4277), *sec14-1$^{ts}$**eaf1Δ cki1Δ*** (YKB4278), ***eaf7Δ*** (YKB3292), *sec14-1$^{ts}$**eaf7Δ*** (YKB4068), ***osh4***Δ (YKB3343), *sec14-1$^{ts}$**osh4***Δ (YKB3344), ***eaf7Δ osh4Δ*** (N/A), *sec14-1$^{ts}$**eaf1Δ osh4Δ*** (N/A), ***cki1***Δ (YKB4273), *sec14-1$^{ts}$**cki1***Δ (YKB4275), ***eaf7Δ cki1Δ*** (YKB4279), *sec14-1$^{ts}$**eaf7Δcki1Δ*** (YKB4281), *esa1-L254P$^{ts}$* (YKB4236), *sec14-1$^{ts}$ esa1-L254P$^{ts}$* (YKB4242), *esa1-L254P$^{ts}$**osh4Δ*** (N/A), *sec14-1$^{ts}$esa1-L254P$^{ts}$**osh4Δ*** (N/A) cultures were grown in YPD at 30°C prior to being diluted to an $OD_{600}$ of 0.1 and 4 times 10-fold serial dilutions were spotted on YPD for two days at 30°C, 32°C, 33.5°C, or 37°C. Representative images of three separate experiments are shown.

A

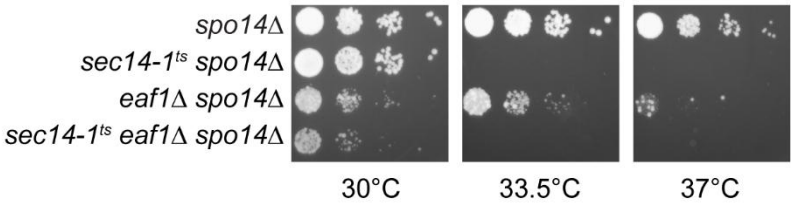
spo14Δ
sec14-1ts spo14Δ
eaf1Δ spo14Δ
sec14-1ts eaf1Δ spo14Δ
30°C
33.5°C
37°C

B

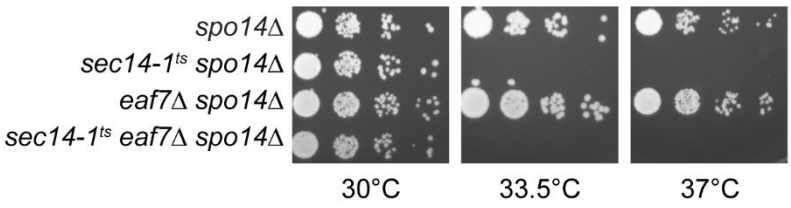
spo14Δ
sec14-1ts spo14Δ
eaf7Δ spo14Δ
sec14-1ts eaf7Δ spo14Δ
30°C
33.5°C
37°C

C

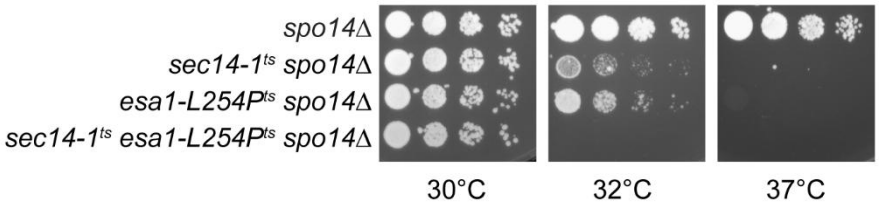
spo14Δ
sec14-1ts spo14Δ
esa1-L254Pts spo14Δ
sec14-1ts esa1-L254Pts spo14Δ
30°C
32°C
37°C

**Figure 3.7 *EAF1* deletion mutant displays synthetic sickness with *SPO14* deletion mutant.A)** *EAF1*, **B)** *EAF7,* and **C)** *ESA1* mutants genetic interaction with *SPO14* deletion mutant. ***spo14Δ*** (YKB3113), ***sec14-1$^{ts}$ spo14Δ*** (YKB4261), ***spo14Δ eaf1Δ*** (YKB4263***), sec14-1$^{ts}$ spo14Δ eaf1Δ*** (YKB4264), ***spo14Δ eaf7Δ*** (YKB4269***), sec14-1$^{ts}$spo14Δ eaf7Δ*** (YKB4271), ***esa1-L254P$^{ts}$spo14Δ*** (YKB4265), and ***sec14-1$^{ts}$esa1-L254P$^{ts}$spo14Δ*** (YKB4267) cultures were grown in YPD at 30°C prior to being diluted to an $OD_{600}$ of 0.1 and 4 times 10-fold serial dilutions were spotted on YPD for two days at 30°C, 32°C, 33.5°C, or 37°C. Representative images of three separate experiments are shown.

of the TINTIN complex (ROSSETTO *et al.* 2014; BHAT *et al.* 2015); therefore its genetic interaction with Sec14 might be independent of NuA4 and would not necessarily share the same interactions as Eaf1. Furthermore, the temperature sensitive Esa1 mutant would not share the same phenotype as a complete null mutation which could explain why we do not see a similar interaction with *spo14Δ* as we did with *eaf1Δ*. For these reasons, we believe that NuA4 is necessary to suppress defects in Sec14 function through a mechanism independent of *SPO14*.

### 3.2.4 ICRE-regulated phospholipid genes are not fully derepressed in *EAF1* mutant background.

Given the importance of transcriptional regulation to lipid homeostasis, we next sought to determine whether the synthetic genetic interaction between *sec14-1$^{ts}$* and NuA4 mutants could reflect misregulation of lipid metabolic genes expression. In collaboration with the Stintzi lab (uOttawa), we compared mRNA gene expression between *sec14-1$^{ts}$* and *sec14-1$^{ts}$eaf1Δ* using RNA deep sequencing. RNA samples from three biological replicates were extracted from mid-log phase cells that were shifted to semi-permissive temperatures (33.5°C) for two hours to briefly inactivate *sec14-1$^{ts}$*. In summary, over 8 million reads were obtained for each sample identifying at least 89% of the annotated open reading frames in the *Saccharomyces* genome database (CHERRY *et al.* 2012; ENGEL *et al.* 2014). Analysis of the ERCC spike-in standard revealed that all samples had an $R^2$ correlation ranging from 0.92-0.95 (**Figure 3.8A**). These results indicate our rRNA depletion and library construction was consistent and unbiased across samples. Principal component analysis determined that the majority of the variance between samples is attributable to the differences between the two different strains and not their biological replicates (**Figure 3.8B**). Only a subset of genes were found to be significantly downregulated (103 genes/1.84%) or upregulated (183 genes/3.11%) in *sec14-1$^{ts}$eaf1Δ* compared to *sec14-1$^{ts}$* by a fold change ≥ 2 and FDR adjusted p-value ≤ 0.05 (**Figure 3.9A, Table S3-S4)**.

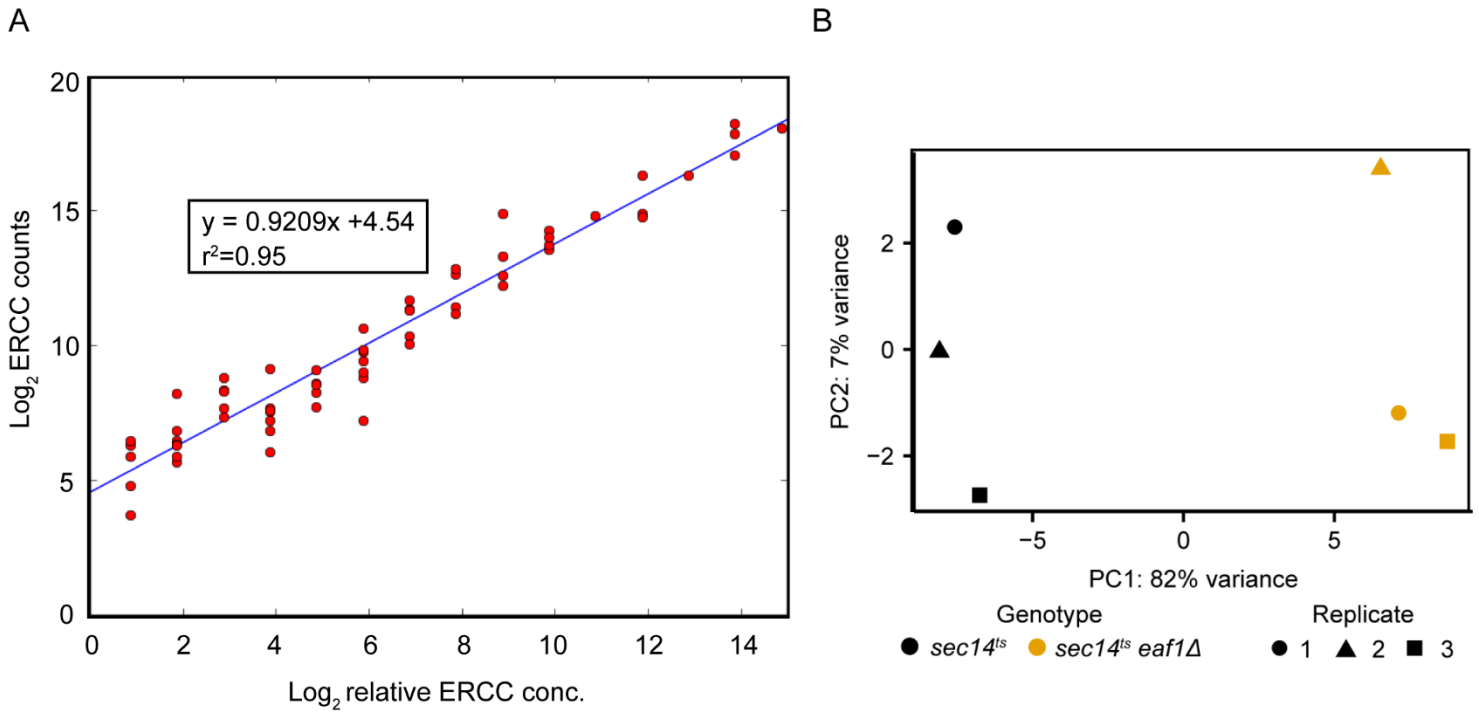
A
B
y = 0.9209x +4.54
r²=0.95
Log2 ERCC counts
Log2 relative ERCC conc.
PC2: 7% variance
PC1: 82% variance
Genotype
sec14ts
sec14ts eaf1Δ
Replicate
1
2
3

**Figure 3.8 ERCC standard validation and principal component analysis for RNA-seq samples. A)** Representative ERCC standard curve. Graph shows standard curve calculated for one biological replicate of *sec14-1$^{ts}$*. Log2 transformed ERCC counts are plotted on the y-axis while Log2 transformed ERCC concentrations are plotted on the x-axis. B) Principal component analysis of the normalized gene counts. The graph plots the first two principal components. As expected, the RNA-seq datasets separate by genotype on PC1, demonstrating that the majority of variance is explained by genotype and not by biological replicate. Annika Flint and James Butcher (Stintzi lab; UOttawa) performed experiments and created graphs.

A

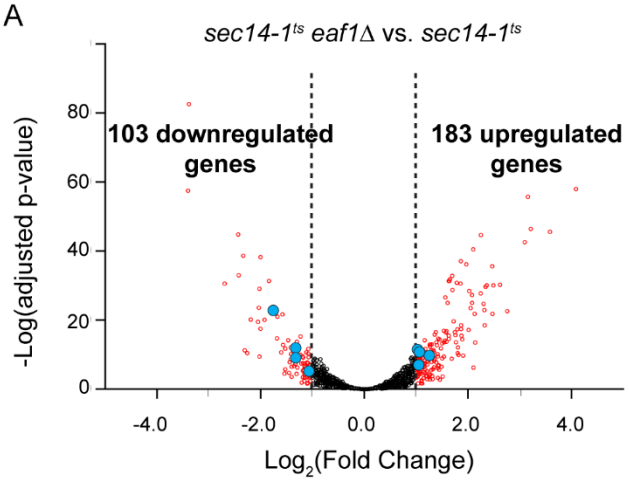


B

Table. Singificantly changed lipid metabolic genes

| Downregulated | $Log_2$ Fold Change | Upregulated | $Log_2$ Fold Change |
|---|---|---|---|
| ***YEH1*** | -1.74 | ***INO1*** | 1.25 |
| ***PLB2*** | -1.33 | ***FAS2*** | 1.06 |
| ***BCP1*** | -1.32 | ***PLB3*** | 1.04 |
| ***CDS1*** | -1.05 | ***FAS1*** | 1.02 |

C

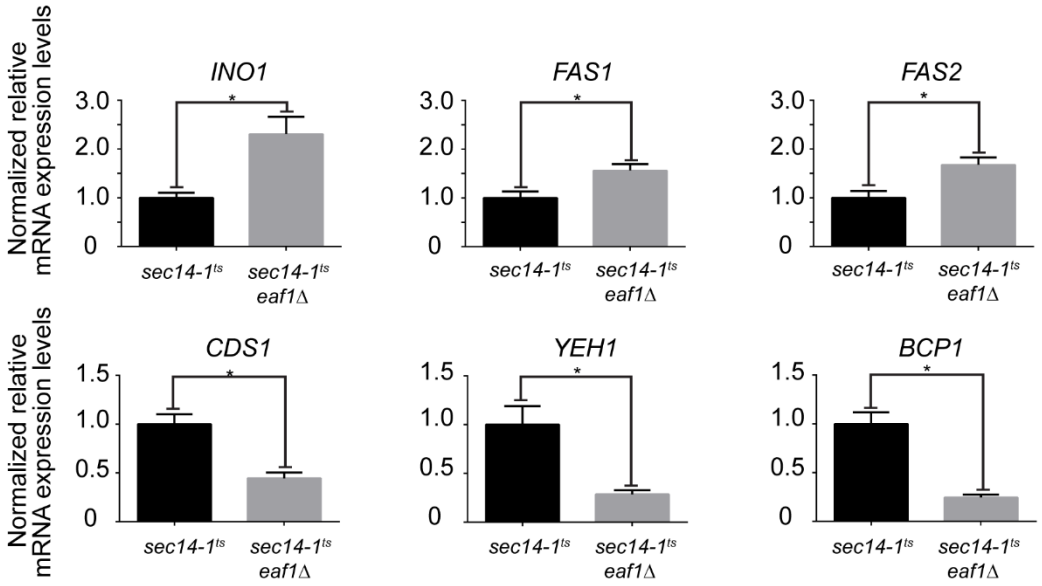


D

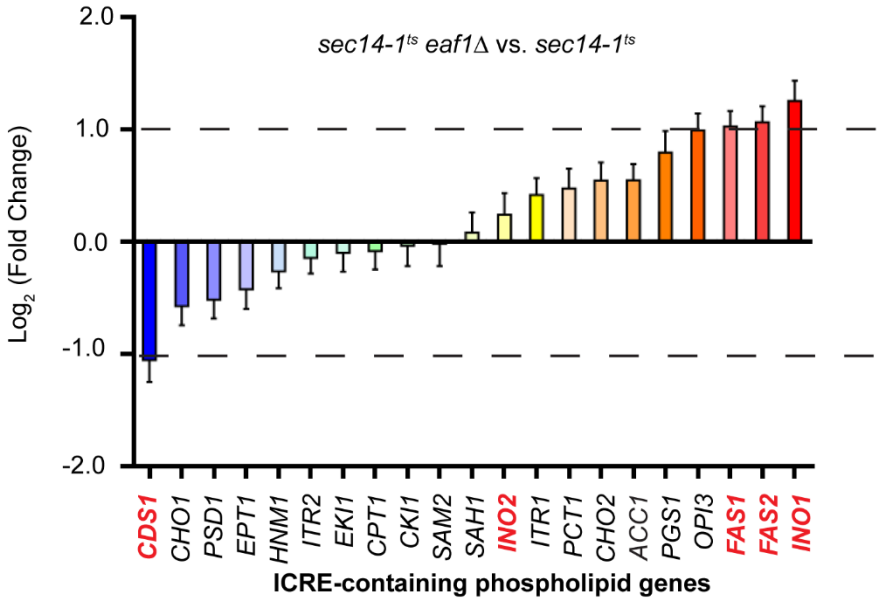

**Figure 3.9 Transcriptional profiling of *sec14-1$^{ts}$eaf1Δ* and *sec14-1$^{ts}$* reveal that ICRE-regulated phospholipid genes are not significantly upregulated.A)** Volcano plot for differentially expressed genes (*sec14-1$^{ts}$eaf1Δ* (YKB3935) vs. *sec14-1$^{ts}$* (YKB3144)) from RNA-sequencing experiments. Differential expression levels of aligned sequences were calculated using significant thresholds set at $Log_2$ fold change≥2 and FDR adjusted p-value≤0.05. Significant differentially expressed genes are in red. In blue are significantly changed lipid metabolic genes described in B). **B)** Table listing significantly downregulated and upregulated lipid metabolic genes. **C)** Confirmation of mRNA expression of lipid metabolic genes identified in transcriptome comparison of *sec14-1$^{ts}$eaf1Δ* and *sec14-1$^{ts}$*. Strains were grown to log phase in YPD at 30°C then shifted to 33.5°C for two hours prior to RNA extraction. mRNA expression levels were normalized to *TDH3* and *ACT1* expression. The mean normalized $Log_2$ fold expression (+S.E.M.) from three biological replicates is shown. Statistical analysis was performed by unpaired two-tailed t-test: *p-value≤0.05. **D)** Relative expression levels of ICRE-containing phospholipid genes between *sec14-1$^{ts}$eaf1Δ* and *sec14-1$^{ts}$*. Genes are ordered from lowest to highest fold-change expression. Annika Flint and James Butcher (Stintzi lab; UOttawa) performed RNA-seq experiments.

Deletion of *EAF1* in the *sec14-1$^{ts}$* background resulted in the decreased expression of the purine biosynthesis genes (*ADE1, ADE12, ADE17*) phosphate metabolic genes (*PHO3, PHO5, PHO11, PHO12*) and a large cluster of genes associated with ribosomal biogenesis (**Table S3-S5**) which is in agreement with previously published studies (REID *et al.* 2000; KROGAN *et al.* 2004; NOURANI *et al.* 2004; LINDSTROM *et al.* 2006; CHENG *et al.* 2015). Upregulated genes common to previous ***eaf1Δ*** transcriptome studies and *sec14-1$^{ts}$**eaf1Δ*** included the stress response genes (*DDR2*, *HSP12, HSP26*) (LINDSTROM *et al.* 2006; CHENG *et al.* 2015) (**Table S4-S6**), altogether demonstrating the genes that are regulated by NuA4 independent of *SEC14*. However, our main purpose was to focus on genes that were both implicated in phospholipid metabolism and that were differentially regulated by NuA4 in *sec14-1$^{ts}$* background

Only 8 genes involved in phospholipid metabolism displayed significant transcriptional change (**Figure 3.9B**). Downregulated genes included the steryl ester hydrolase *YEH1,* the phosphatidate cytidylyltransferase (CDP-diglyceride synthetase) *CDS1*, the phospholipase B *PLB2*, and *BCP1*, which encodes a protein implicated in phosphatidylinositol-4,5-biphosphate (PI-4,5-$P_2$) synthesis. Upregulated genes included the inositol-3-phosphate synthase *INO1*, the fatty acid synthases *FAS1* and *FAS2*, along with the phospholipase B *PLB3*. As recent evidence suggests that the contribution of phospholipase B enzymes toward phospholipid turnover *in-vivo* is negligible (MORA *et al.* 2012), we focused our attention on the remaining six genes. For each of the lipid metabolic genes, the changes in expression detected by next generation sequencing analysis were confirmed through qRT-PCR (**Figure 3.9C**). Intriguingly, four out of the six genes confirmed contain an inositol-choline repressible element (ICRE) in their promoter.

If NuA4 is regulating transcription of ICRE-containing genes, one would anticipate that other ICRE-containing phospholipid metabolic genes would be similarly derepressed as *INO1* (**Figure 3.9D**); however, this was not the case. While the expression of *FAS1* and *FAS2* were significantly upregulated in *sec14-1$^{ts}$eaf1Δ* cells, *CDS1* was down-regulated. Indeed the

expression of the majority of ICRE-containing phospholipid genes did not display significant changes in gene expression in our transcriptome profile, including the transcription factor *INO2*, whose expression remained close to basal level (**Figure 3.9D**). Derepression of *INO1* expression is normally preceded by increased levels of *INO2* which subsequently dimerizes with *INO4* and binds to ICRE-gene promoters to promote transcription (AMBROZIAK AND HENRY 1994; ASHBURNER AND LOPES 1995). Our transcriptome analysis provides evidence of *INO1* derepression happening independently of *INO2* derepression, suggesting that the transcriptional derepression of *INO1* in *sec14-1$^{ts}$eaf1Δ* is not characteristic of the typical Opi- transcriptional response. This demonstrates that the ICRE-regulated phospholipid genes are not properly regulated in NuA4 mutants which could negatively impact phospholipid homeostasis under conditions requiring these genes

### *3.2.5* Overexpression of *CDS1* or *BCP1* do not rescue growth defect of *sec14-1$^{ts}$eaf1Δ*

We next sought to determine if the misregulation of ICRE-regulated phospholipid genes was contributing to the synthetic sickness of *sec14-1$^{ts}$eaf1Δ* strain. We hypothesized that if the sickness defect was the result of decreased Cds1 activity, then overexpression of *CDS1* would rescue the growth defect of *sec14-1$^{ts}$eaf1*Δ cells. To test this we generated a doxycycline-inducible *CDS1-TAP* strain. While overexpression of *CDS1* did not impact growth of wildtype or *sec14-1$^{ts}$* cells, overexpression of *CDS1* caused synthetic dosage sickness with *eaf1*Δ at 30°C and the genetic interaction increased at 33.5°C (**Figure 3.10A**). Further, overexpression of *CDS1* did not rescue *sec14-1$^{ts}$eaf1*Δ cells, indicating that the genetic interaction between *eaf1*Δ and *sec14-1$^{ts}$* is not due to a decrease in *CDS1* gene expression. Similarly overexpression of *BCP1* did not rescue the growth defect of *sec14-1$^{ts}$ eaf1*Δ cells (**Figure 3.10B**).

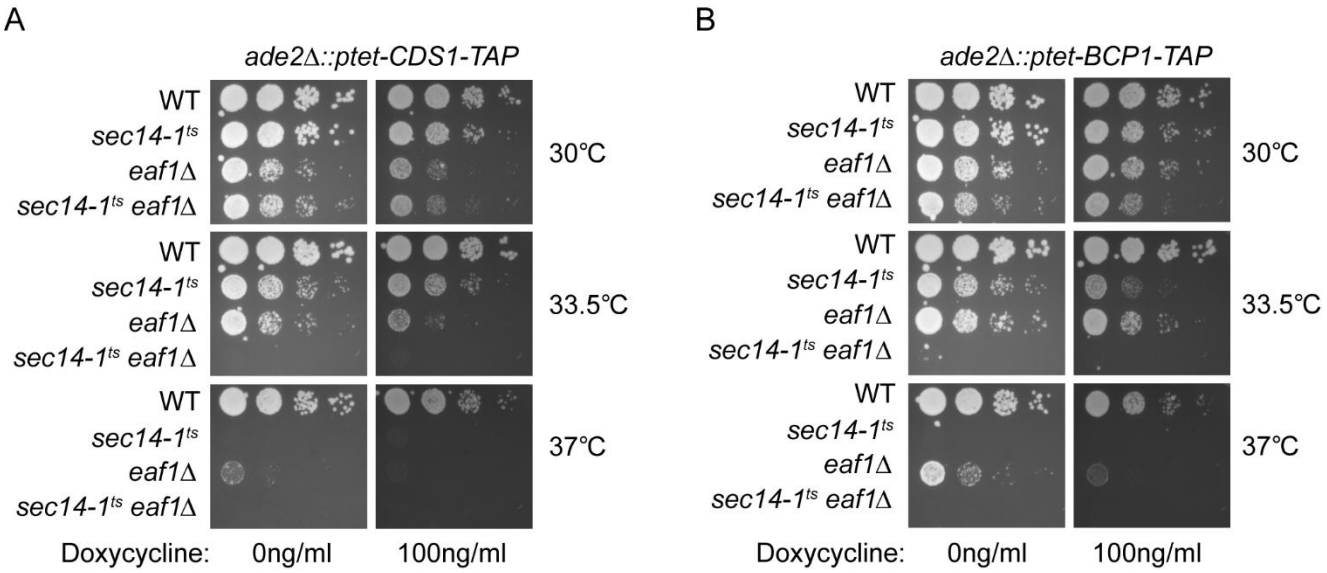
A
ade2Δ::ptet-CDS1-TAP
WT
sec14-1ts
eaf1Δ
sec14-1ts eaf1Δ
30°C
33.5°C
37°C
Doxycycline: 0ng/ml 100ng/ml
B
ade2Δ::ptet-BCP1-TAP
WT
sec14-1ts
eaf1Δ
sec14-1ts eaf1Δ
30°C
33.5°C
37°C
Doxycycline: 0ng/ml 100ng/ml

**Figure 3.10 *CDS1* and *BCP1* overexpression does not suppress the synthetic sickness interaction of *sec14-1$^{ts}$eaf1Δ*. A)** *CDS1* overexpression and **B)** *BCP1* overexpression does not suppress *sec14-1$^{ts}$eaf1Δ*. *CDS1-TAP* or *BCP1-TAP* under a tetracycline-inducible promoter was integrated into the *ADE2* locus region in WT (BY4741), *sec14-1$^{ts}$* (YKB3144), *eaf1Δ* (YKB3333), and *sec14-1$^{ts}$eaf1Δ* (YKB3935) strain backgrounds. Cultures were grown in YPD at 30°C prior to being diluted to an $OD_{600}$ of 0.1 and 4 times 10-fold serial dilutions were spotted on YPD with indicated amount of doxycycline for two days at 30°C, 33.5°C, or 37°C. Representative images of three separate experiments are shown.

### 3.2.6 NuA4 mutants exacerbate the growth defects of *sec14-1$^{ts}$* under inositol-depleted conditions

We next asked if NuA4-dependent regulation of inositol impacted the growth of *sec14-1$^{ts}$.* The growth defects of *sec14-1$^{ts}$* on inositol-depleted media can be suppressed by mutants which exhibit an overproduction of inositol phenotype (Opi-) due to the derepression and transcription of the rate limiting biosynthetic enzyme within this pathway, *INO1* (PATTON-VOGT *et al.* 1997; CHANG *et al.* 2002). Surprisingly, we (Figure 3.9) and others have shown that the NuA4 mutants exhibit a derepression of *INO1* and inositol production or Opi- phenotype (HANCOCK *et al.* 2006; SALAS-SANTIAGO AND LOPES 2014). We then anticipated that NuA4 mutants would suppress the growth defect of *sec14-1$^{ts}$* under inositol-depleted conditions. To test this hypothesis, NuA4 mutants *eaf1Δ, eaf7Δ,* and the temperature sensitive *ESA1* mutant, *esa1-L254P$^{ts}$* (CLARKE *et al.* 1999), were crossed with *sec14-1$^{ts}$* and growth was assessed under both inositol-replete and -depleted conditions (**Figure 3.11**). As expected, *sec14-1$^{ts}$eaf7*Δ cells display synthetic sickness upon increased temperature in inositol-supplemented media (CURWIN *et al.* 2009)(Figure 3.6), and similar interactions were seen for the double mutants of *sec14-1$^{ts}$* with *eaf1*Δ and *esa1-L254P$^{ts}$*. As was also expected, *sec14-1$^{ts}$* cells exhibited a growth defect in inositol-depleted media at the semi-permissive temperature 33.5°C (PATTON-VOGT *et al.* 1997) (**Figure 3.11A**). While the *eaf1Δ* and *eaf7Δ* single mutants grew similarly between both conditions, (**Figure 3.11A-B**), we were surprised to see that *esa1-L254P$^{ts}$* cells displayed growth defects in inositol-depleted media (**Figure 3.11C**). In combination, the double mutants *sec14-1$^{ts}$eaf1Δ*, *sec14-1$^{ts}$eaf7Δ*, and *sec14-1$^{ts}$esa1-L254P$^{ts}$* all showed a synthetic growth defect at 30°C in inositol-depleted media compared to *sec14-1$^{ts}$* (**Figure 3.11**). These results suggest that, though *eaf1Δ* and *eaf7Δ* do not display detectable growth defects under inositol-depleted conditions like *esa1-L254P$^{ts}$*, these mutants do in fact exacerbate these growth defects for *sec14-1$^{ts}$* under normally permissive temperatures. However as the synthetic sickness between NuA4 mutants and *sec14-1$^{ts}$* at the semi-permissive temperature could not be

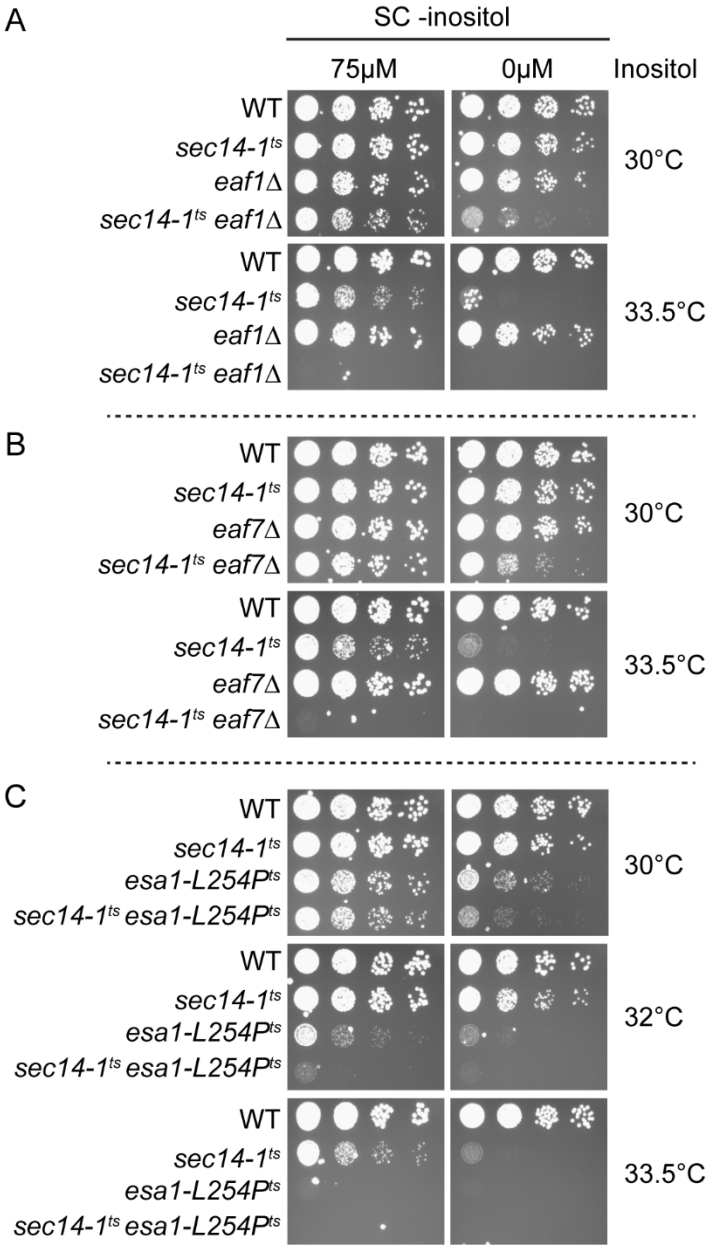
A
SC -inositol
75μM
0μM
Inositol
WT
sec14-1ts
eaf1Δ
sec14-1ts eaf1Δ
30°C
WT
sec14-1ts
eaf1Δ
sec14-1ts eaf1Δ
33.5°C
B
WT
sec14-1ts
eaf7Δ
sec14-1ts eaf7Δ
30°C
WT
sec14-1ts
eaf7Δ
sec14-1ts eaf7Δ
33.5°C
C
WT
sec14-1ts
esa1-L254Pts
sec14-1ts esa1-L254Pts
30°C
WT
sec14-1ts
esa1-L254Pts
sec14-1ts esa1-L254Pts
32°C
WT
sec14-1ts
esa1-L254Pts
sec14-1ts esa1-L254Pts
33.5°C

**Figure 3.11 NuA4 mutants exacerbate the growth defects of *sec14-1$^{ts}$* in inositol-depleted media.**Combination of the NuA4 mutants **A)** *eaf1Δ*, **B)** *eaf7Δ*, and **C)** *esa1-L254P$^{ts}$* increase the growth defects of the *SEC14* temperature-sensitive mutant, *sec14-1$^{ts}$*, under inositol-depleted conditions. Wildtype (YKB1079), *sec14-1$^{ts}$* (YKB3144), *eaf1Δ* (YKB3333), *sec14-1$^{ts}$eaf1Δ* (YKB3935), *eaf7*Δ (YKB3292), *sec14-1$^{ts}$eaf7*Δ (YKB4068), *esa1-L254P$^{ts}$* (YKB4236), and *sec14-1$^{ts}$esa1-L254P$^{ts}$* (YKB4242) cultures were grown to mid-log phase prior to being diluted to an $OD_{600}$ of 0.1 and 4 times 10-fold serial dilutions were spotted on SC-inositol media supplemented with indicated amount of myo-inositol. Plates were incubated for two days at 30°C, 32°C, or 33.5°C and images are representative of three biological replicates.

rescued by supplemented inositol, this suggest that inositol defects are not the root-cause of the *OSH4*/*CKI1*-independent mechanisms by which NuA4 is required to buffer *sec14-1$^{ts}$* defects.

### 3.2.7 Lipid droplet formation is impaired in *sec14-1$^{ts}$eaf1Δ*

Given the fact that ICRE-regulated genes are misregulated in NuA4 mutants, we wanted to determine which, if any, lipid metabolic pathways were affected in *sec14-1$^{ts}$eaf1Δ*. Under inositol depleted conditions, not only do cells require inositol but also the ability to synthesize both TAG and SE, or neutral lipids, for survival (GASPAR *et al.* 2011). Intriguingly, like *sec14-1$^{ts}$eaf1*Δ cells, *dga1Δlro1Δare1Δare2Δ* cells- a strain with abolished triacylglycerol (TAG) and steryl ester (SE) biosynthesis- is not able to grow in the absence of inositol at higher temperatures, this despite *INO1* expression (GASPAR *et al.* 2011). Therefore, we asked if *sec14-1$^{ts}$eaf1Δ* increased growth defects under inositol-depleted conditions were due to defects in TAG and SE biosynthesis. The formation of lipid droplets is an established proxy for TAG and SE biosynthesis (WANG 2015). Therefore, we examined lipid droplet formation under inositol-replete and -depleted conditions in the wildtype, *sec14-1$^{ts}$, eaf1Δ,* and *sec14-1$^{ts}$eaf1Δ* strains at 30°C using a fluorescent lipid-droplet marker (**Figure 3.12A**). Upon inositol-depletion, both wildtype and *sec14-1$^{ts}$* cells emitted a nearly 3-fold increase in fluorescence density compared to inositol-supplemented conditions, which is in agreement with previous reports of increased neutral lipid levels in cells under inositol-depleted conditions (**Figure 3.12A-B**) (GASPAR *et al.* 2011). In contrast, deletion of *eaf1Δ* in either the wild type or *sec14-1$^{ts}$* background resulted in a reduction in the fluorescence intensity of lipid droplets. This finding suggests that neutral lipid biogenesis is significantly impaired in *eaf1Δ*, which could explain the increased growth defects of *sec14-1$^{ts}$eaf1*Δ cells under inositol-depleted conditions.

### *3.2.8* Inhibition of *de novo* fatty acid biosynthesis has a detrimental effect on *sec14-1$^{ts}$* growth and is epistatic with *eaf1Δ*

To investigate if defects in neutral lipid biosynthesis were the cause of the *sec14-1$^{ts}$eaf1Δ* increased growth defects under inositol-depleted conditions, we examined the growth

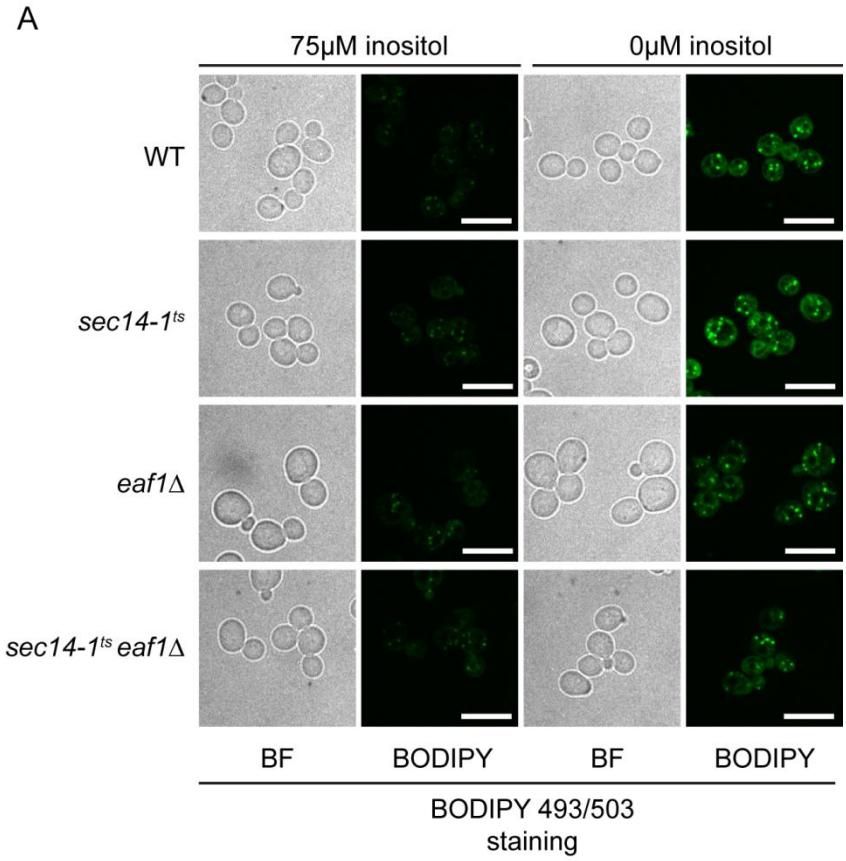
A
75μM inositol
0μM inositol
WT
sec14-1ts
eaf1Δ
sec14-1ts eaf1Δ
BF
BODIPY
BF
BODIPY
BODIPY 493/503
staining

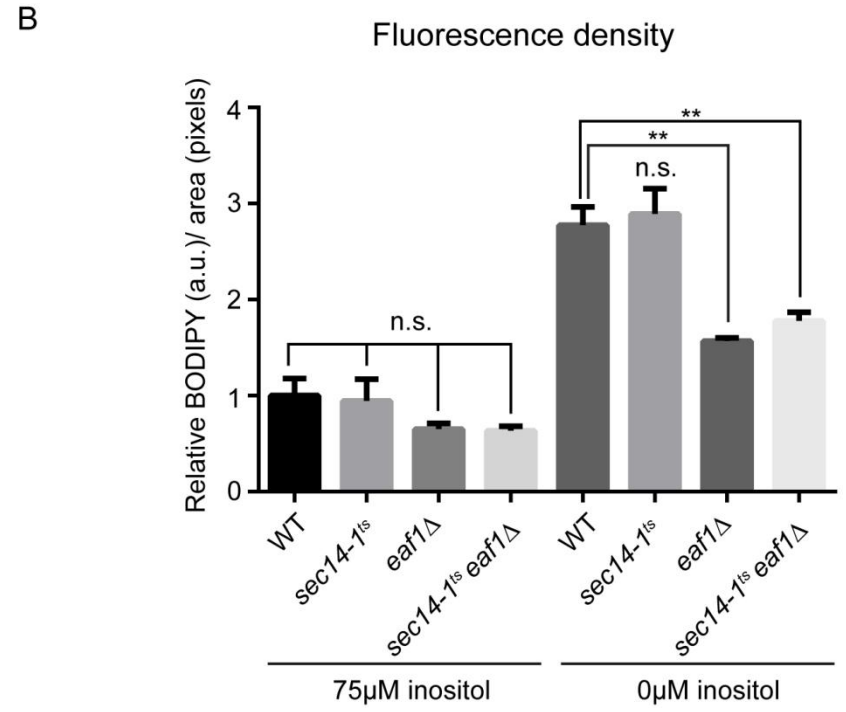
B
Fluorescence density
Relative BODIPY (a.u.)/ area (pixels)
0
1
2
3
4
n.s.
**
**
n.s.
WT
sec14-1ts
eaf1Δ
sec14-1ts eaf1Δ
WT
sec14-1ts
eaf1Δ
sec14-1ts eaf1Δ
75μM inositol
0μM inositol

**Figure** 3**.12 Lipid droplet dynamics is impaired in *EAF1* deletion mutants. A)** Wildtype (YKB1079), *sec14-1$^{ts}$* (YKB3144), ***eaf1Δ*** (YKB3333), and *sec14-1$^{ts}$**eaf1Δ*** (YKB3935) were grown to mid-log phase in SC media at 30°C before shifting to inositol-supplemented (75 µM myo-inositol) SC media or inositol-depleted SC media for 2 hours at 30°C prior to being stained with 10µM BOPIDY 493/503 for 10 min before imaging. Images shown are mid-field view of representative cells for each sample (Scale bar =10 µm). **B)** Graphic display of the mean relative fluorescence density for each strain and condition. Cells were first segmented from brightfield images using a custom Matlab script then fluorescence was measured for each cell using the outlines (see Materials and Methods for details). Mean fluorescence density was measured from 100 cells across three biological replicates relative to WT fluorescence in inositol supplemented media (+S.E.M.). Statistical analysis was performed by one-way ANOVA with Tukey's multiple comparisons test: *p-value <0.05; n.s. not significant. Danny Salem (Kaerns lab; UOttawa) measured fluorescence density (Figure 3.12A).

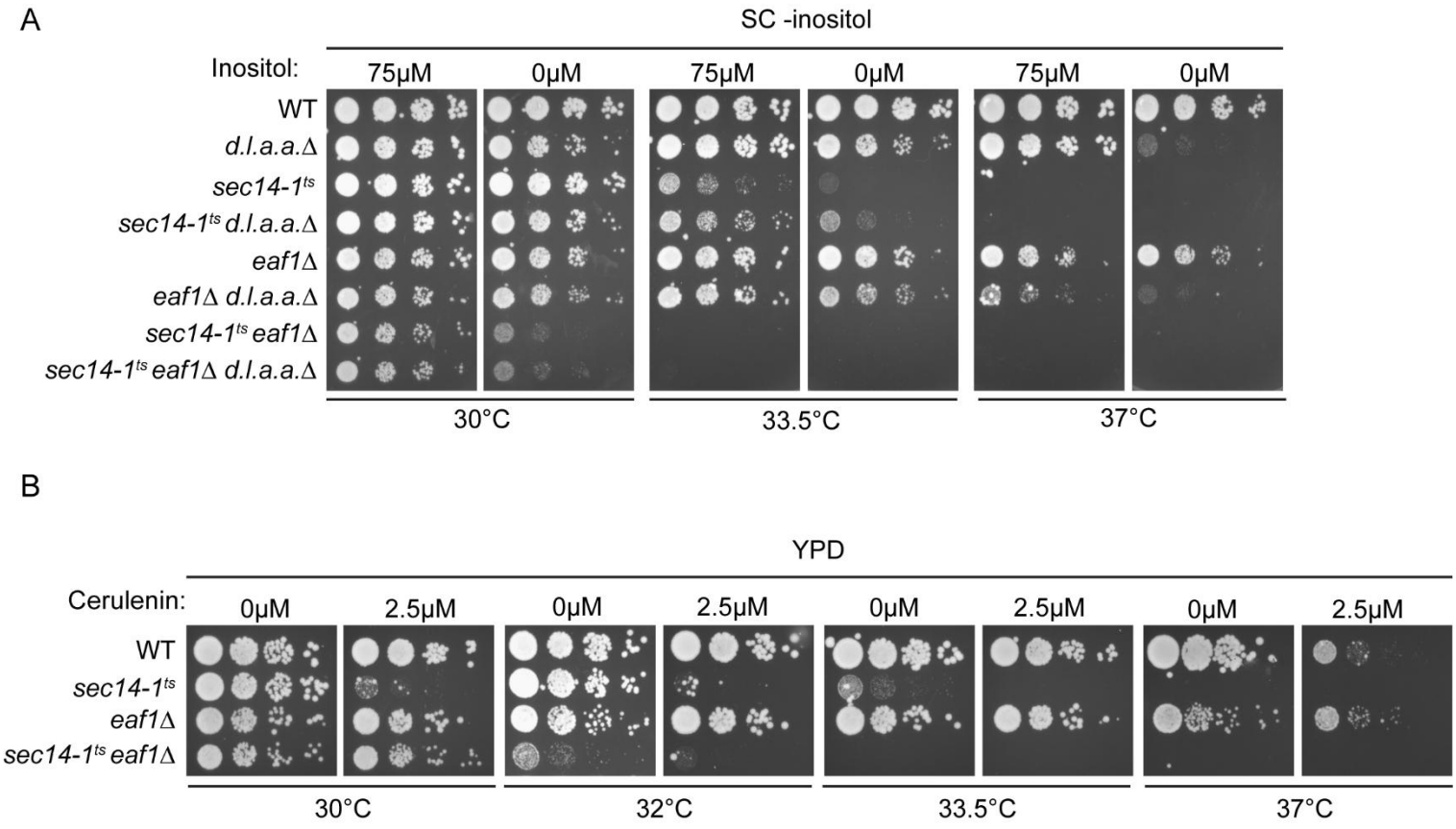
A
SC -inositol
Inositol:
75μM
0μM
75μM
0μM
75μM
0μM
WT
d.l.a.a.Δ
sec14-1ts
sec14-1ts d.l.a.a.Δ
eaf1Δ
eaf1Δ d.l.a.a.Δ
sec14-1ts eaf1Δ
sec14-1ts eaf1Δ d.l.a.a.Δ
30°C
33.5°C
37°C
B
YPD
Cerulenin:
0μM
2.5μM
0μM
2.5μM
0μM
2.5μM
0μM
2.5μM
WT
sec14-1ts
eaf1Δ
sec14-1ts eaf1Δ
30°C
32°C
33.5°C
37°C

**Figure 3.13 Inhibition of fatty acid biosynthesis causes synthetic growth defect in *sec14-1$^{ts}$* A)** Genetic inhibition of triacylglycerol and steryl ester biosynthesis does not affect the growth of *sec14-1$^{ts}$*. Wildtype (YKB1079), *dga1Δlro1Δare1Δare2Δ* (d.l.a.a.Δ; YKB4336), *sec14-1$^{ts}$* (YKB3144), *sec14-1$^{ts}$d.l.a.a.Δ* (YKB4337), *eaf1Δ* (YKB3333), *eaf1Δd.l.a.a.Δ* (YKB4338), *sec14-1$^{ts}$eaf1Δ* (YKB3935), and *sec14-1$^{ts}$eaf1Δ d.l.a.a.Δ* (YKB4339) cultures were grown in YPD at 30°C prior to being diluted to an $OD_{600}$ of 0.1 and 4 times 10-fold serial dilutions were spotted on SC-inositol media supplemented with indicated amount of myo-inositol and incubated for two days at 30°C. **B)** Inhibition of fatty acid biosynthesis by cerulenin treatment causes synthetic growth defect with *sec14-1$^{ts}$*. Wildtype (YKB1079), *sec14-1$^{ts}$* (YKB3144), *eaf1Δ* (YKB3333), *sec14-1$^{ts}$eaf1Δ* (YKB3935), cultures were grown in YPD at 30°C prior to being diluted to an $OD_{600}$ of 0.1 and 4 times 10-fold serial dilutions were spotted on YPD with indicated amounts of cerulenin for two days at 30°C. Images are representative of three biological replicates.

of *sec14-1$^{ts}$* strains when both TAG and SE biosynthesis are eliminated (**Figure 3.13A**). TAG and SE biosynthesis can be completely abolished in yeast by deleting Dga1, Lro1, Are1, and Are2- the proteins responsible for all neutral lipid biosynthesis in yeast (OELKERS *et al.* 2002; SANDAGER *et al.* 2002). As previously shown, *dga1Δlro1Δare1Δare2Δ* (*d.l.a.a.Δ*) cells do not display defects in inositol-replete conditions, but become inositol auxotrophs at 37°C (GASPAR *et al.* 2011) (**Figure 3.13A**). In inositol-replete or depleted conditions at 30°C, *dga1Δlro1Δare1Δare2Δ* (*d.l.a.a.Δ*) combined with *sec14-1$^{ts}$* or *eaf1Δ* does not impair growth. Further, the addition of *dga1Δlro1Δare1Δare2Δ* does not increase the growth defects of *sec14-1$^{ts}$eaf1*Δ cells at 30°C. This suggests the growth defect of *sec14-1$^{ts}$eaf1Δ* under inositol-depleted conditions or at higher temperatures is not due to defects in neutral lipid biosynthesis.

However, while inhibition of TAG and SE biosynthesis is not the cause of the growth defects of *sec14-1$^{ts}$eaf1Δ* in inositol-depleted media, loss of lipid droplet formation reflects defects somewhere downstream of the neutral lipid biosynthesis pathway. Therefore, we examined whether the *de novo* biosynthesis of fatty acids, a requisite precursor for neutral lipid biosynthesis, was involved in the negative genetic interaction between *sec14-1$^{ts}$* and *eaf1Δ*. For this purpose, we used cerulenin -a fatty acid analog which inhibits the enzymatic activity of fatty acid synthases *FAS1* and *FAS2* (KAWAGUCHI *et al.* 1979; KAWAGUCHI *et al.* 1982), to determine the effect of inhibiting fatty acid biosynthesis on *sec14-1$^{ts}$* growth. We found that while the growth of wildtype and *eaf1Δ* cells were not impacted by 2.5 µM cerulenin treatment at 30°C, growth of *sec14-1$^{ts}$* cells were hypersensitive to these conditions (**Figure 3.13B**). Interestingly, the cerulenin sensitivity at 30°C of *sec14-1$^{ts}$* cells was rescued by deletion of *EAF1*. At 32°C and 33.5°C, cerulenin treatment affected *sec14-1*$^{ts}$ growth to a similar extent as *sec14-1$^{ts}$eaf1*Δ in the absence of cerulenin treatment which demonstrates an epistatic effect between deleting *EAF1* and inhibiting the fatty acid synthases *FAS1/FAS2* on the observed *sec14-1$^{ts}$* growth defect, at least at higher temperatures. This suggests that the cause of the disrupted

phospholipid homeostasis in NuA4 mutants, including their negative genetic interaction with *sec14-1*$^{ts}$ and the loss of lipid droplets, originates from defects within the fatty acid biosynthesis pathway.

## 3.3 Discussion

**The lysine acetyltransferase complex NuA4 is required for the *sec14* bypass**

The *sec14* bypass phenotype offers important insight on pathways and mechanism which coordinate lipid homeostasis in compensation for Sec14-deficient conditions. We report a novel role for the lysine acetyltransferase complex, NuA4, as a mediator of these compensatory pathways. Deletion or mutants of NuA4 subunits caused a consistent growth defect both in *sec14-1*$^{ts}$ background and in *OSH4*-overexpressed conditions (**Figure 3.4**). This proved to be an effect particular to NuA4 mutants as most of the other KAT mutants and KDAC mutants, other than *rtt109Δ*, did not affect the growth under *sec14* conditions or of *OSH4*-overexpressed conditions (**Figure 3.1-3.2**). We chose not to pursue our investigation into the role of Rtt109 on the function of Sec14 as the deletion mutant's effect on growth were not as important as Eaf1 (**Figure 2.1-2.2**) and the negative genetic interaction between *rtt109Δ* and *eaf1Δ* suggested distinct parallel roles between the two KATs on Sec14 (**Figure 3.3**).

Deletion of either *OSH4* or *CKI1* only partially suppressed Sec14-deficient growth defect in a NuA4 mutant background (**Figure 3.6**). This implies that the *sec14* bypass pathway relies heavily on a functional NuA4 complex. However, a partial suppression also suggests that NuA4 mutants might genetically interact with *sec14-1*$^{ts}$ through pathway both dependent and independent of *OSH4/CKI1*. Recent communication with our collaborators at A&M University in Texas, Dr. Vytas Bankaitis and Dr. Ju Huang, also noted that in their own strain background, SEY6210/SEY6211, deletion of *OSH4* completely suppresses the negative growth defects of *sec14-1*$^{ts}$*eaf1Δ* at 37°C, but deletion of *CKI1* does not (Huang *et al.* 2016; preparing for submission to *Cell*). This lead us to conclude that NuA4 might have multiple target within the

lipid biosynthesis pathway that effect Sec14-deficient conditions, including some targets whose function depend on *OSH4*. The subject of my second chapter will touch more on this subject. For this aim, we decided to continue our investigation into the *OSH4*-idenpendent targets of NuA4.

**NuA4 mutants increase the inositol auxotrophy of *sec14$^{ts}$* cells despite *INO1* induction**

NuA4 mutants are known to exhibit the Opi- phenotype, which is the overproduction of inositol caused by the derepression and transcription of *INO1* (HANCOCK *et al.* 2006; SALAS-SANTIAGO AND LOPES 2014). Although s*ec14-1$^{ts}$* had been previously reported as having growth defects under inositol-depleted conditions (PATTON-VOGT *et al.* 1997), a high-throughput study that tested non-essential mutants for inositol auxotrophy did not identify any NuA4 mutants with this phenotype (VILLA-GARCIA *et al.* 2011). We initially hypothesized that the introduction of NuA4 mutants into a *sec14-1$^{ts}$* background would restore *INO1* expression and rescue growth on inositol-depleted media. Instead, we found that the combination of *sec14-1$^{ts}$* and NuA4 mutants resulted in an increased growth defect under inositol-depleted conditions, this despite *INO1* derepression (**Figure 3.9- 3.11**). In contrast, deletion mutants of genes within the CDP-choline pathway, *CKI1*, *PCT1* and *CPT1*, required for phosphatidylcholine synthesis have been shown to not only exhibit an Opi- phenotype but also suppress the growth defect of the *sec14-1$^{ts}$* mutant under inositol-depleted conditions (PATTON-VOGT *et al.* 1997; CHANG *et al.* 2002).

Although the mutants of the CDP-choline pathway exhibit a relatively stronger Opi- phenotype then NuA4 mutants (HANCOCK *et al.* 2006), we did not expect the growth defect of *sec14-1$^{ts}$* under inositol-depleted conditions to worsen in combination with NuA4 mutants. This suggests that survival under inositol-depleted conditions requires more than just *INO1* induction. Our transcriptional data showed that derepression and transcription of *INO1* was occurring in *sec14-1$^{ts}$eaf1Δ*, but derepression was not extended to all ICRE-regulated phospholipid genes. The main transcriptional activator of ICRE-regulated genes, *INO2*, which is normally induced

under similar conditions as *INO1,* remained at basal levels of transcription in *sec14-1$^{ts}$eaf1Δ* cells (**Figure 3.9D**). This suggests that the induction of *INO1* in *sec14-1$^{ts}$eaf1Δ* cells, and other NuA4 mutants (HANCOCK *et al.* 2006; SALAS-SANTIAGO AND LOPES 2014), may not be dependent on *INO2*, potentially explaining why most ICRE-regulated genes are not induced in *sec14-1$^{ts}$eaf1Δ* cells.

One possible mechanism for the induction of *INO1* expression in *sec14-1$^{ts}$eaf1Δ* cells could be through the downregulation of *CDS1* expression (**Figure 3.9**). It has been shown that lowering expression of the essential gene *CDS1* causes on Opi- phenotype and induction of *INO1* expression, much like NuA4 mutants (SHEN AND DOWHAN 1996; SALAS-SANTIAGO AND LOPES 2014). However, reduction of *CDS1* causes an increase in both PA and TAG levels resulting in super-sized lipid droplets (FEI *et al.* 2011), which is not seen in *eaf1Δ* cells (**Figure 3.12**). One intriguing possibility is the Opi- phenotype of NuA4 mutants is an indirect consequence of the cell trying to compensate for defects in TAG and SE biosynthesis, resulting in the reduction of *CDS1.* This may also explain why overexpression of *CDS1* is toxic in eaf1Δ cells (**Figure 3.10A**). Indeed, it remains to be determined if NuA4-dependent acetylation of histones is directly regulating the transcription of the eight lipid metabolism genes identified in our screen, or if the changes in gene expression reflect a transcriptional compensation mechanism independent of NuA4's nuclear activity.

**NuA4 regulates lipid droplet formation through the fatty acid biosynthesis pathway**

A decrease in lipid droplet formation despite the derepression of *INO1* expression is characteristic of the quadruple mutant *dga1Δlro1Δare1Δare2Δ* that is unable to synthesize neutral lipids (MULLNER AND DAUM 2004; GASPAR *et al.* 2011). Further, like our *esa1-L254P$^{ts}$* mutant cells (**Figure 3.11C**), *dga1Δlro1Δare1Δare2Δ* cells are sensitive to inositol-depleted conditions (GASPAR *et al.* 2011). However, the loss of neutral lipid biosynthesis did not account

for the negative genetic interaction between NuA4 and Sec14 nor did it account for the increased growth of *sec14-1$^{ts}$eaf1Δ* on inositol-depleted media at 30°C (**Figure 3.13A**).

An alternative explanation could be that defective lipid droplet formation in ***eaf1Δ*** cells is caused by a lack of fatty acid substrate. We demonstrated that the inhibition of the fatty acid biosynthesis pathway by cerulenin dramatically increased the growth defect of *sec14-1$^{ts}$* to a similar extent as untreated *sec14-1$^{ts}$eaf1Δ at* 32°C and 33.5°C (**Figure 3.13B**). As inhibition of the fatty acid biosynthesis pathway did not further decrease the viability of *sec14-1$^{ts}$eaf1Δ,* it would suggest that fatty acid biosynthesis may already be compromised in ***eaf1Δ*** cells at higher temperatures. The suppressive effect of *sec14-1$^{ts}$eaf1Δ* on cerulenin treatment compared to *sec14-1$^{ts}$*at 30°C remains unresolved. Potentially, increased expression of both *FAS1* and *FAS2* in *sec14-1$^{ts}$eaf1Δ* (**Figure 3.9**) may be able to buffer the effects of cerulenin at 30°C, but, upon increasing temperatures, the negative effect of ***eaf1Δ*** on *sec14-1$^{ts}$* outweighs the negative effect of cerulenin. The fact remains that the effect of inhibiting fatty acid synthases in *sec14-1$^{ts}$* cells is non-additive to the effect of deleting *EAF1,* which suggests an epistatic interaction between *EAF1* and *FAS1/FAS2*.

Our proposed theory that NuA4 regulates the fatty acid biosynthesis pathway accounts for most of the phenotypes reported in this paper. Inhibition of the fatty acid biosynthesis pathway negatively affects neutral lipid biosynthesis and lipid droplet formation as they are the principal substrates in these pathways (HENRY *et al.* 2012; WANG 2015). Similarly to NuA4 mutants, downregulation of the fatty acid biosynthesis pathway leads to the derepression and transcription of *INO1* (SHIRRA et al. 2001). Whether or not the inhibition of the fatty acid biosynthesis pathway is the primary cause behind *INO1* transcriptional activation in NuA4 mutants remains to be confirmed. One potential experiment to test this hypothesis would be to determine the effect of overexpressing *FAS1/FAS2* in the NuA4 mutants to see whether or not they can suppress *INO1* transcriptional activation and lipid droplet decrease. Conversely, the

opposite effect is observed when this pathway is activated. Overexpression of genes responsible for fatty acid biosynthesis represses the transcription of *INO1* (SHIRRA *et al.* 2001; FEDDERSEN *et al.* 2007) and increased fatty acid biosynthesis causing a dramatic accumulation of lipid droplet (HOFBAUER *et al.* 2014). This suggests that NuA4 is a positive regulator of the fatty acid biosynthesis pathway. While this could occur through NuA4-dependent regulation of transcriptional events, NuA4 may also have potential targets within the fatty acid biosynthesis pathway. Indeed, lysine acetylation of proteins in this pathway, including Fas1 and Fas2, have been detected in both yeast and higher organisms (CHOUDHARY *et al.* 2009; HENRIKSEN *et al.* 2012; WEINERT *et al.* 2014; DOWNEY *et al.* 2015; MADSEN *et al.* 2015). In order to determine if acetylation of Fas1/Fas2 is regulating their function, one could determine the specific lysine residues that are targeted by acetylation and conduct fatty acid synthase activity assay on mutants that mimic either its acetylated form (lysine to glutamine) or unacetylated form (lysine to arginine). Alternatively, hyper-activation of AMPK1/Snf1 in NuA4 mutants (LU *et al.* 2011) might also contribute to downregulation of the fatty acid biosynthesis pathway (HOFBAUER *et al.* 2014). In order to determine if this is the case, we could compare lipid droplet formation and *INO1* transcription in mutant strains that express the Snf1 hyperactive mutant (LU *et al.* 2011). While the mechanism(s) through which NuA4 is contributing to cellular lipid homeostasis remain to be deciphered, our work introduces that NuA4 have underappreciated roles in lipid homeostasis.

# 4 Chapter 2: The effect of lysine acetylation on Oxysterol-Binding Proteins

## 4.1 Brief introduction

In the previous chapter, we had demonstrated that NuA4 mutants had deleterious effects on both *OSH4*- and *CKI1*-dependent *sec14* bypass (**Figure 3.6**). However, we had also discussed the possibility that NuA4 has multiple targets within the phospholipid metabolic pathways, some of which whose function were dependent on *OSH4*. The growth defect between NuA4 mutant *eaf1Δ* and Sec14 mutant, *sec14-1$^{ts}$*, were at least somewhat dependent on *OSH4* because *osh4Δ* partially suppressed *sec14-1$^{ts}$eaf1Δ* growth defects (**Figure 2.6A**). Additionally, we have evidence that the extent of the suppressive effect of *osh4Δ* on *sec14-1$^{ts}$eaf1Δ* is even greater in another yeast background (Huang *et al.* 2016; preparing for submission to *Cell*). Furthermore, we found within a previously conducted genome-wide synthetic dosage lethal screen that ***eaf7Δ*** specifically inhibited *CKI1*-dependent *sec14* bypass but not *OSH4*-dependent *sec14* bypass (FAIRN *et al.* 2007). Therefore, we hypothesized that NuA4 could be targeting proteins whose function directly related to Osh4. Osh4 is a conserved lipid-binding protein that regulates PI-4-P metabolism by stimulating the activity of the PI-4-P phosphatase Sac1 which subsequently hydrolyses PI-4-P into PI (FAIRN *et al.* 2007; STEFAN *et al.* 2011). Prior to the start of our investigation, results from a high-throughput acetylome study identified three acetylation sites on Osh4: K109, K168, and K247 (HENRIKSEN *et al.* 2012). The function of Osh4 depends on its lipid-binding affinity towards PI-4-P and sterols that requires specific interactions between the lipid and several side chains of the amino acid sequence of Osh4, including lysine K109 and K168 (IM *et al.* 2005; RAYCHAUDHURI *et al.* 2006; DE SAINT-JEAN *et al.* 2011). This led us to believe that lysine acetylation could potentially regulate the function of Osh4.

In this study, we screened point mutants of Osh4 that replicated either acetylated lysine or unacetylated lysine and discovered that the acetylated mimic, K109Q, inhibited both the function and localization of the protein *in-vivo* while the unacetylated mimic, K109R, retained some function and was localized similar to wildtype Osh4. Finally, we discovered that one other homologue of Osh4, Osh1, is also acetylated on the Osh4 K109-equivalent lysine residue, K874. Altogether our model suggests a potentially conserved mechanism by which acetylation inhibits the function of Oxysterol-Binding Proteins.

## 4.2 Results

### 4.2.1 Osh4 conserved lysine residue and potential acetylation site, K109, is critical for function

We initially attempted to confirm the acetylation sites on Osh4 using a mass spectrometry-based approach adapted for purified protein complexes (MITCHELL *et al.* 2013). As a proof of our mass spectrometry method, we analyzed the peptide sequences of a purified Osh4 recombinant protein sample containing an incorporated acetyl group on lysine K109 (Osh4-K109Ac) (**Table 4.1 ID#1**) (Huang *et al.* 2016; Preparing for submission to *Cell*). As expected, we were able to detect acetylation on lysine K109 on six unique peptides from Osh4-K109Ac samples. In comparison, we could not detect any acetylation sites on wildtype Osh4 recombinant protein without the incorporated acetyl group (**Table 4.1 ID#2**). The fact that we could detect acetylation on lysine K109 of Osh4 on the recombinant protein validates this particular method used to identify acetylation on purified Osh4.

Our next goal was to attempt to identify naturally occurring acetylation sites on Osh4 purified from yeast cells. For experimental purposes, we varied the purification strategy of Osh4 by using different epitope tags (GFP, TAP), different growth conditions (log phase, stationary phase, temperatures), and different strain backgrounds (*rpd3Δsir2Δ*, *sec14-1$^{ts}$*) in order to increase our chance of finding acetylation sites on Osh4 (**Table 4.1 ID#3-9**). For each

**Table 4.1 LC/MS/MS experiment conducted on Osh4 samples**

| ID | LC/MS/MS experiment* | # of replicates | Total peptides (Unique peptides) | Protein sequence coverage | Detected acetylation site(s) (# peptide(s)) |
|---|---|---|---|---|---|
| **1** | Osh4-K109Ac (recombinant protein) | 1 | 280 (82) | 76% | K109 (6) |
| **2** | Osh4 (recombinant protein) | 1 | 570 (98) | 81% | - |
| **3** | IP-GFP: Osh4-GFP | 1 | 361(118) | 85.7% | - |
| **4** | IP-TAP: Osh4-TAP | 2 | 760 (85)<br>646 (76) | 85%<br>84% | - |
| **5** | IP-TAP: Osh4-TAP (stationary phase) | 1 | 71 (60) | 81.6% | - |
| **6** | IP-TAP: Osh4-TAP (*rpd3Δ sir2Δ*) | 2 | 403(79)<br>763(83) | 84%<br>85% | -<br>- |
| **7** | IP-TAP: Osh4-TAP (stationary phase; *rpd3Δ sir2Δ*) | 1 | 71(63) | 73.3% | - |
| **8** | IP-GFP: Osh4-GFP (*sec14-1$^{ts}$;* non-permissive temperature) | 1 | 78(59) | 77% | - |
| **9** | IP-TAP: Osh4-TAP (*sec14-1$^{ts}$;* non-permissive temperature) | 1 | 135(64) | 71% | - |

* Complete MS results, including spectras, are available upon request

experiment, the protein sequence coverage of Osh4 surpassed 70% and included coverage of the regions surrounding all three previously identified acetylation sites (K109, K168, K247). However, despite favorable sequence coverage, including peptides covering K109 amino acid, we were unable to detect acetylation on any peptide sequences of Osh4. Furthermore, subsequent analysis for different post-translation modifications failed to identify any significant modifications on Osh4. Our results would suggest that lysine acetylation does not target Osh4 to an appreciable extent. However, as methods for detecting acetylation sites on extracted proteins are still being optimized, our results cannot conclusively refute the hypothesis that Osh4 is acetylated *in-vivo*. We therefore pursued our investigation on the previously identified acetylation sites.

We generated point mutations by site-directed mutagenesis on each of the previously detected acetylation sites (K109, K168, K247) to either mimic its acetylated state (lysine (K) to glutamine (Q)) or mimic its unacetylated state (lysine (K) to arginine (R)). We confirmed stable protein expression for each generated point mutants by immunoblot which, at the same time, suggests that acetylation does not affect protein levels of Osh4 (**Figure 4.1A**). Two distinct growth assays were used to assess the effect of each mutant on the function of the protein (**Figure 4.1B-C**). The first growth assay addressed the ability of each mutant to rescue the lethality of an Osh-deficient strain. In yeast, the seven Oxysterol-Binding Protein homologues share a redundant essential function for growth and viability and the expression of a functional copy of Osh4, or any other Osh protein, is sufficient to rescue this lethal phenotype (BEH *et al.* 2001). Therefore, we expressed a copy of each Osh4 acetylation mimics into an Osh-deficient strain to compare their ability to rescue this lethal phenotype (**Figure 4.1B**). The strain background we used for this experiment lacked expression of all seven *OSH* genes apart from a single copy of a temperature-sensitive point mutant of Osh4, *osh4-1*$^{ts}$, whose growth is only impaired at non-permissive temperatures of 37°C (*osh1-7Δ osh4-1*$^{ts}$) (BEH AND RINE 2004). As

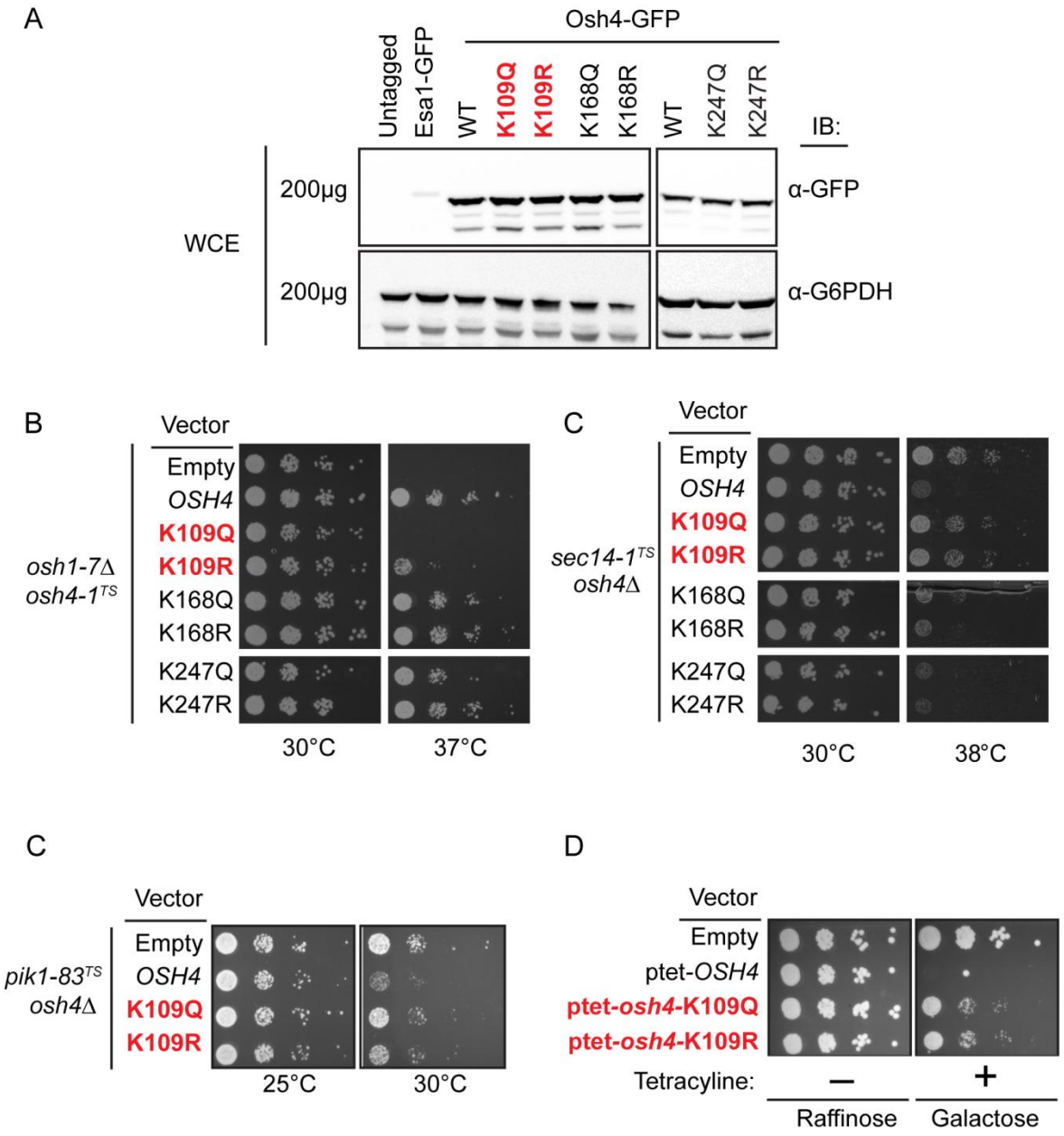
A
Osh4-GFP
Untagged
Esa1-GFP
WT
K109Q
K109R
K168Q
K168R
WT
K247Q
K247R
IB:
WCE
200µg
α-GFP
200µg
α-G6PDH
B
Vector
Empty
OSH4
K109Q
K109R
K168Q
K168R
K247Q
K247R
osh1-7Δ
osh4-1TS
30°C
37°C
C
Vector
Empty
OSH4
K109Q
K109R
K168Q
K168R
K247Q
K247R
sec14-1TS
osh4Δ
30°C
38°C
C
Vector
Empty
OSH4
K109Q
K109R
pik1-83TS
osh4Δ
25°C
30°C
D
Vector
Empty
ptet-OSH4
ptet-osh4-K109Q
ptet-osh4-K109R
Tetracyline:
–
+
Raffinose
Galactose

**Figure 4.1 Osh4 acetylation mimic, K109Q, inhibits in-vivo function whereas the unacetylated mimic, K109R, displays partial function. A)** Protein levels of Osh4 are unaffected by point mutations that mimics either acetylated lysine (K to Q) or mimics unacetylated lysine (K to R) on potential acetylation sites. *osh4*Δ (YKB3344) was transformed with empty vector (untagged; pRS415) or a plasmid expressing different construct of GFP-tagged Osh4. The transformed strains as well as endogenously GFP-tagged Esa1 (YKB2002) were grown in YPD media to mid-log phase, harvested and lysed. GFP-tagged protein was purified by GFP-immunopurification from 12.5mg of WCE. Immunoprecipitates were run on 9% acrylamide gel through SDS-PAGE and transferred to a nitrocellulose membrane. Membranes were immunoblotted using indicated antibodies. **B)** The K109 acetylation mimic of Osh4, K109Q, prevents the rescue of *OSH* deficient cells whereas the unacetylated mimic, K109R, partially rescues growth. *osh1-7Δ osh4-1*$^{ts}$ (YKB3197) was transformed with a empty vector (pRS416) or with a plasmid expressing different construct of *OSH4* . **C)** Both the K109 acetylation and unacetylated mimic of Osh4, K109Q and K109R, inhibit *OSH4*-dependent *sec14-1*$^{ts}$ growth defect. *sec14-1*$^{ts}$ *osh4Δ* (YKB3344) strain was transformed with a empty vector (pRS416) or with a plasmid expressing different construct of *OSH4*. **D)** Both the K109 acetylation and unacetylated mimic of Osh4, K109Q and K109R, inhibit *OSH4*-dependent *pik1ts* growth defect. *pik1-83*$^{ts}$ *osh4Δ* (YKB3707) strain was transformed with a empty vector (pRS416) or with a plasmid expressing Osh4, osh4-K109Q or osh4-K109R. **E)** Osh4 acetylation mimic, K109Q, and unacetylated mimic, K109R, inhibits *OSH4* overexpression-induced toxicity. Wildtype (YKB1079) strain was transformed with an empty vector (pRS413), or a GAL-dependent tetracycline inducible reporter with different construct of *OSH4*: WT construct (ptet-*OSH4*; PKB299), acetylated mimic (ptet-*osh4-K109Q*; PKB300), unacetylated mimic (ptet-*osh4-K109R*; PKB301). All cultures were grown in selective media at 30°C prior to being diluted to an $OD_{600}$ of 0.1 and 4 times 10-fold serial dilutions were spotted on indicated media for 2-3 days at indicated temperatures. Representative figures from three separate experiments are shown.

expected, expression of the wildtype copy, *OSH4,* was sufficient to rescue growth at 37°C. Comparatively, expression of the lysine K168 and lysine K247 mutants did not impair the Osh4s' ability to restore growth suggesting that acetylation of those lysine residues does not affect function. However, the expression of the lysine K109 point mutants did have an effect on the function of Osh4. Expression of the acetylated mimic, K109Q, was unable to rescue growth at 37°C, whereas expression of the unacetylated mimic, K109R, partially rescued growth at 37°C. This demonstrated that lysine K109 of Osh4 is critical for function. Additionally, it provides evidence of functional distinction between the acetylated mimic (inactive) and unacetylated mimic of Osh4 (active).

The second growth assay addressed the ability of each acetylation mimic to prevent the suppression of *OSH4*-dependent *sec14* bypass. As mentioned in the previous chapter, *sec14-1$^{ts}$* lethal growth defect can be suppressed by deleting *OSH4* (FANG *et al.* 1996). Expression of a functional copy of Osh4 is sufficient to prevent growth of a *sec14-1$^{ts}$ osh4Δ* background (LI *et al.* 2002). Therefore, we compared the ability of each mutant to inhibit growth of the *sec14-1$^{ts}$osh4Δ* strain at non-permissive temperatures (**Figure 4.1C**). As expected, expression of wildtype *OSH4* inhibited the growth of *sec14-1$^{ts}$osh4Δ* at 38°C which confirms that expression of a functional copy of Osh4 prevents growth in this background (LI *et al.* 2002). Of the six acetylation mimics screened, once again, only the expression of lysine K109 point mutants had an effect on the ability of Osh4 to inhibit growth. The expression of both the acetylated mimic, K109Q, and unacetylated mimic, K109R, did not inhibit growth of *sec14-1$^{ts}$osh4Δ* at 38°C.This provided further evidence that lysine K109 of Osh4 is critical for function; however, unlike with Osh-deficient strain rescue, both K109Q and K109R were non-functional. Given the fact that mutants of lysine K168 and lysine K247 did not affect the function of Osh4 in either screens, we decided to focus our attention on the effect of lysine acetylation on lysine K109.

To further characterize the differences between the acetylated mimic and unacetylated mimic of lysine K109, we subjected these mutants to two more growth assays. Sec14 directly stimulates the activity of the PI-kinase, Pik1 (SCHAAF *et al.* 2008). Much like with *sec14-1$^{ts}$*, the growth defects a temperature sensitive mutant of Pik1, *pik1-83$^{ts}$,* can be at least partially suppressed by deleting *OSH4* (FAIRN *et al.* 2007). However, unlike wildtype *OSH4*, we found that expression of the K109Q and K109R mutants did not impair the growth of a *pik1-83$^{ts}$osh4Δ* strain at semi-permissive temperatures (30°C) (**Figure 4.1D**). Finally, we compared the ability of each mutant to confer a toxic effect on growth once overexpressed (**Figure 4.1E**). Overexpression of Osh4 causes a growth defect caused by the hyperactivation of the PI-4-phosphatase Sac1 and subsequent depletion of PI-4-P (LEBLANC AND MCMASTER 2010; ALFARO *et al.* 2011). We found that, unlike wildtype *OSH4*, overexpression of K109Q and K109R did not induce growth defects. Collectively, our *in-vivo* growth assays suggest a crucial role for lysine K109 on the function of Osh4.

### 4.2.2 The acetylated mimic of lysine K109 prevents the localization of Osh4 to cytosolic punctate structures

An additional measure of Osh4 function is its ability to localize to punctate regions within the cells on Golgi-membranes and on vesicles trafficking towards the plasma membrane (LI *et al.* 2002; ALFARO *et al.* 2011). Using GFP-tagged constructs of Osh4, we compared the localization pattern of the K109 mutants with wildtype Osh4 (**Figure 4.2A**). As expected, wildtype Osh4-GFP localized both diffusely in the cytoplasm as well as in punctate regions within the cells. Interestingly, the acetylated mimic, K109Q, only localized in a diffuse pattern whereas the unacetylated mimic, K109R, maintained a similar pattern of localization as wildtype (**Figure 4.2A-B**). This suggests that the acetylated mimic, K109Q, is potentially non-functional due to its inability to properly localize within the cells, whereas the unacetylated mimic, K109R, can still maintain some of its function due to its proper localization.

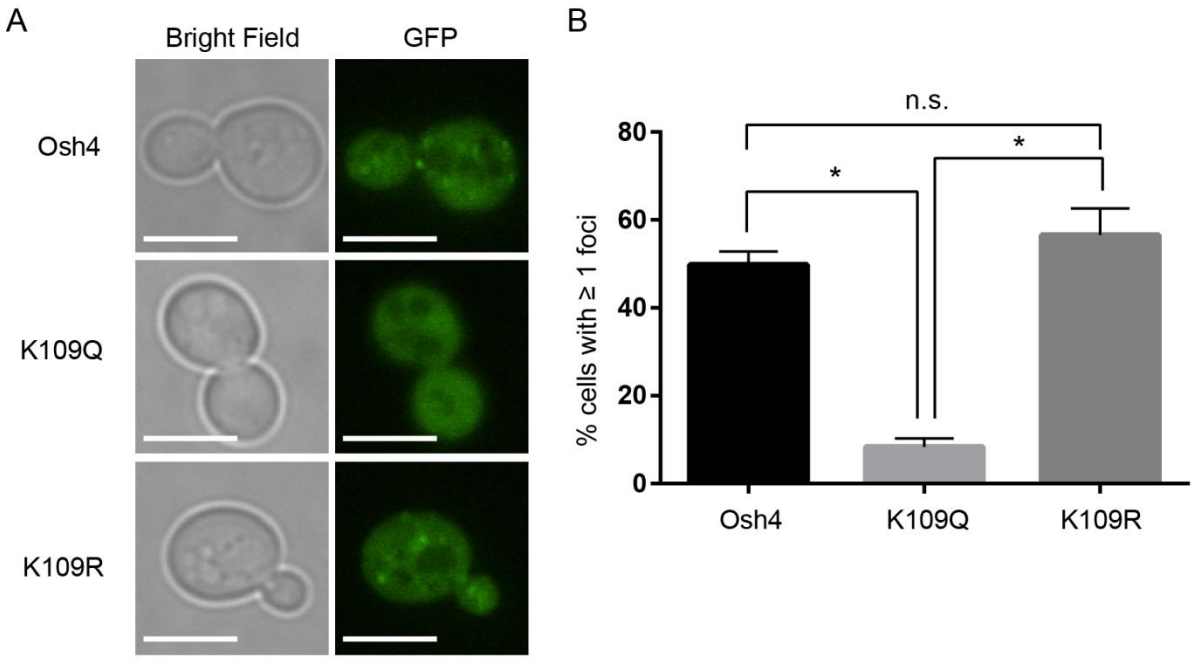
A
Bright Field
GFP
Osh4
K109Q
K109R
B
n.s.
*
*
80
60
40
20
0
% cells with ≥ 1 foci
Osh4
K109Q
K109R

**Figure 4.2 The acetylated mimic of Osh4-K109Q, adopts a diffused localization within the cell whereas the unacetylated mimic, K109R, maintains wildtype punctate localization. A)** *osh4Δ* (YKB3343) was transformed with a plasmid expressing different construct of GFP-tagged Osh4 : wildtype construct (Osh4-GFP; PKB289), acetylation mimic (osh4-GFP-K109Q; PKB211), and unacetylated mimic (osh4-GFP-K109R). Cells were grown to mid-log phase in SD-Leu at 30°C and imaged at room temperature. Cells shown are representative of the localization distribution observed for each construct. White scale bar = 5µm **B)** Quantification of localization changes between the acetylated mimic and unacetylated mimic of Osh4 of the cells represented in A). The graph displays the average amount of cells (%) with at least one foci detected (+SEM) from three separate experiments scoring more than 80 cells in each replicate. Statistical analysis was performed by one-way ANOVA with Tukey's multiple comparisons test: *p-value<0.05; n.s. not significant.

### 4.2.3 *In-vitro* PI-4-P binding affinity and Sac1 stimulation is unaffected by lysine K109 mutants

It has been previously reported that lysine K109 of Osh4 is important for the lipid-binding affinity towards PI-4-P (DE SAINT-JEAN *et al.* 2011). We decided to try and determine if acetylation of this particular lysine residue would affect lipid-binding affinity by comparing the PI-4-P binding affinity of the acetylated mimic, K109Q, and the unacetylated mimic, K109R. For this purpose, we performed a relatively simple lipid-binding assay of purified Osh4 recombinant protein on a nitrocellulose membrane spotted with serial dilutions of PI-4-P (MUNNIK AND WIERZCHOWIECKA 2013) (**Figure 4.3A**). As expected, wildtype Osh4 could bind to PI-4-P but not to the control lipid PI. We were surprised to find that both K109Q and K109R maintained their specific affinity for PI-4-P. This suggests that the PI-4-P binding affinity of Osh4 is independent of lysine K109. We also decided to compare the ability of the K109 mutants to stimulate the phosphatase activity of Sac1. Purified Osh4 recombinant protein has the ability to stimulate the PI-4-phosphatase activity of Sac1 *in-vitro* (STEFAN *et al.* 2011). We repeated the same experiment to compare the function of the acetylated mimic, K109Q, versus the unacetylated mimic, K109R, on *in-vitro* Sac1 phosphatase activity (**Figure 4.3B**). As expected, we found that adding wildtype Osh4 protein significantly increased the activity levels of Sac1 compared to the blank control. However, despite our hypothesis, we found that both K109Q and K109R mutants also stimulated Sac1 activity to a similar extent as wildtype. This evidence suggests that the neither the PI-4-P binding affinity nor the Sac1 activation function of Osh4 is dependent on lysine K109.

### 4.2.4 Osh1, a yeast homologue of Osh4, is also acetylated *in-vivo*

The lysine K109 residue of Osh4 is conserved throughout the family of Oxysterol-Binding Related Protein (ORP) family both in yeast and in humans. Therefore, it was possible that this mechanism of regulation by lysine acetylation existed throughout the entire ORP family of proteins. In yeast, there are seven ORP homologous genes termed Osh proteins

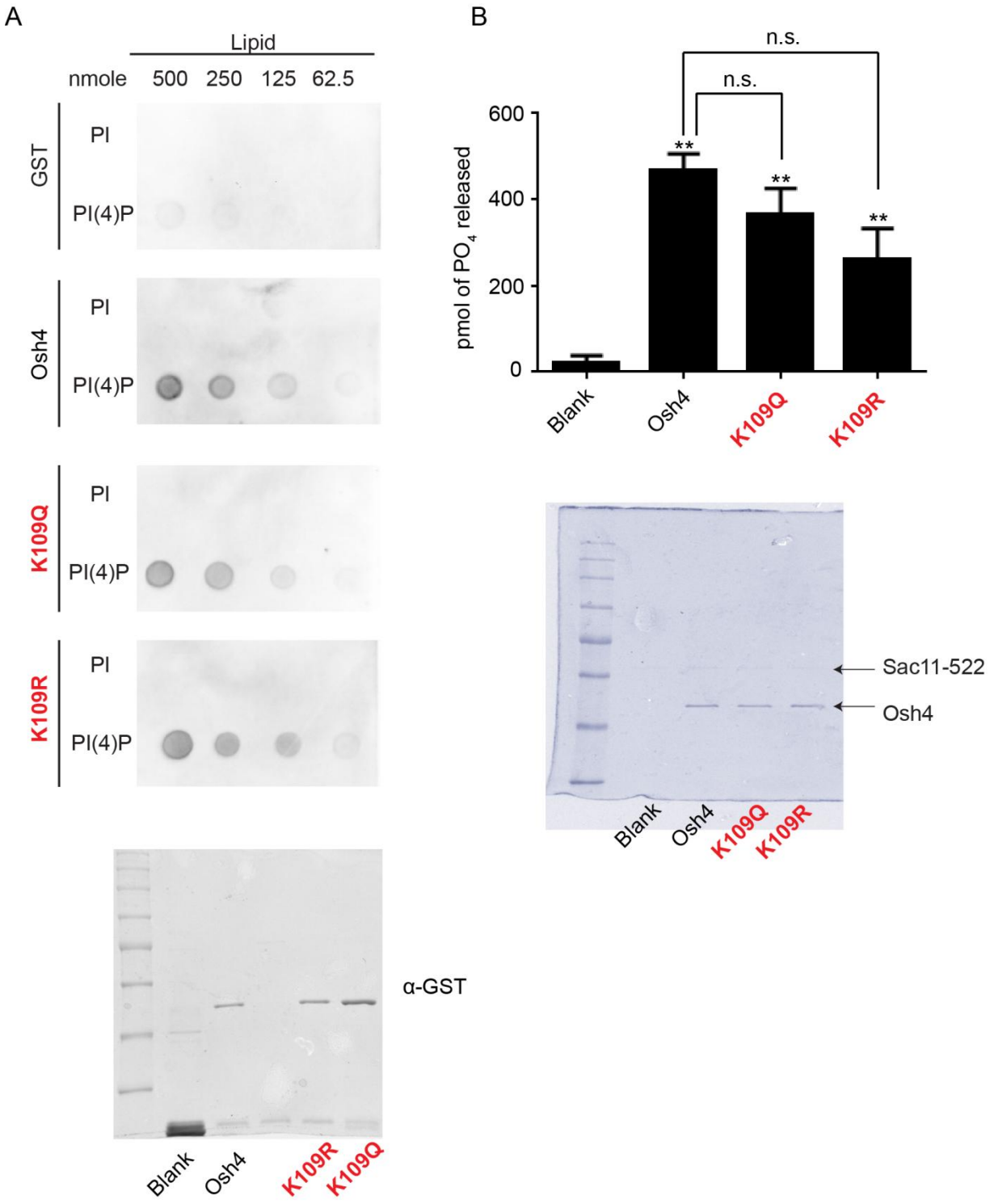
A
Lipid
nmole 500 250 125 62.5
GST
PI
PI(4)P
Osh4
PI
PI(4)P
K109Q
PI
PI(4)P
K109R
PI
PI(4)P
α-GST
Blank
Osh4
K109R
K109Q
B
n.s.
n.s.
600
400
200
0
pmol of PO4 released
**
**
**
Blank
Osh4
K109Q
K109R
Sac11-522
Osh4
Blank
Osh4
K109Q
K109R

**Figure 4.3 Osh4 K109 mutants does not impair PI-4-P binding on nitrocellulose membrane or Osh4-dependent in-vitro Sac1 activation.** A) Lipid overlay assay of recombinant Osh4 WT, K109Q, and K109R mutant proteins on PI-4-P. Indicated amounts of serially diluted lipids (PI and PI-4-P) were spotted on nitrocellulose membranes and dried. Purified recombinant Osh4 constructs and GST (4 µg/ml) in PBS were incubated on blocked membranes overnight. Thereafter, membranes were washed and immunoblotted using anti-Osh4 antibodies. Images shown are representative results from two technical replicates. Immunoblot of GST-tagged recombinant proteins used for assay is shown below. B) In-vitro Sac1 phosphatase assay with recombinant GST-tagged Osh4, K109Q, and K109R mutants. Each protein sample (1.2 µM) were incubated with recombinant GST-tagged $sac1^{1-522}$ protein (300 ng) using short acyl chain diC8-PI4P in excess as substrate, for 10 minutes at 25˚C. Reactions were stopped with 50mM of N-ethylmaleimide (NEM), and phosphate release was measured by malachite green PO4 assay. Results shown are averages from three separate experiments. Statistical analyses were performed by one-way ANOVA with Sidak's multiple comparisons test: ** = $p < 0.05$; n.s.= not significant. Reaction mix for each separate sample were resolved on a 9% acrylamide gel and subsequently stained with Coomassie. Bands corresponding for the Sac1 catalytic domain ($sac1^{1-522}$) and the Osh4 recombinant protein are indicated. Both experiments were conducted by Dr. Michael Kennedy from our lab.

(BEH *et al.* 2001). To determine if any other Osh proteins are acetylated *in-vivo*, we screened each protein for acetylation by immunoblotting (**Figure 4.4**). GFP-tagged Osh proteins, along with a positive control for acetylation, Esa1 (MITCHELL *et al.* 2013), were purified from mid-log phase yeast cells and immunoblot analysis was performed using pan-acetyl lysine antibodies. As expected, acetylation was detected on Esa1-GFP and a weak yet consistent acetylation signal was detected on Osh4-GFP. Intriguingly, a very strong acetylation signal was detected on the Osh1-GFP protein, this despite its protein levels being noticeably less abundant than Osh4. The five other Osh proteins did not appear to have any detectable acetylation.

In order to identify the acetylation sites on Osh1, TAP-tagged construct of Osh1 were purified from yeast in both wildtype and *rpd3Δsir2Δ* backgrounds and sequenced by mass spectrometry. In total, six acetylation sites were detected between two biological replicates of each strain backgrounds (**Table 4.2**). The detection of six different acetylation sites on Osh1 would explain the much stronger acetylation signal detected by immunoblotting compared to Osh4. More importantly, a peptide containing the K109 equivalent residue of Osh1, K874, was identified as an acetylation site. K109 of Osh4 and K874 of Osh1 fall within the same conserved lysine residue shared across all ORPs (**Figure 4.5**). This supports the hypothesis that acetylation of the conserved lysine residue of ORP could potentially be a general method for regulating ORP function.

### 4.2.5 Lysine acetylation site of Osh1, K874, is critical for function but not for localization

Unlike Osh4, the functions of Osh1 have not been as extensively studied. Like for all Osh proteins, Osh1 can rescue a strain deficient of all Osh genes (BEH *et al.* 2001). Furthermore, Osh1 localizes both to the Golgi as well as to nucleus-vacuole junction (NVJ) sites (LEVINE AND MUNRO 2001). The entire Osh protein family appear to be required for piecemeal microautophagy of the nucleus, one function of NVJ sites, however this role remains undefined

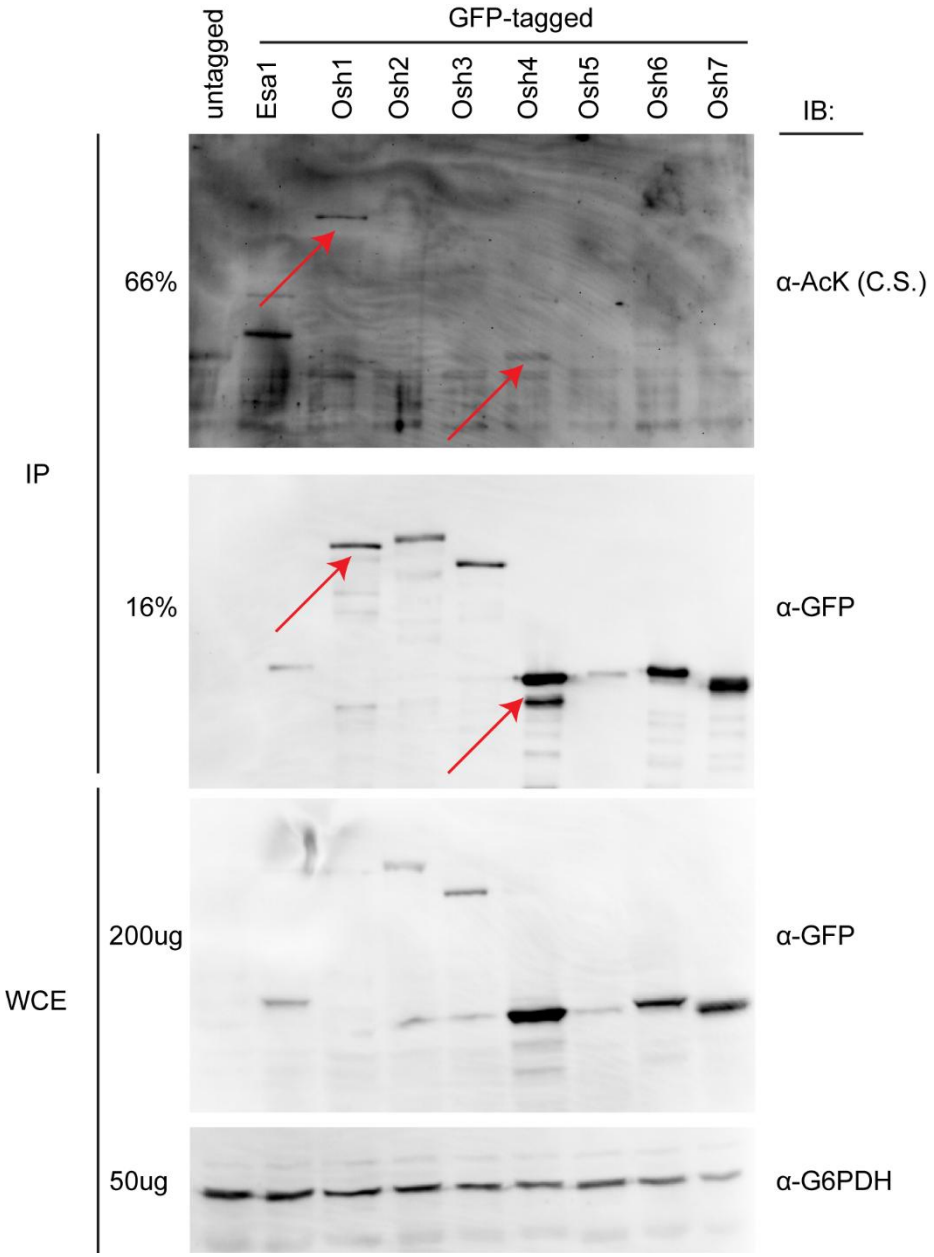
GFP-tagged
untagged
Esa1
Osh1
Osh2
Osh3
Osh4
Osh5
Osh6
Osh7
IB:
IP
66%
α-AcK (C.S.)
16%
α-GFP
WCE
200ug
α-GFP
50ug
α-G6PDH

**Figure 4.4 Osh1 and Osh4 are acetylated *in-vivo*.** GFP-tagged Osh proteins and GFP-tagged Esa1 (YKB2002) was purified by GFP-immunopurification from 12.5mg of WCE. Immunoprecipitates whole cell lysates were resolved on 9% SDS-PAGE gel, and subjected to immunoblot analysis with indicated antibodies. Representative images of three separate experiments are shown.

**Table 4.2 LC/MS/MS experiment conducted on Osh1 samples.**

| LC/MS/MS experiment | # of replicates | Total peptides (Unique peptides) | Protein sequence coverage | Detected acetylation site(s) (# peptide(s)) |
|---|---|---|---|---|
| **TAP IP: Osh1-TAP** | 2 | 1031 (170)<br>1092 (156) | 84%<br>84% | K915 (1)<br>K974 (2)<br>K999 (2) |
| **TAP-IP: Osh1-TAP *rpd3Δ sir2Δ* background** | 2 | 787 (151)<br>1450 (177) | 79%<br>87% | K231 (3)<br>K814 (1)<br>K874 (1)<br>K974 (3) |

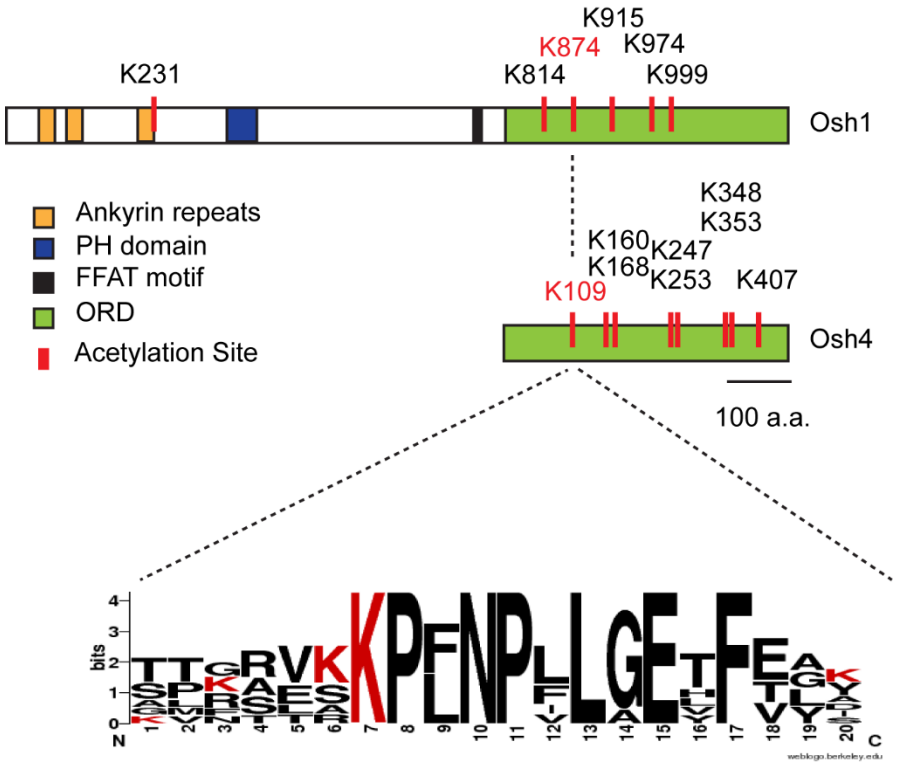
K915
K874
K974
K231
K814
K999
Osh1
Ankyrin repeats
PH domain
FFAT motif
ORD
Acetylation Site
K348
K353
K160
K247
K168
K253
K407
K109
Osh4
100 a.a.
bits
N
C

**Figure 4.5 Schematic of the acetylation sites detected on both Osh1 and Osh4 by LC/MS/MS.** Lysine K874 of Osh1 and lysine K109 of Osh4, located on the Oxysterol-Binding Protein-Related Domain (ORD), is highly conserved throughout the Oxysterol-Binding Protein family in yeast as well as with the canonical mammalian OSBP, as demonstrated by the sequence logo below. Osh1 acetylation sites were detected in this study. Osh4 acetylation sites were compiled from previous high-throughput acetylome studies done in yeast: (HENRIKSEN *et al.* 2012; WEINERT *et al.* 2014; DOWNEY *et al.* 2015; MADSEN *et al.* 2015)

(KVAM AND GOLDFARB 2004). To determine the effect of acetylation on the function and localization of Osh1 the K874 residue was mutated to either mimic its acetylated state, K874Q, or mimic its unacetylated state, K874R. Protein expression of Osh1 was relatively similar across all generated mutants with only some minor yet inconsistent changes (**Figure 4.6A**). Osh1 acetylation mimetics were expressed in the Osh deficient strain (*osh1-7Δ osh4-1$^{ts}$*) to assess their ability to rescue growth and determine its functional capability (**Figure 4.6B**). Unlike the wildtype copy of *OSH1*, both the acetylated mimic, K874Q, and the unacetylated mimic, K874R, could not rescue growth of the Osh deficient strain at non-permissive temperature (37°C). This would indicate the importance of this lysine residue for the function of Osh1.

We next wanted to compare the localization pattern of Osh1 between each mutant. GFP-tagged constructs of the Osh1 mutants were created and to our surprise, despite inhibiting the function of Osh1, localization of both the acetylated mimic, K874Q, and unacetylated mimic, K874R, appeared similar to wildtype Osh1, suggesting that, unlike Osh4, the conserved lysine residue is not important for localization (**Figure 4.6C**). In conclusion, K874 of Osh1 appears to be critical for its function but not for its localization. This is in contrast to lysine K109 of Osh4 which was critical for both function and localization.

## 4.3 Discussion

### Osh Acetylation

The data we collected suggests a conserved mechanism for the regulation Oxysterol-Binding Proteins throughout the entire family of proteins. Not only are Oxysterol-Binding Proteins highly conserved, but the lysine residue of interest, K109 of Osh4 and K874 of Osh1, is conserved throughout all OSBP proteins. We can hypothesize an initial model for how the acetylation of lysine K109 of Osh4 can regulate its function *in-vivo* (**Figure 4.7**). In our model, we propose that the acetylation of lysine K109 drives Osh4 away from the Golgi and vesicles

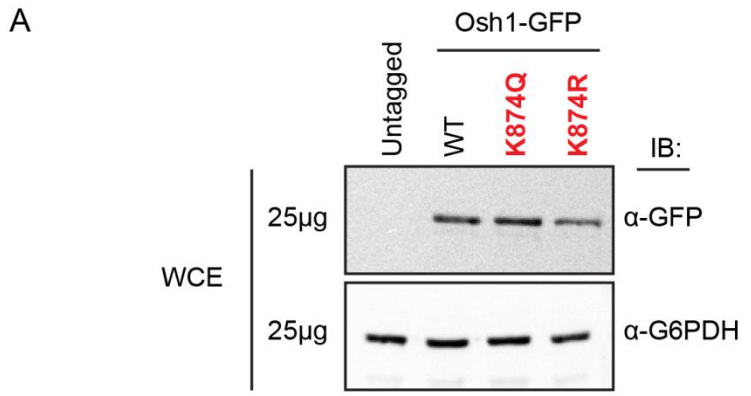
A
Osh1-GFP
Untagged
WT
K874Q
K874R
IB:
25µg
α-GFP
WCE
25µg
α-G6PDH

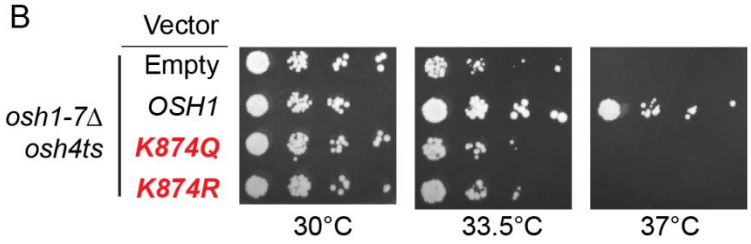
B
Vector
Empty
OSH1
K874Q
K874R
osh1-7Δ
osh4ts
30°C
33.5°C
37°C

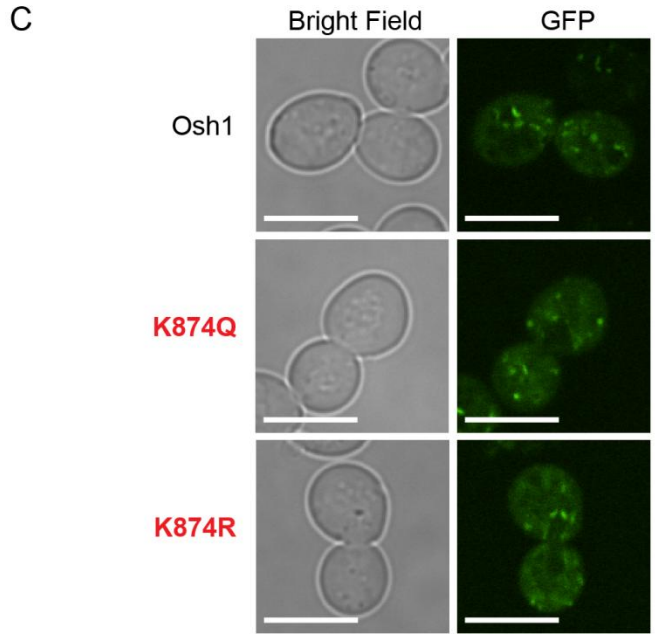
C
Bright Field
GFP
Osh1
K874Q
K874R

**Figure 4.6 Osh1 K109-equivalent lysine residue and potential acetylation site, K874, is also critical for function but not for localization. A)** Protein levels of Osh4 are unaffected by point mutations that mimics either acetylated lysine (K to Q) or mimics unacetylated lysine (K to R) on lysine K874. *osh1*Δ (YKB4145) was transformed with empty vector (Untagged; pRS416) or a plasmid expressing different construct of GFP-tagged Osh1. The transformed strains were grown in YPD media to mid-log phase, harvested and lysed. GFP-tagged protein was purified by GFP-immunopurification from 10 mg of WCE. Immunoprecipitates were run on 7% acrylamide gel through SDS-PAGE and transferred to a nitrocellulose membrane. Membranes were immunoblotted using indicated antibodies. **B)** Osh1 acetylation mimic, K874Q, and unacetylated mimic, K874R, cannot rescue *osh1-7Δosh4-1*$^{ts}$ strain. *osh1-7Δosh4-1*$^{ts}$ (YKB3197) was transformed with a empty vector (pRS326) or with a plasmid expressing different construct of *OSH1*: WT construct (*OSH1*; PKB308), acetylated mimic (*osh1*-K874Q; PKB309), and unacetylated mimic (*osh1*-K874R; PKB310). Cultures were grown in SD-Ura at 30°C prior to being diluted to an $OD_{600}$ of 0.1 and 4 times 10-fold serial dilutions were spotted on SD-Ura for three days at 30°C, 33.5°C, or 37°C **C)** Osh1 acetylation mimic, K874Q, and unacetylated mimic, K874R, does not affect the localization of Osh1. osh1Δ (YKB4145) was transformed with a plasmid expressing different construct of GFP-tagged Osh1: WT construct (Osh1-GFP; PKB305), acetylated mimic (osh1-GFP-K874Q; PKB306), and unacetylated mimic (osh1-GFP-K874R). Cells were grown to mid-log phase in SD-Ura at 30°C and imaged at room temperature. Cells shown are representative of the localization distribution observed for each construct. White scale bar = 5µm.

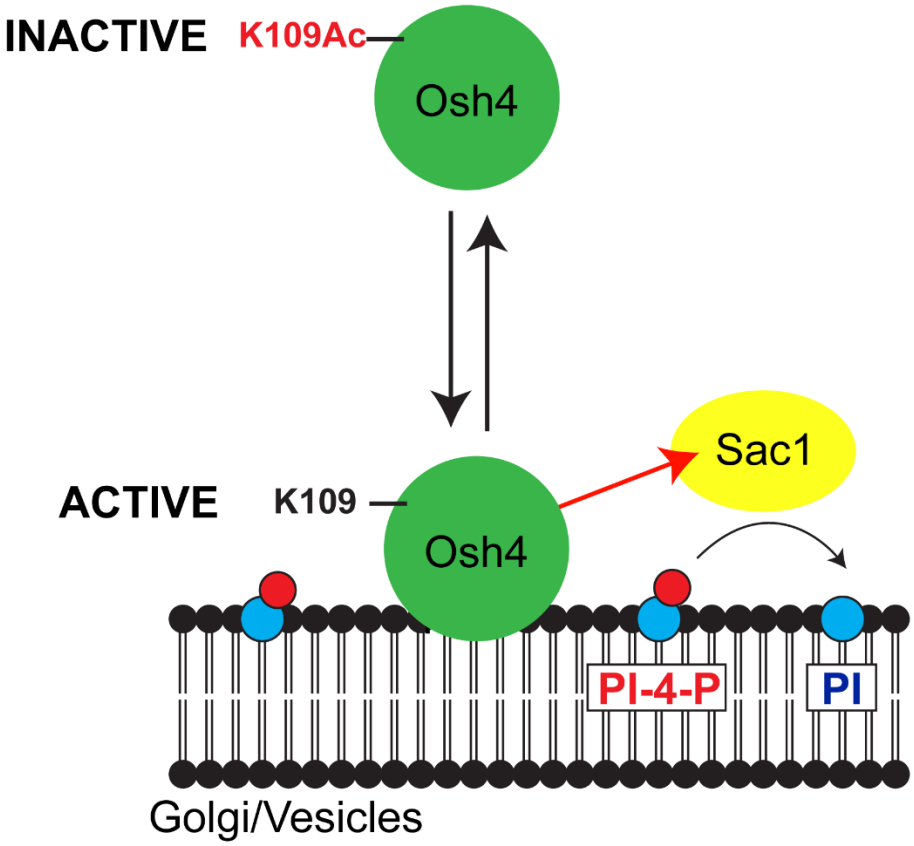
INACTIVE
K109Ac
Osh4
ACTIVE
K109
Osh4
Sac1
PI-4-P
PI
Golgi/Vesicles

**Figure 4.7 Schematic of the proposed mechanism by which acetylation regulates the function of Osh4.** In this model, acetylation of lysine K109 of Osh4 prevents its association with Golgi/ vesicle membranes which inhibits the ability of Osh4 to interact with PI-4-P. Localization of Osh4 to Golgi membranes and Sac1 stimulation requires deacetylation of lysine K109.

preventing it from interacting with PI-4-P and stimulating Sac1-dependent PI-4-P dephosphorylation. Although we failed to confirm acetylation on Osh4 by mass spectrometry, the fact that we could detect acetylation on the equivalent site on Osh1 strongly suggests a conserved nature for this method of regulation.

**Acetylation of Osh4 and Osh1 *in-vivo***

Despite detection of acetylation on Osh4 in acetylome studies by mass spectrometry (HENRIKSEN *et al.* 2012), and immunoblotting using pan acetyl-antibodies (KALUARACHCHI DUFFY *et al.* 2012), we failed to detect any naturally occurring acetylation sites on Osh4 (**Table 4.1**). As three other acetylome studies also failed to identify acetylation on lysine K109 of Osh4 (WEINERT *et al.* 2014; DOWNEY *et al.* 2015; MADSEN *et al.* 2015), one possibility is that acetylation of K109 on Osh4 was a false positive of the Henriksen 2012 screen, and does not occur *in-vivo*. However, several reasons could explain why both we and others could not detect acetylation on lysine K109.

Though all the acetylome studies enriched for acetylated peptides by immunoprecipitation using pan acetyl-lysine antibodies, there are were differences in the methodologies that could account for discrepancies in the acetylome (HENRIKSEN *et al.* 2012; WEINERT *et al.* 2014; DOWNEY *et al.* 2015; MADSEN *et al.* 2015).The most important of which is the inherent variability of the specificity of the pan acetyl-lysine antibodies used for enriching acetylated peptides. Different batches of antibodies could lead to preferential sequence binding from one source to the next leading to distinctive results. Thus, the fact that acetylation sites were not perfectly replicated in each of the acetylome screens could very easily be attributed to their different sources of antibodies.

Secondly, our own experimental method of identifying acetylation sites is different from the one used in the Henriksen 2012 screen. In our study, purified protein of interest was simply

purified from yeast extracts without any regards to its acetylation. By removing the enrichment step for acetylated peptides, the probability of detecting an acetylated peptide became dependent on the relative abundancy of the modified peptide to the unmodified peptide. A more recent acetylome study has undertaken the task of determining the relative abundancy of peptides that are acetylated on proteins (WEINERT *et al.* 2014). They estimated that the ratio of acetylated peptides to unacetylated peptides is relatively low, especially for proteins outside the nucleus. These results imply that we are unlikely to encounter an acetylated peptide among the entire pool of peptides collected, especially without enriching for acetylated peptides by immunoprecipitation. Although we purified large amount of protein to compensate for the lack of enrichment, chances are unacetylated peptides were preferentially pulled out over acetylated peptide thus preventing identification of acetylation sites.

Finally, there is the possibility that the modified peptide can simply not be detected *in-vivo* due to different modifications occurring on the peptide. For example, if phosphorylation of a specific serine of threonine were occurring on the same peptide which acetylation occurs, unless it specifically entered into the analysis procedure, the algorithm that solves peptide sequences would be unable to resolve this peptide. One would have to try inserting multiple variables in the modification imput of the algorithm to even attempt correctly sequencing and identifying the modified peptide.

In contrast to Osh4, we were able to consistently detect acetylation sites on Osh1 in all four biological replicates. Unlike Osh4, all four high-throughput acetylome in yeast failed to detect any acetylated peptides belonging to Osh1 (HENRIKSEN *et al.* 2012; WEINERT *et al.* 2014; DOWNEY *et al.* 2015; MADSEN *et al.* 2015). We were able to find that not only was Osh1 acetylated, but that the acetylation appears much more abundant on Osh1 than on Osh4 both by means of immunoblotting and mass spectrometry which identified six distinct acetylation sites (**Figure 4.4, Table 4.2**). Importantly we determined that the equivalent lysine residue of

Osh4-K109 was acetylated on Osh1: K874 (**Figure 4.5, Table 4.2**). As suggested by the immunoblots, mass spectrometry detection of acetylation on Osh1 was likely successful due to the apparent increase in the percentage of cellular Osh1 that is acetylated. Altogether, we can support the claim that Osh1 is acetylated *in-vivo* as we detected acetylated by both immunoblot and mass spectrometry. As methods for detecting acetylation are still in their infancy, we should expect better methods designed in the future to validate these acetylation sites on both Osh4 and Osh1.

**Acetylation of lysine K109 inhibits the function of Osh4**

Of the three acetylation sites we investigated, only lysine K109 appeared to be critical for the function of Osh4. Lysine K109 had previously been shown to be essential for function, localization, and lipid-binding (LI *et al.* 2002; IM *et al.* 2005; RAYCHAUDHURI *et al.* 2006; DE SAINT-JEAN *et al.* 2011). However, our study showed for the first time that mutating lysine K109 to either mimic acetylated lysine or mimic unacetylated lysine gave two distinct phenotypes. Our acetylated mimic, K109Q, was completely non-functional as it could not complement any Osh4 phenotype and did not localize properly within the cell (**Figure 4.1- 4.2**). In contrast, the unacetylated mimic, K109R, was able to complement one of Osh4 phenotype and maintain proper localization (**Figure 4.1- 4.2**). This suggests a model in which acetylation causes inhibition of function by mislocalizing the protein (**Figure 4.7**).

An important question still remaining is how acetylation regulates the localization of Osh4. Structural analysis of Osh4 crystallized with PI-4-P determined that lysine K109 formed a hydrogen bond (H-bond) with the 1'-phosphate group of PI-4-P (DE SAINT-JEAN *et al.* 2011). Disrupting the hydrogen bond by incorporating an acetyl group would in theory prevent the protein from binding PI-4-P. In fact, previous mutation of that lysine to an alanine did negatively affect the proteins ability to extract PI-4-P from liposomes (DE SAINT-JEAN *et al.* 2011). Yet, our

own lipid-binding experiment determined that our acetylated mimic, K109Q, was still able to bind PI-4-P (**Figure 4.3A**). However, there is a major difference between the method we used to measure PI-4-P affinity and what has been used before. Our version of the lipid-binding assay assessed the ability of the protein to simply bind to PI-4-P-stained nitrocellulose membrane. Although this method is widely used for lipid-binding assays, it does not perfectly complement *in-vivo* conditions. Osh4 needs to bind-to and extract lipids from the Golgi to present it to the ER-localized Sac1 phosphatase (DE SAINT-JEAN *et al.* 2011; STEFAN *et al.* 2011). Our method of measuring PI-4-P binding affinity does not take the lipid-extraction ability of Osh4 into account which would suggest our method is not ideal. A more relevant PI-4-P binding assay using a liposome extraction method has been conducted with the K109Q mutant and does demonstrate that this mutant has severe PI-4-P binding defect (Huang *et al.* 2016; preparing for submission to *Cell*). This provides evidence that acetylation on lysine K109 of Osh4 would prevent PI-4-P binding affinity which could in theory explain why our K109Q does not localize to Golgi membranes.

Another interesting question is why our K109R mutant does not demonstrate all the phenotype we would expect from our unacetylated mimic (**Figure 4.7**). In our model, the unacetylated protein should be able to bind to PI-4-P and localize to Golgi membranes. We were able to show that Osh4 K109R mutant does in fact localize to Golgi membranes (**Figure 4.2**), yet this protein does not fully complement the function of the wildtype protein *in-vivo* (**Figure 4.1**). Several plausible explanations could account for these encountered discrepancies. For example, although we use arginine to mimic the unacetylated lysine residue, the side chain of arginine and lysine differ both in terms of charge and size. The pKa values of their side chains are 12.48 and 10.54 for arginine and lysine, respectively. This means that the positive charge on the arginine side chain is slightly more stable than lysine which would in theory create stronger electrostatic bonds. Additionally, the charge on the end of the side chain

of arginine is more delocalized due to the proximity of double C-H bonds. Both the strength of the charge and the localization of the charge would affect the possible function of the residue. Therefore, a change in the charge of the side chain could affect its ability to interact with certain molecule. Alternatively, the arginine residue might also affect the local structure of the protein by creating new or destroying old interactions between opposing side chains or water molecules. However, if this mutation does confer structural changes, it does not appear to affect protein stability (**Figure 4.1A**). In context with our study, the differences between the function wildtype Osh4 and the unacetylated mimic, K109R, demonstrates that arginine is not a perfect mimic of an unacetylated lysine residue.

**Osh1 is a novel target of lysine acetylation**

This lysine residue K874 on Osh1 is conserved throughout the family of Oxysterol-Binding Proteins from yeast to humans, which highlights the importance of this residue for the function of the family of proteins. As mentioned before, lysine K109 of Osh4 is essential for function and this is due to its role in binding PI-4-P (DE SAINT-JEAN *et al.* 2011). Other than Osh4, many other Oxysterol-Binding Proteins have been found to bind to PI-4-P including Osh3 and Osh6 in yeast and OSBP, ORP4, ORP5, ORP8, and ORP9 in mammals (TONG *et al.* 2016). Crystal structure of Osh3 and Osh6 with PI-4-P demonstrates that all the residues which help the protein bind to PI-4-P are conserved, including the lysine residue equivalent to lysine K109 of Osh4 (TONG *et al.* 2013; WANG 2015). Coupled to the fact that we also found that lysine K874 of Osh1 is critical for function (**Figure 4.6B**), we suggest that lysine acetylation would directly regulate the PI-4-P binding affinity of Osh1 much like we had discussed in the previous section.

One important difference between Osh1 and Osh4 is the affect of our mutants on the localization of the protein. Unlike with Osh4 (**Figure 4.2**), localization of both the acetylated mimic K874Q and the unacetylated mimic K874R remained similar to wildtype (**Figure 4.6C**). The difference between the effect of lysine acetylation between Osh1 and Osh4 could be due to

the length of their respective amino acid sequence (**Figure 4.5**). Osh4 has 434 amino acids and contains only one identified domain, the conserved Oxysterol-Binding Protein related domain (ORD) domain. The ORD constitute the lipid-binding region of the Oxysterol-Binding Protein family that folds into a semi-complete β-barrel enclosed by a lid allowing for extraction of lipids from membranes into a hydrophobic compartment (IM *et al.* 2005). Lysine K109 is positioned within this domain at the opening of the barrel (IM *et al.* 2005; DE SAINT-JEAN *et al.* 2011). Osh1 is an 1188 amino acid sequence that not only contains the ORD, but also contains a Pleckstrin Homology domain (PH) as well as several Ankyrin repeats on the C-terminal tail of the protein (**Figure 4.5**). Its PH domain appear to be critical for the localization of Osh1 to Golgi membranes, whereas its Ankyrin repeats help anchor the protein at the NVJ sites (LEVINE AND MUNRO 2001). Thus, it appears the localization of Osh1 is independent on the ORD domain which is where lysine K874 resides. One possible theory explaining the difference between Osh1 and Osh4 is that given the lack of additional C-terminal domains, the localization of Osh4 is more dependent on PI-4-P binding by its ORD domain. Regulation of Osh1 would more likely involve the inhibition of PI-4-P binding, but without impairing localization.

**Identifying the KATs and KDACs acetylating Osh4/Osh1**

Although we made great efforts at characterizing the mechanisms by which acetylation regulates Osh proteins, we did not address the enzymes that were responsible for their acetylation. Our initial screens in Chapter 1 did provide evidence that NuA4 is responsible for several aspects of phospholipid homeostasis including some which are dependent on Osh4's function. Deleting *OSH4* in the *sec14-1$^{ts}$eaf1Δ* did partially suppress the growth defects (**Figure 3.6A**) and our collaborators even have evidence that in their specific strain background, deleting *OSH4* completely suppresses the growth defects of *sec14-1$^{ts}$eaf1Δ* (Huang *et al.* 2016; preparing for submission to *Cell*). The partial dependence of NuA4 mutant's interaction on *OSH4* does suggest that part of its function is directed through that protein. If NuA4 was

acetylating and inhibiting Osh4, than we would hypothesize that inhibiting NuA4 would activate Osh4. NuA4 mutants do in fact increase the growth defects of *sec14-1*$^{ts}$ and overexpressed *OSH4* (**Figure 3.4**), much like a functional and active Osh4 protein would (**Figure 4.1**). Despite this, more would need to done to confirm the theory that NuA4 acetylates and inhibits the function of Osh4. Osh4 was not a part of the list of acetylation targets detected in either the NuA4 *in-vitro* KAT assay screen on a protein microarray or the mChIP-KAT-MS experiment with the NuA4 catalytic domain, Esa1 (LIN *et al.* 2009; MITCHELL *et al.* 2013), yet, more could be added to those experiments. The protein microarray in the Lin 2009 screen only confirmed NuA4 KAT activity by immunoblotting which is entirely dependent on the specificity and batch of the pan-acetyl antibodies used. Whereas the Mitchell 2013 screen did not include an enrichment step for acetylated peptides which, as we discussed previously, is dependent on the abundancy of the modified peptide. Both these examples could explain why Osh4 was not identified in either screen. Once again, given the rate of scientific advances towards identifying acetylation sites (reviewed in DOWNEY AND BAETZ 2016), we would expect methods of identifying KATs and KDACs regulating acetylation of specific proteins to become more obtainable.

**Conclusion**

Our research provides evidence that the function of Osh1 and Osh4 is regulated through the acetylation of the conserved lysine residue critical for PI-4-P-binding. Given the conservation of PI-4-P binding, we extend our hypothesis towards the regulation of all Oxysterol-Binding Proteins by lysine acetylation. The most recent model for Oxysterol-Binding Protein conserved function is the regulation of the lipid composition between two opposing membranes by exchanging PI-4-P with another lipid ligand (OLKKONEN 2015). Activation of the Sac1 phosphatase has been suggested to be a conserved function for all Oxysterol-Binding proteins (STEFAN *et al.* 2011). The coupling of PI-4-P transport to Sac1-mediated PI-4-P

dephosphorylation would allow for a specific lipid gradient to form between the membranes (OLKKONEN 2015). By altering the PI-4-P binding affinity of Oxysterol-Binding Protein, lysine acetylation could then regulate the PI-4-P metabolic flux and help establish proper lipid composition for PI-4-P containing membranes.

# 5 References


Aitken, J. F., G. P. van Heusden, M. Temkin and W. Dowhan, 1990 The gene encoding the phosphatidylinositol transfer protein is essential for cell growth. J Biol Chem 265**:** 4711-4717.

Alfaro, G., J. Johansen, S. A. Dighe, G. Duamel, K. G. Kozminski *et al.*, 2011 The sterol-binding protein Kes1/Osh4p is a regulator of polarized exocytosis. Traffic 12**:** 1521-1536.

Ambroziak, J., and S. A. Henry, 1994 INO2 and INO4 gene products, positive regulators of phospholipid biosynthesis in Saccharomyces cerevisiae, form a complex that binds to the INO1 promoter. J Biol Chem 269**:** 15344-15349.

Ashburner, B. P., and J. M. Lopes, 1995 Autoregulated expression of the yeast INO2 and INO4 helix-loop-helix activator genes effects cooperative regulation on their target genes. Mol Cell Biol 15**:** 1709-1715.

Audhya, A., and S. D. Emr, 2002 Stt4 PI 4-kinase localizes to the plasma membrane and functions in the Pkc1-mediated MAP kinase cascade. Dev Cell 2**:** 593-605.

Audhya, A., M. Foti and S. D. Emr, 2000 Distinct roles for the yeast phosphatidylinositol 4-kinases, Stt4p and Pik1p, in secretion, cell growth, and organelle membrane dynamics. Mol Biol Cell 11**:** 2673-2689.

Auesukaree, C., A. Damnernsawad, M. Kruatrachue, P. Pokethitiyook, C. Boonchird *et al.*, 2009 Genome-wide identification of genes involved in tolerance to various environmental stresses in Saccharomyces cerevisiae. J Appl Genet 50**:** 301-310.

Auger, A., L. Galarneau, M. Altaf, A. Nourani, Y. Doyon *et al.*, 2008 Eaf1 is the platform for NuA4 molecular assembly that evolutionarily links chromatin acetylation to ATP-dependent exchange of histone H2A variants. Mol Cell Biol 28**:** 2257-2270.

Bachhawat, N., Q. Ouyang and S. A. Henry, 1995 Functional characterization of an inositol-sensitive upstream activation sequence in yeast. A cis-regulatory element responsible for inositol-choline mediated regulation of phospholipid biosynthesis. J Biol Chem 270**:** 25087-25095.

Bankaitis, V. A., J. R. Aitken, A. E. Cleves and W. Dowhan, 1990 An essential role for a phospholipid transfer protein in yeast Golgi function. Nature 347**:** 561-562.

Bankaitis, V. A., D. E. Malehorn, S. D. Emr and R. Greene, 1989 The Saccharomyces cerevisiae SEC14 gene encodes a cytosolic factor that is required for transport of secretory proteins from the yeast Golgi complex. J Cell Biol 108**:** 1271-1281.

Becker, G. W., and R. L. Lester, 1977 Changes in phospholipids of Saccharomyces cerevisiae associated with inositol-less death. J Biol Chem 252**:** 8684-8691.

Beh, C. T., L. Cool, J. Phillips and J. Rine, 2001 Overlapping functions of the yeast oxysterol-binding protein homologues. Genetics 157**:** 1117-1140.

Beh, C. T., and J. Rine, 2004 A role for yeast oxysterol-binding protein homologs in endocytosis and in the maintenance of intracellular sterol-lipid distribution. J Cell Sci 117**:** 2983-2996.

Bhat, W., S. Ahmad and J. Cote, 2015 TINTIN, at the interface of chromatin, transcription elongation, and mRNA processing. RNA Biol 12**:** 486-489.

Brachmann, C. B., A. Davies, G. J. Cost, E. Caputo, J. Li *et al.*, 1998 Designer deletion strains derived from Saccharomyces cerevisiae S288C: a useful set of strains and plasmids for PCR-mediated gene disruption and other applications. Yeast 14**:** 115-132.

Cai, Y., J. Jin, C. Tomomori-Sato, S. Sato, I. Sorokina *et al.*, 2003 Identification of new subunits of the multiprotein mammalian TRRAP/TIP60-containing histone acetyltransferase complex. J Biol Chem 278**:** 42733-42736.

Carman, G. M., and G. S. Han, 2011 Regulation of phospholipid synthesis in the yeast Saccharomyces cerevisiae. Annu Rev Biochem 80**:** 859-883.

Chang, H. J., E. W. Jones and S. A. Henry, 2002 Role of the unfolded protein response pathway in regulation of INO1 and in the sec14 bypass mechanism in Saccharomyces cerevisiae. Genetics 162**:** 29-43.

Cheng, X., A. Auger, M. Altaf, S. Drouin, E. Paquet *et al.*, 2015 Eaf1 Links the NuA4 Histone Acetyltransferase Complex to Htz1 Incorporation and Regulation of Purine Biosynthesis. Eukaryot Cell 14**:** 535-544.

Cheng, X., and J. Cote, 2014 A new companion of elongating RNA Polymerase II: TINTIN, an independent sub-module of NuA4/TIP60 for nucleosome transactions. Transcription 5**:** e995571.

Cherry, J. M., E. L. Hong, C. Amundsen, R. Balakrishnan, G. Binkley *et al.*, 2012 Saccharomyces Genome Database: the genomics resource of budding yeast. Nucleic Acids Res 40**:** D700-705.

Chittuluru, J. R., Y. Chaban, J. Monnet-Saksouk, M. J. Carrozza, V. Sapountzi *et al.*, 2011 Structure and nucleosome interaction of the yeast NuA4 and Piccolo-NuA4 histone acetyltransferase complexes. Nat Struct Mol Biol 18**:** 1196-1203.

Choudhary, C., C. Kumar, F. Gnad, M. L. Nielsen, M. Rehman *et al.*, 2009 Lysine acetylation targets protein complexes and co-regulates major cellular functions. Science 325**:** 834-840.

Choudhary, C., B. T. Weinert, Y. Nishida, E. Verdin and M. Mann, 2014 The growing landscape of lysine acetylation links metabolism and cell signalling. Nat Rev Mol Cell Biol 15**:** 536-550.

Clancey, C. J., S. C. Chang and W. Dowhan, 1993 Cloning of a gene (PSD1) encoding phosphatidylserine decarboxylase from Saccharomyces cerevisiae by complementation of an Escherichia coli mutant. J Biol Chem 268**:** 24580-24590.

Clarke, A. S., J. E. Lowell, S. J. Jacobson and L. Pillus, 1999 Esa1p is an essential histone acetyltransferase required for cell cycle progression. Mol Cell Biol 19**:** 2515-2526.

Cleves, A. E., T. P. McGee, E. A. Whitters, K. M. Champion, J. R. Aitken *et al.*, 1991 Mutations in the CDP-choline pathway for phospholipid biosynthesis bypass the requirement for an essential phospholipid transfer protein. Cell 64**:** 789-800.

Cleves, A. E., P. J. Novick and V. A. Bankaitis, 1989 Mutations in the SAC1 gene suppress defects in yeast Golgi and yeast actin function. J Cell Biol 109**:** 2939-2950.

Culbertson, M. R., and S. A. Henry, 1975 Inositol-requiring mutants of Saccharomyces cerevisiae. Genetics 80**:** 23-40.

Curwin, A. J., G. D. Fairn and C. R. McMaster, 2009 Phospholipid transfer protein Sec14 is required for trafficking from endosomes and regulates distinct trans-Golgi export pathways. J Biol Chem 284**:** 7364-7375.

de Saint-Jean, M., V. Delfosse, D. Douguet, G. Chicanne, B. Payrastre *et al.*, 2011 Osh4p exchanges sterols for phosphatidylinositol 4-phosphate between lipid bilayers. J Cell Biol 195**:** 965-978.

Dean-Johnson, M., and S. A. Henry, 1989 Biosynthesis of inositol in yeast. Primary structure of myo-inositol-1-phosphate synthase (EC 5.5.1.4) and functional analysis of its structural gene, the INO1 locus. J Biol Chem 264**:** 1274-1283.

Delage, E., J. Puyaubert, A. Zachowski and E. Ruelland, 2013 Signal transduction pathways involving phosphatidylinositol 4-phosphate and phosphatidylinositol 4,5-bisphosphate: convergences and divergences among eukaryotic kingdoms. Prog Lipid Res 52**:** 1-14.

Desrivieres, S., F. T. Cooke, P. J. Parker and M. N. Hall, 1998 MSS4, a phosphatidylinositol-4-phosphate 5-kinase required for organization of the actin cytoskeleton in Saccharomyces cerevisiae. J Biol Chem 273**:** 15787-15793.

Donahue, T. F., and S. A. Henry, 1981 myo-Inositol-1-phosphate synthase. Characteristics of the enzyme and identification of its structural gene in yeast. J Biol Chem 256**:** 7077-7085.

Dowd, S. R., M. E. Bier and J. L. Patton-Vogt, 2001 Turnover of phosphatidylcholine in Saccharomyces cerevisiae. The role of the CDP-choline pathway. J Biol Chem 276**:** 3756-3763.

Downey, M., and K. Baetz, 2016 Building a KATalogue of acetyllysine targeting and function. Brief Funct Genomics 15**:** 109-118.

Downey, M., J. R. Johnson, N. E. Davey, B. W. Newton, T. L. Johnson *et al.*, 2015 Acetylome profiling reveals overlap in the regulation of diverse processes by sirtuins, gcn5, and esa1. Mol Cell Proteomics 14**:** 162-176.

Doyon, Y., and J. Cote, 2004 The highly conserved and multifunctional NuA4 HAT complex. Curr Opin Genet Dev 14**:** 147-154.

Doyon, Y., W. Selleck, W. S. Lane, S. Tan and J. Cote, 2004 Structural and functional conservation of the NuA4 histone acetyltransferase complex from yeast to humans. Mol Cell Biol 24**:** 1884-1896.

Drazic, A., L. M. Myklebust, R. Ree and T. Arnesen, 2016 The world of protein acetylation. Biochim Biophys Acta 1864**:** 1372-1401.

Engel, S. R., F. S. Dietrich, D. G. Fisk, G. Binkley, R. Balakrishnan *et al.*, 2014 The reference genome sequence of Saccharomyces cerevisiae: then and now. G3 (Bethesda) 4**:** 389-398.

Esposito, M., P. Konarzewska, O. Odeyale and C. H. Shen, 2010 Gene-wide histone acetylation at the yeast INO1 requires the transcriptional activator Ino2p. Biochem Biophys Res Commun 391**:** 1285-1290.

Fairn, G. D., A. J. Curwin, C. J. Stefan and C. R. McMaster, 2007 The oxysterol binding protein Kes1p regulates Golgi apparatus phosphatidylinositol-4-phosphate function. Proc Natl Acad Sci U S A 104**:** 15352-15357.

Fang, M., B. G. Kearns, A. Gedvilaite, S. Kagiwada, M. Kearns *et al.*, 1996 Kes1p shares homology with human oxysterol binding protein and participates in a novel regulatory pathway for yeast Golgi-derived transport vesicle biogenesis. EMBO J 15**:** 6447-6459.

Faulhammer, F., G. Konrad, B. Brankatschk, S. Tahirovic, A. Knodler *et al.*, 2005 Cell growth-dependent coordination of lipid signaling and glycosylation is mediated by interactions between Sac1p and Dpm1p. J Cell Biol 168**:** 185-191.

Feddersen, S., T. B. Neergaard, J. Knudsen and N. J. Faergeman, 2007 Transcriptional regulation of phospholipid biosynthesis is linked to fatty acid metabolism by an acyl-CoA-binding-protein-dependent mechanism in Saccharomyces cerevisiae. Biochem J 407**:** 219-230.

Fei, W., G. Shui, Y. Zhang, N. Krahmer, C. Ferguson *et al.*, 2011 A role for phosphatidic acid in the formation of "supersized" lipid droplets. PLoS Genet 7**:** e1002201.

Flanagan, C. A., E. A. Schnieders, A. W. Emerick, R. Kunisawa, A. Admon *et al.*, 1993 Phosphatidylinositol 4-kinase: gene structure and requirement for yeast cell viability. Science 262**:** 1444-1448.

Foti, M., A. Audhya and S. D. Emr, 2001 Sac1 lipid phosphatase and Stt4 phosphatidylinositol 4-kinase regulate a pool of phosphatidylinositol 4-phosphate that functions in the control of the actin cytoskeleton and vacuole morphology. Mol Biol Cell 12**:** 2396-2411.

Galarneau, L., A. Nourani, A. A. Boudreault, Y. Zhang, L. Heliot *et al.*, 2000 Multiple links between the NuA4 histone acetyltransferase complex and epigenetic control of transcription. Mol Cell 5**:** 927-937.

Gaspar, M. L., H. F. Hofbauer, S. D. Kohlwein and S. A. Henry, 2011 Coordination of storage lipid synthesis and membrane biogenesis: evidence for cross-talk between triacylglycerol metabolism and phosphatidylinositol synthesis. J Biol Chem 286**:** 1696-1708.

Ghosh, R., and V. A. Bankaitis, 2011 Phosphatidylinositol transfer proteins: negotiating the regulatory interface between lipid metabolism and lipid signaling in diverse cellular processes. Biofactors 37**:** 290-308.

Gibellini, F., and T. K. Smith, 2010 The Kennedy pathway--De novo synthesis of phosphatidylethanolamine and phosphatidylcholine. IUBMB Life 62**:** 414-428.

Greenberg, M. L., B. Reiner and S. A. Henry, 1982 Regulatory mutations of inositol biosynthesis in yeast: isolation of inositol-excreting mutants. Genetics 100**:** 19-33.

Grigat, M., Y. Jaschke, F. Kliewe, M. Pfeifer, S. Walz *et al.*, 2012 Multiple histone deacetylases are recruited by corepressor Sin3 and contribute to gene repression mediated by Opi1 regulator of phospholipid biosynthesis in the yeast Saccharomyces cerevisiae. Mol Genet Genomics 287**:** 461-472.

Hama, H., E. A. Schnieders, J. Thorner, J. Y. Takemoto and D. B. DeWald, 1999 Direct involvement of phosphatidylinositol 4-phosphate in secretion in the yeast Saccharomyces cerevisiae. J Biol Chem 274**:** 34294-34300.

Han, G. S., A. Audhya, D. J. Markley, S. D. Emr and G. M. Carman, 2002 The Saccharomyces cerevisiae LSB6 gene encodes phosphatidylinositol 4-kinase activity. J Biol Chem 277**:** 47709-47718.

Hancock, L. C., R. P. Behta and J. M. Lopes, 2006 Genomic analysis of the Opi- phenotype. Genetics 173**:** 621-634.

Henriksen, P., S. A. Wagner, B. T. Weinert, S. Sharma, G. Bacinskaja *et al.*, 2012 Proteome-wide analysis of lysine acetylation suggests its broad regulatory scope in Saccharomyces cerevisiae. Mol Cell Proteomics 11**:** 1510-1522.

Henry, S. A., M. L. Gaspar and S. A. Jesch, 2014 The response to inositol: regulation of glycerolipid metabolism and stress response signaling in yeast. Chem Phys Lipids 180**:** 23-43.

Henry, S. A., S. D. Kohlwein and G. M. Carman, 2012 Metabolism and regulation of glycerolipids in the yeast Saccharomyces cerevisiae. Genetics 190**:** 317-349.

Hirsch, J. P., and S. A. Henry, 1986 Expression of the Saccharomyces cerevisiae inositol-1-phosphate synthase (INO1) gene is regulated by factors that affect phospholipid synthesis. Mol Cell Biol 6**:** 3320-3328.

Hofbauer, H. F., F. H. Schopf, H. Schleifer, O. L. Knittelfelder, B. Pieber *et al.*, 2014 Regulation of gene expression through a transcriptional repressor that senses acyl-chain length in membrane phospholipids. Dev Cell 29**:** 729-739.

Homma, K., S. Terui, M. Minemura, H. Qadota, Y. Anraku *et al.*, 1998 Phosphatidylinositol-4-phosphate 5-kinase localized on the plasma membrane is essential for yeast cell morphogenesis. J Biol Chem 273**:** 15779-15786.

Hosaka, K., J. Nikawa, T. Kodaki and S. Yamashita, 1994 Cloning and characterization of the SCS1 gene required for the expression of genes in yeast phospholipid synthesis. J Biochem 115**:** 131-136.

Huang da, W., B. T. Sherman and R. A. Lempicki, 2009 Bioinformatics enrichment tools: paths toward the comprehensive functional analysis of large gene lists. Nucleic Acids Res 37**:** 1-13.

Hughes, W. E., R. Woscholski, F. T. Cooke, R. S. Patrick, S. K. Dove *et al.*, 2000 SAC1 encodes a regulated lipid phosphoinositide phosphatase, defects in which can be suppressed by the homologous Inp52p and Inp53p phosphatases. J Biol Chem 275**:** 801-808.

Huh, W. K., J. V. Falvo, L. C. Gerke, A. S. Carroll, R. W. Howson *et al.*, 2003 Global analysis of protein localization in budding yeast. Nature 425**:** 686-691.

Im, Y. J., S. Raychaudhuri, W. A. Prinz and J. H. Hurley, 2005 Structural mechanism for sterol sensing and transport by OSBP-related proteins. Nature 437**:** 154-158.

Jackson, C. L., and S. Bouvet, 2014 Arfs at a glance. J Cell Sci 127**:** 4103-4109.

Jaschke, Y., J. Schwarz, D. Clausnitzer, C. Muller and H. J. Schuller, 2011 Pleiotropic corepressors Sin3 and Ssn6 interact with repressor Opi1 and negatively regulate transcription of genes required for phospholipid biosynthesis in the yeast Saccharomyces cerevisiae. Mol Genet Genomics 285**:** 91-100.

Kaluarachchi Duffy, S., H. Friesen, A. Baryshnikova, J. P. Lambert, Y. T. Chong *et al.*, 2012 Exploring the yeast acetylome using functional genomics. Cell 149**:** 936-948.

Kandutsch, A. A., F. R. Taylor and E. P. Shown, 1984 Different forms of the oxysterol-binding protein. Binding kinetics and stability. J Biol Chem 259**:** 12388-12397.

Kawaguchi, A., H. Tomoda, S. Nozoe, S. Omura and S. Okuda, 1982 Mechanism of action of cerulenin on fatty acid synthetase. Effect of cerulenin on iodoacetamide-induced malonyl-CoA decarboxylase activity. J Biochem 92**:** 7-12.

Kawaguchi, A., H. Tomoda, S. Okuda, J. Awaya and S. Omura, 1979 Cerulenin resistance in a cerulenin-producing fungus. Isolation of cerulenin insensitive fatty acid synthetase. Arch Biochem Biophys 197**:** 30-35.

Kodaki, T., and S. Yamashita, 1987 Yeast phosphatidylethanolamine methylation pathway. Cloning and characterization of two distinct methyltransferase genes. J Biol Chem 262**:** 15428-15435.

Kohlwein, S. D., 2010 Triacylglycerol homeostasis: insights from yeast. J Biol Chem 285**:** 15663-15667.

Konarzewska, P., M. Esposito and C. H. Shen, 2012 INO1 induction requires chromatin remodelers Ino80p and Snf2p but not the histone acetylases. Biochem Biophys Res Commun 418**:** 483-488.

Krogan, N. J., K. Baetz, M. C. Keogh, N. Datta, C. Sawa *et al.*, 2004 Regulation of chromosome stability by the histone H2A variant Htz1, the Swr1 chromatin remodeling complex, and the histone acetyltransferase NuA4. Proc Natl Acad Sci U S A 101**:** 13513-13518.

Kuchler, K., G. Daum and F. Paltauf, 1986 Subcellular and submitochondrial localization of phospholipid-synthesizing enzymes in Saccharomyces cerevisiae. J Bacteriol 165**:** 901-910.

Kurat, C. F., H. Wolinski, J. Petschnigg, S. Kaluarachchi, B. Andrews *et al.*, 2009 Cdk1/Cdc28-dependent activation of the major triacylglycerol lipase Tgl4 in yeast links lipolysis to cell-cycle progression. Mol Cell 33**:** 53-63.

Kurdistani, S. K., and M. Grunstein, 2003 Histone acetylation and deacetylation in yeast. Nat Rev Mol Cell Biol 4**:** 276-284.

Kvam, E., and D. S. Goldfarb, 2004 Nvj1p is the outer-nuclear-membrane receptor for oxysterol-binding protein homolog Osh1p in Saccharomyces cerevisiae. J Cell Sci 117**:** 4959-4968.

LeBlanc, M. A., and C. R. McMaster, 2010 Lipid binding requirements for oxysterol-binding protein Kes1 inhibition of autophagy and endosome-trans-Golgi trafficking pathways. J Biol Chem 285**:** 33875-33884.

Lee, H. J., M. Chun and K. V. Kandror, 2001 Tip60 and HDAC7 interact with the endothelin receptor a and may be involved in downstream signaling. J Biol Chem 276**:** 16597-16600.

Lehto, M., S. Laitinen, G. Chinetti, M. Johansson, C. Ehnholm *et al.*, 2001 The OSBP-related protein family in humans. J Lipid Res 42**:** 1203-1213.

Letts, V. A., L. S. Klig, M. Bae-Lee, G. M. Carman and S. A. Henry, 1983 Isolation of the yeast structural gene for the membrane-associated enzyme phosphatidylserine synthase. Proc Natl Acad Sci U S A 80**:** 7279-7283.

Levine, T. P., and S. Munro, 2001 Dual targeting of Osh1p, a yeast homologue of oxysterol-binding protein, to both the Golgi and the nucleus-vacuole junction. Mol Biol Cell 12**:** 1633-1644.

Li, X., M. P. Rivas, M. Fang, J. Marchena, B. Mehrotra *et al.*, 2002 Analysis of oxysterol binding protein homologue Kes1p function in regulation of Sec14p-dependent protein transport from the yeast Golgi complex. J Cell Biol 157**:** 63-77.

Li, X., S. M. Routt, Z. Xie, X. Cui, M. Fang *et al.*, 2000 Identification of a novel family of nonclassic yeast phosphatidylinositol transfer proteins whose function modulates phospholipase D activity and Sec14p-independent cell growth. Mol Biol Cell 11**:** 1989-2005.

Lin, Y. Y., J. Y. Lu, J. Zhang, W. Walter, W. Dang *et al.*, 2009 Protein acetylation microarray reveals that NuA4 controls key metabolic target regulating gluconeogenesis. Cell 136**:** 1073-1084.

Lindstrom, K. C., J. C. Vary, Jr., M. R. Parthun, J. Delrow and T. Tsukiyama, 2006 Isw1 functions in parallel with the NuA4 and Swr1 complexes in stress-induced gene repression. Mol Cell Biol 26**:** 6117-6129.

Loewen, C. J., M. L. Gaspar, S. A. Jesch, C. Delon, N. T. Ktistakis *et al.*, 2004 Phospholipid metabolism regulated by a transcription factor sensing phosphatidic acid. Science 304**:** 1644-1647.

Loewen, C. J., A. Roy and T. P. Levine, 2003 A conserved ER targeting motif in three families of lipid binding proteins and in Opi1p binds VAP. EMBO J 22**:** 2025-2035.

Loewy, B. S., and S. A. Henry, 1984 The INO2 and INO4 loci of Saccharomyces cerevisiae are pleiotropic regulatory genes. Mol Cell Biol 4**:** 2479-2485.

Longtine, M. S., A. McKenzie, 3rd, D. J. Demarini, N. G. Shah, A. Wach *et al.*, 1998 Additional modules for versatile and economical PCR-based gene deletion and modification in Saccharomyces cerevisiae. Yeast 14**:** 953-961.

Lopes, J. M., K. L. Schulze, J. W. Yates, J. P. Hirsch and S. A. Henry, 1993 The INO1 promoter of Saccharomyces cerevisiae includes an upstream repressor sequence (URS1) common to a diverse set of yeast genes. J Bacteriol 175**:** 4235-4238.

Love, M. I., W. Huber and S. Anders, 2014 Moderated estimation of fold change and dispersion for RNA-seq data with DESeq2. Genome Biol 15**:** 550.

Lu, J. Y., Y. Y. Lin, J. C. Sheu, J. T. Wu, F. J. Lee *et al.*, 2011 Acetylation of yeast AMPK controls intrinsic aging independently of caloric restriction. Cell 146**:** 969-979.

Lu, P. Y., N. Levesque and M. S. Kobor, 2009 NuA4 and SWR1-C: two chromatin-modifying complexes with overlapping functions and components. Biochem Cell Biol 87**:** 799-815.

Madsen, C. T., K. B. Sylvestersen, C. Young, S. C. Larsen, J. W. Poulsen *et al.*, 2015 Biotin starvation causes mitochondrial protein hyperacetylation and partial rescue by the SIRT3-like deacetylase Hst4p. Nat Commun 6**:** 7726.

Maeda, K., K. Anand, A. Chiapparino, A. Kumar, M. Poletto *et al.*, 2013 Interactome map uncovers phosphatidylserine transport by oxysterol-binding proteins. Nature 501**:** 257-261.

McGee, T. P., H. B. Skinner, E. A. Whitters, S. A. Henry and V. A. Bankaitis, 1994 A phosphatidylinositol transfer protein controls the phosphatidylcholine content of yeast Golgi membranes. J Cell Biol 124**:** 273-287.

Mendonsa, R., and J. Engebrecht, 2009 Phospholipase D function in Saccharomyces cerevisiae. Biochim Biophys Acta 1791**:** 970-974.

Menzies, K. J., H. Zhang, E. Katsyuba and J. Auwerx, 2016 Protein acetylation in metabolism - metabolites and cofactors. Nat Rev Endocrinol 12**:** 43-60.

Merril, C. R., 1990 Gel-staining techniques. Methods Enzymol 182**:** 477-488.

Mitchell, L., S. Huard, M. Cotrut, R. Pourhanifeh-Lemeri, A. L. Steunou *et al.*, 2013 mChIP-KAT-MS, a method to map protein interactions and acetylation sites for lysine acetyltransferases. Proc Natl Acad Sci U S A 110**:** E1641-1650.

Mitchell, L., J. P. Lambert, M. Gerdes, A. S. Al-Madhoun, I. S. Skerjanc *et al.*, 2008 Functional dissection of the NuA4 histone acetyltransferase reveals its role as a genetic hub and that Eaf1 is essential for complex integrity. Mol Cell Biol 28**:** 2244-2256.

Mitchell, L., A. Lau, J. P. Lambert, H. Zhou, Y. Fong *et al.*, 2011 Regulation of septin dynamics by the Saccharomyces cerevisiae lysine acetyltransferase NuA4. PLoS One 6**:** e25336.

Mora, G., M. Scharnewski and M. Fulda, 2012 Neutral lipid metabolism influences phospholipid synthesis and deacylation in Saccharomyces cerevisiae. PLoS One 7**:** e49269.

Mousley, C. J., P. Yuan, N. A. Gaur, K. D. Trettin, A. H. Nile *et al.*, 2012 A sterol-binding protein integrates endosomal lipid metabolism with TOR signaling and nitrogen sensing. Cell 148**:** 702-715.

Mullner, H., and G. Daum, 2004 Dynamics of neutral lipid storage in yeast. Acta Biochim Pol 51**:** 323-347.

Munnik, T., and M. Wierzchowiecka, 2013 Lipid-binding analysis using a fat blot assay. Methods Mol Biol 1009**:** 253-259.

Natter, K., P. Leitner, A. Faschinger, H. Wolinski, S. McCraith *et al.*, 2005 The spatial organization of lipid synthesis in the yeast Saccharomyces cerevisiae derived from large scale green fluorescent protein tagging and high resolution microscopy. Mol Cell Proteomics 4**:** 662-672.

Nikawa, J., and S. Yamashita, 1984 Molecular cloning of the gene encoding CDPdiacylglycerol-inositol 3-phosphatidyl transferase in Saccharomyces cerevisiae. Eur J Biochem 143**:** 251-256.

Nikawa, J., and S. Yamashita, 1997 Phosphatidylinositol synthase from yeast. Biochim Biophys Acta 1348**:** 173-178.

Nourani, A., R. T. Utley, S. Allard and J. Cote, 2004 Recruitment of the NuA4 complex poises the PHO5 promoter for chromatin remodeling and activation. EMBO J 23**:** 2597-2607.

Novick, P., C. Field and R. Schekman, 1980 Identification of 23 complementation groups required for post-translational events in the yeast secretory pathway. Cell 21**:** 205-215.

Oelkers, P., D. Cromley, M. Padamsee, J. T. Billheimer and S. L. Sturley, 2002 The DGA1 gene determines a second triglyceride synthetic pathway in yeast. J Biol Chem 277**:** 8877-8881.

Oelkers, P., A. Tinkelenberg, N. Erdeniz, D. Cromley, J. T. Billheimer *et al.*, 2000 A lecithin cholesterol acyltransferase-like gene mediates diacylglycerol esterification in yeast. J Biol Chem 275**:** 15609-15612.

Olkkonen, V. M., 2013 OSBP-related proteins: liganding by glycerophospholipids opens new insight into their function. Molecules 18**:** 13666-13679.

Olkkonen, V. M., 2015 OSBP-Related Protein Family in Lipid Transport Over Membrane Contact Sites. Lipid Insights 8**:** 1-9.

Patton-Vogt, J. L., P. Griac, A. Sreenivas, V. Bruno, S. Dowd *et al.*, 1997 Role of the yeast phosphatidylinositol/phosphatidylcholine transfer protein (Sec14p) in phosphatidylcholine turnover and INO1 regulation. J Biol Chem 272**:** 20873-20883.

Petschnigg, J., H. Wolinski, D. Kolb, G. Zellnig, C. F. Kurat *et al.*, 2009 Good fat, essential cellular requirements for triacylglycerol synthesis to maintain membrane homeostasis in yeast. J Biol Chem 284**:** 30981-30993.

Pfaffl, M. W., 2001 A new mathematical model for relative quantification in real-time RT-PCR. Nucleic Acids Res 29**:** e45.

Quinlan, A. R., and I. M. Hall, 2010 BEDTools: a flexible suite of utilities for comparing genomic features. Bioinformatics 26**:** 841-842.

Raychaudhuri, S., Y. J. Im, J. H. Hurley and W. A. Prinz, 2006 Nonvesicular sterol movement from plasma membrane to ER requires oxysterol-binding protein-related proteins and phosphoinositides. J Cell Biol 173**:** 107-119.

Reid, J. L., V. R. Iyer, P. O. Brown and K. Struhl, 2000 Coordinate regulation of yeast ribosomal protein genes is associated with targeted recruitment of Esa1 histone acetylase. Mol Cell 6**:** 1297-1307.

Ricicova, M., M. Hamidi, A. Quiring, A. Niemisto, E. Emberly *et al.*, 2013 Dissecting genealogy and cell cycle as sources of cell-to-cell variability in MAPK signaling using high-throughput lineage tracking. Proc Natl Acad Sci U S A 110**:** 11403-11408.

Roney, I. J., A. D. Rudner, J. F. Couture and M. Kaern, 2016 Improvement of the reverse tetracycline transactivator by single amino acid substitutions that reduce leaky target gene expression to undetectable levels. Sci Rep 6**:** 27697.

Rose, K., S. A. Rudge, M. A. Frohman, A. J. Morris and J. Engebrecht, 1995 Phospholipase D signaling is essential for meiosis. Proc Natl Acad Sci U S A 92**:** 12151-12155.

Rossetto, D., M. Cramet, A. Y. Wang, A. L. Steunou, N. Lacoste *et al.*, 2014 Eaf5/7/3 form a functionally independent NuA4 submodule linked to RNA polymerase II-coupled nucleosome recycling. EMBO J 33**:** 1397-1415.

Rudge, S. A., V. A. Sciorra, M. Iwamoto, C. Zhou, T. Strahl *et al.*, 2004 Roles of phosphoinositides and of Spo14p (phospholipase D)-generated phosphatidic acid during yeast sporulation. Mol Biol Cell 15**:** 207-218.

Salas-Santiago, B., and J. M. Lopes, 2014 Saccharomyces cerevisiae essential genes with an Opi- phenotype. G3 (Bethesda) 4**:** 761-767.

Sandager, L., M. H. Gustavsson, U. Stahl, A. Dahlqvist, E. Wiberg *et al.*, 2002 Storage lipid synthesis is non-essential in yeast. J Biol Chem 277**:** 6478-6482.

Schaaf, G., E. A. Ortlund, K. R. Tyeryar, C. J. Mousley, K. E. Ile *et al.*, 2008 Functional anatomy of phospholipid binding and regulation of phosphoinositide homeostasis by proteins of the sec14 superfamily. Mol Cell 29**:** 191-206.

Schuller, H. J., K. Richter, B. Hoffmann, R. Ebbert and E. Schweizer, 1995 DNA binding site of the yeast heteromeric Ino2p/Ino4p basic helix-loop-helix transcription factor: structural requirements as defined by saturation mutagenesis. FEBS Lett 370**:** 149-152.

Schuller, H. J., R. Schorr, B. Hoffmann and E. Schweizer, 1992 Regulatory gene INO4 of yeast phospholipid biosynthesis is positively autoregulated and functions as a transactivator of fatty acid synthase genes FAS1 and FAS2 from Saccharomyces cerevisiae. Nucleic Acids Res 20**:** 5955-5961.

Schwank, S., R. Ebbert, K. Rautenstrauss, E. Schweizer and H. J. Schuller, 1995 Yeast transcriptional activator INO2 interacts as an Ino2p/Ino4p basic helix-loop-helix heteromeric complex with the inositol/choline-responsive element necessary for expression of phospholipid biosynthetic genes in Saccharomyces cerevisiae. Nucleic Acids Res 23**:** 230-237.

Shahbazian, M. D., and M. Grunstein, 2007 Functions of site-specific histone acetylation and deacetylation. Annu Rev Biochem 76**:** 75-100.

Shen, H., and W. Dowhan, 1996 Reduction of CDP-diacylglycerol synthase activity results in the excretion of inositol by Saccharomyces cerevisiae. J Biol Chem 271**:** 29043-29048.

Shen, H., P. N. Heacock, C. J. Clancey and W. Dowhan, 1996 The CDS1 gene encoding CDP-diacylglycerol synthase in Saccharomyces cerevisiae is essential for cell growth. J Biol Chem 271**:** 789-795.

Shirra, M. K., J. Patton-Vogt, A. Ulrich, O. Liuta-Tehlivets, S. D. Kohlwein *et al.*, 2001 Inhibition of acetyl coenzyme A carboxylase activity restores expression of the INO1 gene in a snf1 mutant strain of Saccharomyces cerevisiae. Mol Cell Biol 21**:** 5710-5722.

Sikorski, R. S., and P. Hieter, 1989 A system of shuttle vectors and yeast host strains designed for efficient manipulation of DNA in Saccharomyces cerevisiae. Genetics 122**:** 19-27.

Skinner, H. B., T. P. McGee, C. R. McMaster, M. R. Fry, R. M. Bell *et al.*, 1995 The Saccharomyces cerevisiae phosphatidylinositol-transfer protein effects a ligand-

dependent inhibition of choline-phosphate cytidylyltransferase activity. Proc Natl Acad Sci U S A 92**:** 112-116.
Sreenivas, A., J. L. Patton-Vogt, V. Bruno, P. Griac and S. A. Henry, 1998 A role for phospholipase D (Pld1p) in growth, secretion, and regulation of membrane lipid synthesis in yeast. J Biol Chem 273**:** 16635-16638.
Stefan, C. J., A. G. Manford, D. Baird, J. Yamada-Hanff, Y. Mao *et al.*, 2011 Osh proteins regulate phosphoinositide metabolism at ER-plasma membrane contact sites. Cell 144**:** 389-401.
Strahl, T., H. Hama, D. B. DeWald and J. Thorner, 2005 Yeast phosphatidylinositol 4-kinase, Pik1, has essential roles at the Golgi and in the nucleus. J Cell Biol 171**:** 967-979.
Suka, N., Y. Suka, A. A. Carmen, J. Wu and M. Grunstein, 2001 Highly specific antibodies determine histone acetylation site usage in yeast heterochromatin and euchromatin. Mol Cell 8**:** 473-479.
Tan, J., and J. A. Brill, 2014 Cinderella story: PI4P goes from precursor to key signaling molecule. Crit Rev Biochem Mol Biol 49**:** 33-58.
Taylor, F. R., S. E. Saucier, E. P. Shown, E. J. Parish and A. A. Kandutsch, 1984 Correlation between oxysterol binding to a cytosolic binding protein and potency in the repression of hydroxymethylglutaryl coenzyme A reductase. J Biol Chem 259**:** 12382-12387.
Taylor, S. C., and A. Posch, 2014 The design of a quantitative western blot experiment. Biomed Res Int 2014**:** 361590.
Tong, J., M. K. Manik, H. Yang and Y. J. Im, 2016 Structural insights into nonvesicular lipid transport by the oxysterol binding protein homologue family. Biochim Biophys Acta 1861**:** 928-939.
Tong, J., H. Yang, H. Yang, S. H. Eom and Y. J. Im, 2013 Structure of Osh3 reveals a conserved mode of phosphoinositide binding in oxysterol-binding proteins. Structure 21**:** 1203-1213.
Tripathi, A., A. H. Nile and V. A. Bankaitis, 2014 Sec14-like phosphatidylinositol-transfer proteins and diversification of phosphoinositide signalling outcomes. Biochem Soc Trans 42**:** 1383-1388.
Trotter, P. J., J. Pedretti and D. R. Voelker, 1993 Phosphatidylserine decarboxylase from Saccharomyces cerevisiae. Isolation of mutants, cloning of the gene, and creation of a null allele. J Biol Chem 268**:** 21416-21424.
Trotter, P. J., J. Pedretti, R. Yates and D. R. Voelker, 1995 Phosphatidylserine decarboxylase 2 of Saccharomyces cerevisiae. Cloning and mapping of the gene, heterologous expression, and creation of the null allele. J Biol Chem 270**:** 6071-6080.
Villa-Garcia, M. J., M. S. Choi, F. I. Hinz, M. L. Gaspar, S. A. Jesch *et al.*, 2011 Genome-wide screen for inositol auxotrophy in Saccharomyces cerevisiae implicates lipid metabolism in stress response signaling. Mol Genet Genomics 285**:** 125-149.
Voelker, D. R., 1997 Phosphatidylserine decarboxylase. Biochim Biophys Acta 1348**:** 236-244.
Wagner, C., M. Dietz, J. Wittmann, A. Albrecht and H. J. Schuller, 2001 The negative regulator Opi1 of phospholipid biosynthesis in yeast contacts the pleiotropic repressor Sin3 and the transcriptional activator Ino2. Mol Microbiol 41**:** 155-166.
Wang, C. W., 2015 Lipid droplet dynamics in budding yeast. Cell Mol Life Sci 72**:** 2677-2695.
Weinert, B. T., V. Iesmantavicius, T. Moustafa, C. Scholz, S. A. Wagner *et al.*, 2014 Acetylation dynamics and stoichiometry in Saccharomyces cerevisiae. Mol Syst Biol 10**:** 716.
White, M. J., J. P. Hirsch and S. A. Henry, 1991 The OPI1 gene of Saccharomyces cerevisiae, a negative regulator of phospholipid biosynthesis, encodes a protein containing polyglutamine tracts and a leucine zipper. J Biol Chem 266**:** 863-872.
Xie, Z., M. Fang, M. P. Rivas, A. J. Faulkner, P. C. Sternweis *et al.*, 1998 Phospholipase D activity is required for suppression of yeast phosphatidylinositol transfer protein defects. Proc Natl Acad Sci U S A 95**:** 12346-12351.

Xiong, Y., and K. L. Guan, 2012 Mechanistic insights into the regulation of metabolic enzymes by acetylation. J Cell Biol 198**:** 155-164.

Yamamoto, T., and M. Horikoshi, 1997 Novel substrate specificity of the histone acetyltransferase activity of HIV-1-Tat interactive protein Tip60. J Biol Chem 272**:** 30595-30598.

Yamashita, S., and J. Nikawa, 1997 Phosphatidylserine synthase from yeast. Biochim Biophys Acta 1348**:** 228-235.

Yang, H., M. Bard, D. A. Bruner, A. Gleeson, R. J. Deckelbaum *et al.*, 1996 Sterol esterification in yeast: a two-gene process. Science 272**:** 1353-1356.

Yi, C., M. Ma, L. Ran, J. Zheng, J. Tong *et al.*, 2012 Function and molecular mechanism of acetylation in autophagy regulation. Science 336**:** 474-477.

Yi, J., X. Huang, Y. Yang, W. G. Zhu, W. Gu *et al.*, 2014 Regulation of histone acetyltransferase TIP60 function by histone deacetylase 3. J Biol Chem 289**:** 33878-33886.

Yoshida, S., Y. Ohya, M. Goebl, A. Nakano and Y. Anraku, 1994a A novel gene, STT4, encodes a phosphatidylinositol 4-kinase in the PKC1 protein kinase pathway of Saccharomyces cerevisiae. J Biol Chem 269**:** 1166-1172.

Yoshida, S., Y. Ohya, A. Nakano and Y. Anraku, 1994b Genetic interactions among genes involved in the STT4-PKC1 pathway of Saccharomyces cerevisiae. Mol Gen Genet 242**:** 631-640.

Zhang, Y., U. Werling and W. Edelmann, 2014 Seamless Ligation Cloning Extract (SLiCE) cloning method. Methods Mol Biol 1116**:** 235-244.

# 6 Contributions of collaborators

James Butcher, Annika Flint, and Dr. Alain Stintzi (UOttawa) performed the RNA-seq experiments. This included creating the cDNA library from the extracted RNA, sequencing, and sequence alignments. They also helped with the editing of my manuscript.

Danny Salem and Dr. Mads Kaern (UOttawa) performed the quantification of the lipid droplet staining. They also helped with the editing of my manuscript.

Dr. Michael Kennedy (UOttawa) did the PI-4-P binding assay and the Sac1 assay in Chapter 2. He also helped with the editing of my manuscript.

Ian Roney and Brendan Camellato (UOtatwa) provided purified genomic extract containing Tet-responsive system.

Mass spectrometry service was provided in part by Dr. Daniel Figeys" laboratory at the University of Ottawa and in part by Dr. Jean-Philippe Lambert who works in Dr. Anne-Claude Gingras laboratory at the University of Toronto.

# 7 Appendices

**Table S1 Strain List**

| Strain | Genotype | Source |
|---|---|---|
| BY4741 | ***MATa*** *his3Δ1 leu2Δ0 met15Δ0 ura3Δ0* | (BRACHMANN *et al.* 1998) |
| YKB3333 | ***MATa*** *his3Δ1 leu2Δ0 met15Δ0 ura3Δ0 eaf1Δ::KANMX* | DMA collection (GE) |
| YKB3484 | ***MATa*** *his3Δ1 leu2Δ0 met15Δ0 ura3Δ0 rtt109Δ::KANMX* | DMA collection (GE) |
| YKB3482 | ***MATa*** *his3Δ1 leu2Δ0 met15Δ0 ura3Δ0 elp3Δ::KANMX* | DMA collection (GE) |
| YKB3489 | ***MATa*** *his3Δ1 leu2Δ0 met15Δ0 ura3Δ0 gcn5Δ::KANMX* | DMA collection (GE) |
| YKB3485 | ***MATa*** *his3Δ1 leu2Δ0 met15Δ0 ura3Δ0 hat1Δ::KANMX* | DMA collection (GE) |
| YKB3486 | ***MATa*** *his3Δ1 leu2Δ0 met15Δ0 ura3Δ0 sas2Δ::KANMX* | DMA collection (GE) |
| YKB3487 | ***MATa*** *his3Δ1 leu2Δ0 met15Δ0 ura3Δ0 sas3Δ::KANMX* | DMA collection (GE) |
| YKB3488 | ***MATa*** *his3Δ1 leu2Δ0 met15Δ0 ura3Δ0 hpa2Δ::KANMX* | DMA collection (GE) |
| YKB3297 | ***MATa*** *his3Δ1 leu2Δ0 met15Δ0 ura3Δ0 hpa3Δ::KANMX* | DMA collection (GE) |
| YKB3303 | ***MATa*** *his3Δ1 leu2Δ0 met15Δ0 ura3Δ0 rpd3Δ::KANMX* | DMA collection (GE) |
| YKB3492 | ***MATa*** *his3Δ1 leu2Δ0 met15Δ0 ura3Δ0 sir2Δ::KANMX* | DMA collection (GE) |
| YKB3491 | ***MATa*** *his3Δ1 leu2Δ0 met15Δ0 ura3Δ0 hda1Δ::KANMX* | DMA collection (GE) |
| YKB3490 | ***MATa*** *his3Δ1 leu2Δ0 met15Δ0 ura3Δ0 hos1Δ::KANMX* | DMA collection (GE) |
| YKB3301 | ***MATa*** *his3Δ1 leu2Δ0 met15Δ0 ura3Δ0 hos2Δ::KANMX* | DMA collection (GE) |
| YKB3302 | ***MATa*** *his3Δ1 leu2Δ0 met15Δ0 ura3Δ0 hos3Δ::KANMX* | DMA collection (GE) |
| YKB3293 | ***MATa*** *his3Δ1 leu2Δ0 met15Δ0 ura3Δ0 hst1Δ::KANMX* | DMA collection (GE) |
| YKB4081 | ***MATa*** *his3Δ1 leu2Δ0 met15Δ0 ura3Δ0 hst2Δ::KANMX* | DMA collection (GE) |
| YKB3295 | ***MATa*** *his3Δ1 leu2Δ0 met15Δ0 ura3Δ0 hst3Δ::KANMX* | DMA collection (GE) |
| YKB3296 | ***MATa*** *his3Δ1 leu2Δ0 met15Δ0 ura3Δ0 hst4Δ::KANMX* | DMA collection (GE) |
| YKB3292 | ***MATa*** *his3Δ1 leu2Δ0 met15Δ0 ura3Δ0 eaf7Δ::KANMX* | DMA collection (GE) |
| YKB4236 | ***MATa*** *his3Δ1 leu2Δ0 met15Δ0 ura3Δ0 esa1Δ::HIS3 esa1-L254P$^{ts}$-URA3* | This study |

| | | |
|---|---|---|
| YKB4073 | ***MATa*** *his3Δ1 leu2Δ0 met15Δ0 ura3Δ0 rtt109Δ::HIS3* | This study |
| CMY505/YKB3144 | ***MATa*** *his3Δ1 leu2Δ0 met15Δ0 ura3Δ0 sec14-1$^{ts}$-NATMX* | (FAIRN *et al.* 2007) |
| YKB3935 | ***MATa*** *his3Δ1 leu2Δ0 met15Δ0 ura3Δ0 sec14-1$^{ts}$-NATMX eaf1Δ::KANMX* | This study |
| YKB4074 | ***MATa*** *his3Δ1 leu2Δ0 met15Δ0 ura3Δ0 sec14-1$^{ts}$-NATMX rtt109Δ::HIS3* | This study |
| YKB3444 | ***MATa*** *his3Δ1 leu2Δ0 met15Δ0 ura3Δ0 sec14-1$^{ts}$-NATMX elp3Δ::KANMX* | This study |
| YKB4080 | ***MATa*** *his3Δ1 leu2Δ0 met15Δ0 ura3Δ0 sec14-1$^{ts}$-NATMX gcn5Δ::KANMX* | This study |
| YKB3442 | ***MATa*** *his3Δ1 leu2Δ0 met15Δ0 ura3Δ0 sec14-1$^{ts}$-NATMX hat1Δ::KANMX* | This study |
| YKB3447 | ***MATa*** *his3Δ1 leu2Δ0 met15Δ0 ura3Δ0 sec14-1$^{ts}$-NATMX sas2Δ::KANMX* | This study |
| YKB3449 | ***MATα*** *his3Δ1 leu2Δ0 met15Δ0 ura3Δ0 sec14-1$^{ts}$-NATMX sas3Δ::KANMX* | This study |
| YKB4065 | ***MATα*** *his3Δ1 leu2Δ0 met15Δ0 ura3Δ0 sec14-1$^{ts}$-NATMX hpa2Δ::KANMX* | This study |
| YKB3451 | ***MATa*** *his3Δ1 leu2Δ0 met15Δ0 ura3Δ0 sec14-1$^{ts}$-NATMX hpa3Δ::KANMX* | This study |
| YKB3509 | ***MATa*** *his3Δ1 leu2Δ0 met15Δ0 ura3Δ0 sec14-1$^{ts}$-NATMX rpd3Δ::KANMX* | This study |
| YKB3936 | ***MATα*** *his3Δ1 leu2Δ0 met15Δ0 ura3Δ0 sec14-1$^{ts}$-NATMX sir2Δ::KANMX* | This study |
| YKB4064 | ***MATa*** *his3Δ1 leu2Δ0 met15Δ0 ura3Δ0 sec14-1$^{ts}$-NATMX hda1Δ::KANMX* | This study |
| YKB3510 | ***MATa*** *his3Δ1 leu2Δ0 met15Δ0 ura3Δ0 sec14-1$^{ts}$-NATMX hos1Δ::KANMX* | This study |
| YKB3512 | ***MATa*** *his3Δ1 leu2Δ0 met15Δ0 ura3Δ0 sec14-1$^{ts}$-NATMX hos2Δ::KANMX* | This study |
| YKB3514 | ***MATa*** *his3Δ1 leu2Δ0 met15Δ0 ura3Δ0 sec14-1$^{ts}$-NATMX hos3Δ::KANMX* | This study |
| YKB3516 | ***MATa*** *his3Δ1 leu2Δ0 met15Δ0 ura3Δ0 sec14-1$^{ts}$-NATMX hst1Δ::KANMX* | This study |
| YKB3518 | ***MATa*** *his3Δ1 leu2Δ0 met15Δ0 ura3Δ0 sec14-1$^{ts}$-NATMX hst2Δ::KANMX* | This study |
| YKB3520 | ***MATa*** *his3Δ1 leu2Δ0 met15Δ0 ura3Δ0 sec14-1$^{ts}$-NATMX hst3Δ::KANMX* | This study |
| YKB3522 | ***MATa*** *his3Δ1 leu2Δ0 met15Δ0 ura3Δ0 sec14-1$^{ts}$-NATMX hst4Δ::KANMX* | This study |
| YKB4068 | ***MATa*** *his3Δ1 leu2Δ0 met15Δ0 ura3Δ0 sec14-1$^{ts}$-NATMX eaf7Δ::KANMX* | This study |
| YKB4242 | ***MATa*** *his3Δ1 leu2Δ0 met15Δ0 ura3Δ0 sec14-1$^{ts}$-NATMX esa1Δ::HIS3 esa1-L254P$^{ts}$-URA3* | This study |
| YKB4083 | ***MATa*** *his3Δ1 leu2Δ0 met15Δ0 ura3Δ0 eaf1Δ::KANMX rtt109Δ::HIS3* | This study |
| YKB4084 | ***MATa*** *his3Δ1 leu2Δ0 met15Δ0 ura3Δ0* | This study |

| | | |
|---|---|---|
| | *sec14-1$^{ts}$-NATMX eaf1Δ::KANMX rtt109Δ::HIS3* | |
| YKB3343 | ***MATa*** *his3Δ1 leu2Δ0 met15Δ0 ura3Δ0 osh4Δ::KANMX* | DMA collection (GE) |
| YKB3344 | ***MATa*** *his3Δ1 leu2Δ0 met15Δ0 ura3Δ0 sec14-1$^{ts}$-NATMX osh4Δ::KANMX* | This study |
| YKB4056 | ***MATa*** *his3Δ1 leu2Δ0 met15Δ0 ura3Δ0 eaf1Δ::KANMX osh4Δ::HIS3* | This study |
| YKB4061 | ***MATa*** *his3Δ1 leu2Δ0 met15Δ0 ura3Δ0 sec14-1$^{ts}$-NATMX eaf1Δ::KANMX osh4Δ::HIS3* | This study |
| YKB4273 | ***MATa*** *his3Δ1 leu2Δ0 met15Δ0 ura3Δ0 cki1Δ::KANMX* | DMA collection (GE) |
| YKB4275 | ***MATa*** *his3Δ1 leu2Δ0 met15Δ0 ura3Δ0 sec14-1$^{ts}$-NATMX cki1Δ::KANMX* | This study |
| YKB4277 | ***MATa*** *his3Δ1 leu2Δ0 met15Δ0 ura3Δ0 eaf1Δ::HIS3 cki1Δ::KANMX* | This study |
| YKB4278 | ***MATa*** *his3Δ1 leu2Δ0 met15Δ0 ura3Δ0 sec14-1$^{ts}$-NATMX eaf1Δ::HIS3 cki1Δ::KANMX* | This study |
| N/A | ***MATa*** *his3Δ1 leu2Δ0 met15Δ0 ura3Δ0 eaf7Δ::KANMX osh4Δ::HIS3* | This study |
| N/A | ***MATa*** *his3Δ1 leu2Δ0 met15Δ0 ura3Δ0 sec14-1$^{ts}$-NATMX eaf7Δ::KANMX osh4Δ::HIS3* | This study |
| YKB4279 | ***MATa*** *his3Δ1 leu2Δ0 met15Δ0 ura3Δ0 eaf7Δ::HIS3 cki1Δ::KANMX* | This study |
| YKB4281 | ***MATa*** *his3Δ1 leu2Δ0 met15Δ0 ura3Δ0 sec14-1$^{ts}$-NATMX eaf7Δ::HIS3 cki1Δ::KANMX* | This study |
| N/A | ***MATa*** *his3Δ1 leu2Δ0 met15Δ0 ura3Δ0 esa1Δ::HIS3 esa1-L254P$^{ts}$-URA3 osh4Δ::KANMX* | This study |
| N/A | ***MATa*** *his3Δ1 leu2Δ0 met15Δ0 ura3Δ0 sec14-1$^{ts}$-NATMX esa1Δ::HIS3 esa1-L254P$^{ts}$-URA3 osh4Δ::KANMX* | This study |
| YKB4283 | ***MATa*** *his3Δ1 leu2Δ0 met15Δ0 ura3Δ0 esa1Δ::HIS3 esa1-L254P$^{ts}$-URA3 cki1ΔKAN* | This study |
| YKB4285 | ***MATa*** *his3Δ1 leu2Δ0 met15Δ0 ura3Δ0 sec14-1$^{ts}$-NATMX esa1Δ::HIS3 esa1-L254P$^{ts}$-URA3 cki1Δ::KANMX* | This study |
| YKB3113 | ***MATa*** *his3Δ1 leu2Δ0 met15Δ0 ura3Δ0 spo14Δ::KANMX* | DMA collection (GE) |
| YKB4261 | ***MATa*** *his3Δ1 leu2Δ0 met15Δ0 ura3Δ0 sec14-1$^{ts}$-NATMX spo14Δ::KANMX* | This study |
| YKB4263 | ***MATa*** *his3Δ1 leu2Δ0 met15Δ0 ura3Δ0 eaf1Δ::HIS3 spo14Δ::KANMX* | This study |
| YKB4264 | ***MATa*** *his3Δ1 leu2Δ0 met15Δ0 ura3Δ0 sec14-1$^{ts}$-NATMX eaf1Δ::HIS3 spo14Δ::KANMX* | This study |
| YKB4269 | ***MATa*** *his3Δ1 leu2Δ0 met15Δ0 ura3Δ0 eaf7Δ::KANMX spo14Δ::KANMX* | This study |
| YKB4271 | ***MATa*** *his3Δ1 leu2Δ0 met15Δ0 ura3Δ0* | This study |

| | | |
|---|---|---|
| | *sec14-1$^{ts}$-NATMX eaf7Δ::KANMX spo14Δ::KANMX* | |
| YKB4265 | ***MATa*** *his3Δ1 leu2Δ0 met15Δ0 ura3Δ0 esa1Δ::HIS3 esa-L254P$^{ts}$-URA3 spo14Δ::KANMX* | This study |
| YKB4267 | ***MATa*** *his3Δ1 leu2Δ0 met15Δ0 ura3Δ0 sec14-1$^{ts}$-NATMX esa1Δ::HIS3 esa1-L254P$^{ts}$-URA3 spo14Δ::KANMX* | This study |
| YJP1078/YKB4336 | ***MATa*** *his3Δ1 leu2Δ0 met15Δ0 ura3Δ0 dga1Δ::KANMX lro1Δ::KANMX are1Δ::KANMX are2Δ::KANMX* | (GASPAR *et al.* 2011) |
| YKB4337 | ***MATa*** *his3Δ1 leu2Δ0 met15Δ0 ura3Δ0 sec14-1$^{ts}$-NATMX dga1Δ::KANMX lro1Δ::KANMX are1Δ::KANMX are2Δ::KANMX* | This study |
| YKB4338 | ***MATa*** *his3Δ1 leu2Δ0 met15Δ0 ura3Δ0 eaf1Δ::URA3 dga1Δ::KANMX lro1Δ::KANMX are1Δ::KANMX are2Δ::KANMX* | This study |
| YKB4339 | ***MATa*** *his3Δ1 leu2Δ0 met15Δ0 ura3Δ0 sec14-1$^{ts}$-NATMX eaf1Δ::URA3 dga1Δ::KANMX lro1Δ::KANMX are1Δ::KANMX are2Δ::KANMX* | This study |
| CBY926/YKB3197 | *MATα ura3-52 his3Δ200 lys2-801 leu2-3,112 trp1Δ901 suc2Δ9 osh1Δ::kan-MX4 osh2Δ::kan-MX4 osh3Δ::LYS2 osh4Δ::HIS3 osh5Δ::LEU2 osh6Δ::LEU2 osh7Δ::HIS3 [osh4-1$^{ts}$-TRP1]* | (BEH AND RINE 2004) |
| YKB3707 | *MATα ura3-52 his3Δ200 lys2-801 leu2-3,112 trp1Δ901 suc2Δ9 pik1Δ::HIS3 pik1-83$^{ts}$-TRP1 osh4Δ::KAN* | This study |
| YKB2002 | ***MATa*** *his3Δ1 leu2Δ0 met15Δ0 ura3Δ0 ESA1-GFP::HIS3* | GFP collection (Thermo) |
| YKB3900 | ***MATa*** *his3Δ1 leu2Δ0 met15Δ0 ura3Δ0 OSH1-GFP::HIS3* | GFP collection (Thermo) |
| YKB4254 | ***MATa*** *his3Δ1 leu2Δ0 met15Δ0 ura3Δ0 OSH2-GFP::HIS3* | GFP collection (Thermo) |
| YKB4255 | ***MATa*** *his3Δ1 leu2Δ0 met15Δ0 ura3Δ0 OSH3-GFP::HIS3* | GFP collection (Thermo) |
| YKB3267 | ***MATa*** *his3Δ1 leu2Δ0 met15Δ0 ura3Δ0 OSH4-GFP::HIS3* | GFP collection (Thermo) |
| YKB4257 | ***MATa*** *his3Δ1 leu2Δ0 met15Δ0 ura3Δ0 OSH5-GFP::HIS3* | This study |
| YKB4256 | ***MATa*** *his3Δ1 leu2Δ0 met15Δ0 ura3Δ0 OSH6-GFP::HIS3* | GFP collection (Thermo) |
| YKB4258 | ***MATa*** *his3Δ1 leu2Δ0 met15Δ0 ura3Δ0 OSH7-GFP::HIS3* | This study |
| YKB4145 | ***MATa*** *his3Δ1 leu2Δ0 met15Δ0 ura3Δ0 osh1Δ::KAN* | DMA collection (GE) |

**Table S2 Plasmid list**

| Plasmid ID | Plasmid components | Source |
|---|---|---|
| PKB19 | pRS413 | (SIKORSKI AND HIETER 1989) |
| PKB299 | pRS413 **ptet-*OSH4*** | This study |
| PKB300 | pRS413 **ptet-*osh4*$^{K109Q}$** | This study |
| PKB301 | pRS413 **ptet-*osh4*$^{K109R}$** | This study |
| PKB302 | pRS413 **ptet-*osh4*$^{Y97F}$** | This study |
| PKB303 | pRS413 **ptet-*osh4*$^{K109Q/\ Y97F}$** | This study |
| PKB304 | pRS413 **ptet-*osh4*$^{K109R/Y97F}$** | This study |
| PKB21 | pRS415 | (SIKORSKI AND HIETER 1989) |
| PKB321 | pRS415 **ptet-*OSH4*** | This study |
| PKB289 | pRS415 ***OSH4-GFP*** | This study |
| PKB212 | pRS415 ***osh4*$^{K109Q}$*-GFP*** | This study |
| PKB211 | pRS415 ***osh4*$^{K109R}$*-GFP*** | This study |
| PKB214 | pRS415 ***osh4*$^{K168Q}$*-GFP*** | This study |
| PKB213 | pRS415 ***osh4*$^{K168R}$*-GFP*** | This study |
| PKB218 | pRS415 ***osh4*$^{K247Q}$*-GFP*** | This study |
| PKB223 | pRS415 ***osh4*$^{K247R}$*-GFP*** | This study |
| PKB23 | pRS416 | (SIKORSKI AND HIETER 1989) |
| PKB286 | pRS416 ***OSH4*** | This study |
| PKB287 | pRS416 ***osh4*$^{K109Q}$** | This study |
| PKB288 | pRS416 ***osh4*$^{K109R}$** | This study |
| PKB269 | pRS416 ***osh4*$^{K168Q}$** | This study |
| PKB270 | pRS416 ***osh4*$^{K168R}$** | This study |
| PKB271 | pRS416 ***osh4*$^{K247Q}$** | This study |
| PKB272 | pRS416 ***osh4*$^{K247R}$** | This study |
| PKB292 | pGST2 | Gift from J-F Couture lab |
| PKB261 | pGST2 ***GST-OSH4*** | This study |
| PKB262 | pGST2 ***GST-osh4*$^{K109Q}$** | This study |
| PKB263 | pGST2 ***GST-osh4*$^{K109R}$** | This study |
| PKB266 | pRSET-B-His6-***SAC1*$^{1-522}$** | (STEFAN *et al.* 2011) |
| PKB308 | pRS326 ***OSH1*** | (LOEWEN *et al.* 2003) |
| PKB309 | pRS326 ***osh1*$^{K874Q}$** | This study |
| PKB310 | pRS326 ***osh1*$^{K874R}$** | This study |
| PKB305 | pRS416 **p*PHO5-OSH1-GFP*** | (LOEWEN *et al.* 2003) |
| PKB306 | pRS416 **p*PHO5-osh1*$^{K874Q}$*-GFP*** | This study |
| PKB307 | pRS416 **p*PHO5-osh1*$^{K874R}$*-GFP*** | This study |

**Table S3 List of significantly downregulated genes from RNA-seq experiment**

| Gene symbol | Log2 Fold Change (*sec14-1$^{ts}$eaf1Δ/sec14-1$^{ts}$*) | FDR-adjusted p-value |
|---|---|---|
| ***TSR2*** | -1.002 | 1.01E-04 |
| ***HUF*** | -1.002 | 3.33E-05 |
| ***SER2*** | -1.012 | 3.00E-05 |
| ***DAS2*** | -1.015 | 1.65E-05 |
| ***TRM11*** | -1.017 | 1.25E-05 |
| ***PHO5*** | -1.018 | 6.16E-07 |
| ***NOP14*** | -1.020 | 1.08E-06 |
| ***NAG1*** | -1.020 | 1.30E-04 |
| ***RPA49*** | -1.022 | 7.02E-06 |
| ***SLX9*** | -1.027 | 6.54E-05 |
| ***NOP6*** | -1.032 | 1.68E-05 |
| ***SQT1*** | -1.034 | 4.89E-07 |
| ***VMR1*** | -1.042 | 2.71E-06 |
| ***YAR068W*** | -1.045 | 3.05E-04 |
| ***REI1*** | -1.047 | 7.17E-08 |
| ***DDI2*** | -1.049 | 4.23E-03 |
| ***NIP7*** | -1.050 | 3.12E-05 |
| ***TRM112*** | -1.051 | 4.00E-06 |
| ***CDS1*** | -1.054 | 2.17E-06 |
| ***HPT1*** | -1.056 | 7.92E-07 |
| ***NUS1*** | -1.058 | 1.01E-07 |
| ***RRP8*** | -1.061 | 1.57E-06 |
| ***NOP13*** | -1.062 | 3.07E-05 |
| ***ESF2*** | -1.067 | 7.62E-05 |
| ***YLR446W*** | -1.077 | 6.29E-06 |
| ***GLN4*** | -1.077 | 5.55E-10 |
| ***BAT2*** | -1.079 | 2.03E-12 |
| ***RRP5*** | -1.082 | 4.37E-11 |
| ***NUG1*** | -1.084 | 2.46E-08 |
| ***NBL1*** | -1.091 | 7.13E-05 |
| ***RNA170*** | -1.092 | 1.40E-02 |
| ***NOP7*** | -1.094 | 4.81E-07 |
| ***TRM8*** | -1.095 | 4.33E-05 |
| ***NOB1*** | -1.097 | 2.31E-07 |
| ***TRX3*** | -1.098 | 3.46E-04 |
| ***YOR008C_A*** | -1.102 | 2.34E-02 |
| ***SVF1*** | -1.104 | 1.64E-08 |
| ***DDI3*** | -1.125 | 3.46E-04 |
| ***IPI3*** | -1.125 | 2.35E-07 |
| ***SNO3*** | -1.146 | 4.93E-04 |
| ***ADE12*** | -1.149 | 3.47E-08 |
| ***LTV1*** | -1.150 | 1.56E-07 |
| ***SNO2*** | -1.152 | 5.99E-05 |
| ***IMP3*** | -1.158 | 2.06E-05 |
| ***YER187W*** | -1.158 | 3.86E-03 |
| ***PAC11*** | -1.163 | 2.17E-06 |
| ***GON7*** | -1.168 | 1.91E-06 |
| ***RIX1*** | -1.180 | 6.26E-10 |

| | | |
|---|---|---|
| ***YCL049C*** | -1.181 | 2.37E-08 |
| ***YLR030W*** | -1.185 | 4.47E-06 |
| ***RGM1*** | -1.188 | 3.29E-04 |
| ***DHR2*** | -1.191 | 2.81E-10 |
| ***PAU13*** | -1.211 | 1.17E-02 |
| ***YDR541C*** | -1.212 | 3.43E-08 |
| ***RDS1*** | -1.224 | 1.64E-10 |
| ***BIO5*** | -1.232 | 1.09E-10 |
| ***BMS1*** | -1.233 | 5.41E-16 |
| ***UTP23*** | -1.293 | 4.67E-07 |
| ***TIS11*** | -1.301 | 1.75E-14 |
| ***YGR035W_A*** | -1.309 | 3.33E-05 |
| ***BRX1*** | -1.323 | 3.98E-08 |
| ***BCP1*** | -1.324 | 5.55E-10 |
| ***PLB2*** | -1.326 | 8.20E-13 |
| ***TIR1*** | -1.329 | 5.26E-08 |
| ***FPR4*** | -1.339 | 4.39E-09 |
| ***RBG2*** | -1.342 | 5.30E-11 |
| ***SNZ3*** | -1.357 | 2.01E-07 |
| ***IMD2*** | -1.363 | 7.86E-10 |
| ***YMR310C*** | -1.385 | 4.18E-12 |
| ***YDL241W*** | -1.403 | 2.58E-04 |
| ***YIR042C*** | -1.403 | 3.06E-07 |
| ***AAD3*** | -1.414 | 6.52E-11 |
| ***TDA4*** | -1.419 | 1.88E-09 |
| ***AIF1*** | -1.421 | 8.20E-13 |
| ***YCR087C_A*** | -1.441 | 1.36E-08 |
| ***SOM1*** | -1.455 | 1.70E-05 |
| ***FRE4*** | -1.468 | 6.13E-15 |
| ***TMA46*** | -1.523 | 1.51E-12 |
| ***PHM6*** | -1.524 | 1.55E-06 |
| ***YOL014W*** | -1.539 | 3.02E-05 |
| ***ADE1*** | -1.572 | 1.37E-13 |
| ***TNA1*** | -1.581 | 2.12E-22 |
| ***IZH4*** | -1.601 | 1.99E-11 |
| ***FIT3*** | -1.675 | 9.39E-22 |
| ***IRC7*** | -1.686 | 1.51E-15 |
| ***YEH1*** | -1.744 | 1.71E-23 |
| ***FET4*** | -1.841 | 3.94E-32 |
| ***YHB1*** | -1.925 | 7.65E-21 |
| ***ARN2*** | -2.001 | 5.43E-39 |
| ***COS10*** | -2.003 | 2.91E-18 |
| ***YGL039W*** | -2.023 | 7.79E-30 |
| ***YNR075C_A*** | -2.024 | 3.61E-10 |
| ***PHO11*** | -2.038 | 2.19E-24 |
| ***ADE17*** | -2.055 | 2.81E-20 |
| ***REE1*** | -2.193 | 6.15E-21 |
| ***PAU18*** | -2.261 | 3.46E-11 |
| ***PAU6*** | -2.310 | 5.22E-12 |
| ***PHO3*** | -2.336 | 1.84E-39 |
| ***PHO12*** | -2.426 | 9.28E-34 |

| | | |
|---|---|---|
| ***SIT1*** | -2.434 | 1.22E-45 |
| ***FIT2*** | -2.694 | 2.51E-31 |
| ***ENB1*** | -3.389 | 2.33E-83 |
| ***EAF1*** | -3.404 | 2.67E-58 |

**Table S4 List of significantly upregulated genes from RNA-seq experiment**

| Gene symbol | Log2 Fold Change (*sec14-1$^{ts}$eaf1Δ/sec14-1$^{ts}$*) | FDR-adjusted p-value |
|---|---|---|
| ***DDR2*** | 4.085 | 9.16E-59 |
| ***HSP12*** | 3.587 | 2.40E-46 |
| ***HSP26*** | 3.215 | 3.82E-47 |
| ***CTT1*** | 3.159 | 1.60E-56 |
| ***PUT1*** | 3.098 | 2.31E-43 |
| ***FMP16*** | 2.756 | 2.41E-23 |
| ***TSL1*** | 2.618 | 5.15E-31 |
| ***SOL4*** | 2.492 | 7.41E-31 |
| ***PUT4*** | 2.473 | 1.22E-22 |
| ***ALD3*** | 2.471 | 2.24E-36 |
| ***YRO2*** | 2.365 | 7.41E-31 |
| ***NQM1*** | 2.340 | 1.83E-30 |
| ***YDR034W_B*** | 2.326 | 2.78E-19 |
| ***HSP42*** | 2.318 | 1.14E-23 |
| ***FMP45*** | 2.303 | 1.54E-25 |
| ***TDH1*** | 2.251 | 2.07E-45 |
| ***GPG1*** | 2.246 | 1.50E-28 |
| ***YNR034W_A*** | 2.139 | 2.87E-14 |
| ***GND2*** | 2.128 | 1.22E-22 |
| ***YER053C_A*** | 2.110 | 4.77E-07 |
| ***YGP1*** | 2.102 | 2.64E-41 |
| ***SDH1*** | 2.082 | 8.34E-26 |
| ***MSC1*** | 2.078 | 4.95E-28 |
| ***TPO2*** | 2.051 | 2.90E-24 |
| ***YBR085C_A*** | 2.024 | 3.30E-29 |
| ***SNA2*** | 2.013 | 5.68E-18 |
| ***ENO1*** | 1.972 | 6.47E-37 |
| ***TMA10*** | 1.910 | 1.56E-10 |
| ***STR3*** | 1.892 | 3.63E-15 |
| ***SIP4*** | 1.873 | 3.01E-16 |
| ***SDH2*** | 1.867 | 2.98E-19 |
| ***GLK1*** | 1.867 | 3.37E-18 |
| ***GPH1*** | 1.864 | 7.74E-38 |
| ***NCE102*** | 1.858 | 2.47E-31 |
| ***AAC1*** | 1.819 | 1.15E-10 |
| ***TKL2*** | 1.807 | 7.77E-13 |
| ***XBP1*** | 1.803 | 3.44E-11 |
| ***HOR7*** | 1.799 | 4.41E-18 |
| ***COR1*** | 1.785 | 1.38E-31 |
| ***YCL042W*** | 1.771 | 2.36E-14 |
| ***YJL133C_A*** | 1.761 | 2.14E-16 |
| ***RPM2*** | 1.750 | 2.74E-17 |
| ***PTR2*** | 1.725 | 1.97E-20 |
| ***PGM2*** | 1.705 | 1.55E-29 |
| ***URA2*** | 1.698 | 1.46E-33 |
| ***RPM1*** | 1.685 | 1.46E-09 |
| ***GLT1*** | 1.652 | 1.22E-32 |
| ***YDL124W*** | 1.640 | 4.38E-32 |

| | | |
|---|---|---|
| ***AGP1*** | 1.633 | 2.72E-16 |
| ***BDF2*** | 1.631 | 4.38E-32 |
| ***SDH3*** | 1.631 | 2.44E-15 |
| ***KAR2*** | 1.608 | 9.93E-26 |
| ***UBX6*** | 1.588 | 1.36E-17 |
| ***AI2*** | 1.587 | 1.07E-14 |
| ***AI3*** | 1.585 | 1.75E-14 |
| ***CAR2*** | 1.578 | 3.50E-17 |
| ***AI4*** | 1.566 | 2.57E-14 |
| ***GDS1*** | 1.566 | 2.38E-27 |
| ***AI5_ALPHA*** | 1.565 | 2.28E-14 |
| ***ATP6*** | 1.551 | 7.98E-15 |
| ***COX1*** | 1.544 | 2.43E-14 |
| ***COX2*** | 1.537 | 1.07E-17 |
| ***PHM7*** | 1.536 | 3.36E-10 |
| ***SPG4*** | 1.516 | 1.94E-04 |
| ***TPO4*** | 1.505 | 1.21E-09 |
| ***TFS1*** | 1.501 | 4.93E-14 |
| ***SGA1*** | 1.494 | 3.06E-07 |
| ***AI1*** | 1.481 | 1.26E-12 |
| ***MET28*** | 1.464 | 2.70E-06 |
| ***YBR200W_A*** | 1.458 | 1.77E-03 |
| ***HSP104*** | 1.451 | 3.29E-15 |
| ***SPS4*** | 1.448 | 1.84E-06 |
| ***YGR161W_C*** | 1.439 | 1.01E-07 |
| ***ATP8*** | 1.424 | 1.36E-07 |
| ***PNC1*** | 1.423 | 2.14E-15 |
| ***YLR157C_C*** | 1.422 | 4.71E-04 |
| ***CYC1*** | 1.420 | 6.98E-07 |
| ***RTN2*** | 1.419 | 2.95E-10 |
| ***CWP2*** | 1.416 | 6.76E-11 |
| ***TPS2*** | 1.404 | 1.58E-13 |
| ***GAD1*** | 1.390 | 2.16E-14 |
| ***OM45*** | 1.390 | 1.67E-08 |
| ***YJL017W*** | 1.382 | 3.15E-17 |
| ***YKL151C*** | 1.361 | 1.27E-16 |
| ***INH1*** | 1.356 | 1.96E-09 |
| ***YPC1*** | 1.349 | 4.58E-07 |
| ***STF2*** | 1.346 | 6.19E-09 |
| ***TPS1*** | 1.346 | 3.37E-12 |
| ***MIG2*** | 1.339 | 1.21E-11 |
| ***YER158C*** | 1.338 | 4.48E-12 |
| ***QCR9*** | 1.334 | 3.78E-10 |
| ***QCR10*** | 1.326 | 1.27E-06 |
| ***CYC7*** | 1.322 | 2.82E-03 |
| ***SIP18*** | 1.321 | 1.11E-03 |
| ***YLR161W*** | 1.313 | 1.33E-04 |
| ***RTS3*** | 1.303 | 9.73E-14 |
| ***YCH1*** | 1.299 | 1.05E-08 |
| ***SKS1*** | 1.298 | 5.22E-12 |
| ***HBT1*** | 1.294 | 3.42E-14 |

| | | |
|---|---|---|
| ***BTN2*** | 1.293 | 1.75E-06 |
| ***GIP2*** | 1.291 | 2.86E-06 |
| ***YHR097C*** | 1.281 | 4.56E-13 |
| ***STP4*** | 1.275 | 9.95E-14 |
| ***YLR159W*** | 1.273 | 5.34E-05 |
| ***YLR159C_A*** | 1.268 | 1.36E-03 |
| ***CIR2*** | 1.267 | 4.56E-13 |
| ***Q0255*** | 1.262 | 1.09E-13 |
| ***CYT1*** | 1.261 | 4.51E-11 |
| ***MDJ1*** | 1.253 | 3.62E-10 |
| ***INO1*** | 1.252 | 1.66E-10 |
| ***YLR157W_A*** | 1.252 | 9.04E-05 |
| ***YLR156W*** | 1.245 | 2.81E-04 |
| ***YBR230W_A*** | 1.218 | 1.43E-04 |
| ***BI2*** | 1.217 | 6.68E-08 |
| ***YGR050C*** | 1.216 | 1.06E-03 |
| ***UTR5*** | 1.208 | 1.97E-04 |
| ***NRG1*** | 1.208 | 5.96E-06 |
| ***PIR3*** | 1.208 | 1.13E-08 |
| ***ATG40*** | 1.207 | 4.71E-10 |
| ***IGD1*** | 1.189 | 1.07E-04 |
| ***COB*** | 1.183 | 2.46E-08 |
| ***HXK1*** | 1.181 | 1.94E-12 |
| ***PCL1*** | 1.175 | 4.03E-09 |
| ***HSP30*** | 1.174 | 1.33E-06 |
| ***CMC4*** | 1.174 | 1.61E-05 |
| ***GAP1*** | 1.170 | 3.16E-08 |
| ***MUP1*** | 1.165 | 6.01E-15 |
| ***BI3*** | 1.159 | 3.40E-07 |
| ***PUN1*** | 1.145 | 2.84E-11 |
| ***ATG39*** | 1.144 | 6.40E-04 |
| ***DUR1_2C2*** | 1.143 | 5.96E-12 |
| ***ICY1*** | 1.140 | 8.87E-06 |
| ***BI4*** | 1.139 | 9.67E-08 |
| ***PMP3*** | 1.130 | 1.36E-05 |
| ***HAP4*** | 1.130 | 4.66E-07 |
| ***CLN1*** | 1.130 | 2.02E-08 |
| ***GPD1*** | 1.129 | 2.89E-10 |
| ***YAK1*** | 1.122 | 7.45E-10 |
| ***YGL007C_A*** | 1.119 | 2.05E-02 |
| ***ROX1*** | 1.116 | 4.36E-08 |
| ***YLR154C_H*** | 1.109 | 2.44E-03 |
| ***COX4*** | 1.109 | 7.41E-08 |
| ***BUR6*** | 1.107 | 2.67E-11 |
| ***SWI1*** | 1.106 | 1.73E-10 |
| ***COX3*** | 1.103 | 5.17E-07 |
| ***YML100W_A*** | 1.102 | 5.36E-03 |
| ***QCR8*** | 1.102 | 2.75E-05 |
| ***VHR1*** | 1.100 | 1.14E-10 |
| ***YBR072C_A*** | 1.098 | 2.03E-02 |
| ***PBI2*** | 1.093 | 3.86E-05 |

| | | |
|---|---|---|
| ***ATP1*** | 1.091 | 2.43E-10 |
| ***HSL1*** | 1.089 | 1.04E-11 |
| ***YPS1*** | 1.087 | 5.66E-10 |
| ***HSP78*** | 1.083 | 7.32E-06 |
| ***MCP1*** | 1.076 | 9.63E-06 |
| ***CYT2*** | 1.075 | 1.36E-05 |
| ***HAC1*** | 1.072 | 6.46E-09 |
| ***YDR222W*** | 1.071 | 1.22E-09 |
| ***SPI1*** | 1.070 | 4.28E-05 |
| ***FAS2*** | 1.061 | 1.21E-11 |
| ***RNR2*** | 1.060 | 4.05E-09 |
| ***YNL190W*** | 1.057 | 2.46E-09 |
| ***MCD4*** | 1.052 | 3.28E-12 |
| ***YBR126W_A*** | 1.047 | 2.43E-07 |
| ***YKR041W*** | 1.043 | 1.75E-06 |
| ***YJR120W*** | 1.043 | 1.85E-04 |
| ***PLB3*** | 1.042 | 8.73E-08 |
| ***NCA3*** | 1.039 | 1.75E-04 |
| ***TPO3*** | 1.036 | 3.48E-06 |
| ***YGR146C_A*** | 1.034 | 2.12E-02 |
| ***PDI1*** | 1.033 | 1.56E-07 |
| ***UGP1*** | 1.032 | 2.50E-07 |
| ***YDR524W_A*** | 1.029 | 1.04E-05 |
| ***QCR6*** | 1.027 | 1.90E-06 |
| ***MTH1*** | 1.025 | 2.51E-04 |
| ***FAS1*** | 1.024 | 3.38E-12 |
| ***ECM33*** | 1.023 | 5.91E-11 |
| ***SCW10*** | 1.023 | 1.64E-07 |
| ***CIT2*** | 1.022 | 5.70E-08 |
| ***ATG17*** | 1.015 | 5.68E-05 |
| ***FMP48*** | 1.009 | 4.46E-04 |
| ***YMR196W*** | 1.007 | 2.26E-08 |
| ***SIL1*** | 1.002 | 3.97E-10 |

**Table S5 Gene clustering GO term analysis of significantly downregulated genes**

| Enriched GO term biological process | Enrichment Score: | p-value | Fold enrichment |
|---|---|---|---|
| **ribosome biogenesis** | 5.308802009524532 | 1.80E-21 | 1.30E+01 |
| **phosphate metabolic process** | 2.0605013595220907 | 3.40E-03 | 1.10E+01 |
| **Siderophore transport** | 1.9896881696205484 | 6.90E-13 | 2.70E+02 |
| **purine ribonucleoside monophosphate biosynthetic process** | 1.4769184564461462 | 6.90E-10 | 1.70E+02 |

**Table S6 Gene clustering GO term analysis of significantly upregulated genes**

| Enriched GO term biological process | Enrichment Score: | p-value | Fold enrichment |
|---|---|---|---|
| **respiratory electron transport chain** | 9.152353887660338 | 3.10E-32 | 1.00E+02 |
| **intron homing** | 5.332023441986259 | 2.30E-13 | 2.10E+01 |
| **glycogen metabolic process** | 3.9587134850705996 | 2.10E-07 | 1.20E+02 |
| **pentose-phosphate shunt** | 3.2885669151366286 | 2.40E-08 | 2.40E+02 |
| **cell wall organization** | 1.5822704791565951 | 2.40E-03 | 8.30E+00 |
| **amine transport** | 1.0875144233351073 | 1.80E-10 | 5.00E+01 |
| **protein amino acid phosphorylation** | 0.7922842001078272 | 2.20E-05 | 2.60E+01 |
| **regulation of transcription, DNA-dependent** | 0.5475037058344772 | 6.50E-08 | 9.20E+00 |

# 8 *Curriculum vitae*

## Louis Dacquay

### Education:

May 2014 to Present
**M.Sc. Biochemistry;** *The role of lysine acetylation on phospholipid metabolic pathways*
(Candidate- expected graduation date: Dec 2016)
Faculty of Medicine; University of Ottawa; Ottawa, Ontario, Canada

September 2009 to April 2014
**B.Sc. Honours Bachelor of Science with Specialization in Biochemistry**
(Graduated: May 2014- *Magna cum laude*)
Faculty of Science; University of Ottawa; Ottawa, Ontario, Canada

### Awards:

September 2015 to August 2016
**NSERC:** Canada Graduate Scholarships-Master's (CGS M) (17,500$)

September 2014 to August 2015
**OGS:** Ontario Graduate Scholarship- Master's (15,000$)

May 2014 to April 2015
**CTPNL:** CIHR Training Program in Neurodegenerative Lipidomics
Graduate Student Award- Master's (7,000$)

January 2012 to April 2012
**NSERC:** Industrial Undergraduate Student Research Awards (4,500$)

### Recent Work History:

May 2013 to April 2014
**Undergraduate student- Honors project**
**Supervisor:** Dr. Kristin Baetz
**University of Ottawa** - 451 Smyth Rd., Ottawa, ON
Description:
- Researched the role of lysine acetylation on the function of the Oxysterol-Binding Protein homologue Osh4/Kes1 in yeast

September 2012 to December 2012
**Co-op student: Laboratory Technician**
**Supervisor:** Monique Tremblay
**Tembec Inc. Chemical Products Group** – 10 Chemin Gatineau, Temiscaming, QC
Description:
- Participated in R&D work to improve quality of lignosulphonate products derived from the byproducts of the pulp and paper manufacturing process.

May 2012 to August 2012
**Co-op student: Laboratory Technician**
**Supervisor:** Hassan Malekeddine
**Lallemand Inc. R&D Quality Control Laboratory** -6100 Royalmount Ave, Montreal, QC
Description:
- Conducted quality control of yeast samples derived from the R&D laboratories

January 2012 to April 2012

**Co-op student: Laboratory Technician**
**Supervisor:** Dr. Zhigen Zhang
**Lallemand Inc. R&D Yeast Process Research Laboratory** -6100 Royalmount Ave, Montreal,
Description:

- Optimized the yeast fermentation process for industrial purposes.

## Invited presentations:

July 2016
**Dacquay L***, Kennedy M, Flint A, Butcher J, Stintzi A, and Baetz K; The lysine acetyltransferase complex NuA4 regulates cellular phosphatidylinositol-4-phospahate and phospholipid metabolism. The Allied Genetics Conference, Genetic Society of America ; Orlando, Florida, USA (**abstract selected for talk**)

May 2015
**Dacquay L***, Kennedy M, Lambert J-P, Gingras A-C, and Baetz K; The yeast Lysine Acetyltransferases NuA4 and Rtt109 inhibit the function of Osh4p, 58th Annual Meeting, Canadian Society for Molecular Biosciences; Halifax Nova-Scotia Canada (**abstract selected for talk**)

## Other presentations:

July 2016
**Dacquay L***, Kennedy M, Flint A, Butcher J, Stintzi A, and Baetz K; The lysine acetyltransferase complex NuA4 regulates cellular phosphatidylinositol-4-phospahate and phospholipid metabolism. Work in Progress seminar (Oral presentation)

March 2016
**Dacquay L***, Kennedy M, Flint A, Butcher J, Stintzi A, and Baetz K; The conserved lysine acetyltransferase complex, NuA4, is a novel regulator of phosphatidylinositol-4-phosphate metabolism and signalling in yeast. University of Ottawa, B.M.I. seminar day (Oral presentation)

April 2015
**Dacquay L***, Kennedy M, Lambert J-P, Gingras A-C, and Baetz K; The yeast Lysine Acetyltransferases NuA4 and Rtt109 inhibit the function of Osh4p, Work in Progress seminar. (Oral presentation)

## Publications:

**Dacquay L***, Flint A, Butcher J, Salem D, Kennedy M, Kaern M, Stintzi A, and Baetz K; The essential NuA4 complex in *Saccaromyces cerevisae* has crucial roles for the transcriptional regulation of phospholipid metabolic genes. (Manuscript in preparation)

Huang J, Mousley C, **Dacquay L**, Maitra N, Drin G, He C, Kennedy M, Kennedy B, Baetz K, Polymenis M, and Bankaitis V; The Kes1-Sec14 Lipid Signaling Axis Exerts Dual Control of Cell Cycle and Membrane Trafficking Systems. (Manuscript in preperation)

## Language skills:

Fully bilingual:

**French:** Maternal language; written and spoken
**English:** Secondary language, written and spoken, high school equivalency

- Primary language used for M.Sc. Biochemistry

## References:

Available on request